Extending metrological traceability in qNMR beyond the first dimension

Fahmina FARDUS-REID

Submitted in accordance to Kingston Universities requirements for the degree of Doctor of Philosophy

In Collaboration with LGC

February 2017

Author Contributions

Chapter 2 contains work from the publication:

A. Le Gresley, F. Fardus, J. Warren, *J. Crit. Rev. Anal. Chem.* 2015, 45, 300-310

Chapter 3 contains work from the publication:

F. Fardus-Reid, J. Warren, A. Le Gresley, *Anal. Methods,* 2016, 8, 2013-2019

(This paper was voted within the top 25 papers most assessed in 2016 for the Journal: Analytical Methods 2016 Most Accessed Articles Collection)

Chapter 3 data was presented at the Practical Applications of NMR In Industry Conference (PANIC) in 2015, poster can be found in Appendix D.

Acknowledgements

I would like to thank my supervisors Adam Le Gresley and John Warren. Adam kept the scientific passion constant throughout the six years which I have admired and found highly motivating. I owe a lot from my PhD to John Warren, for his infinite knowledge of the subject and cannot thank him enough for passing his skills down to me. Both John and Adam have helped in the many achievements accomplished along the way and towards the successful completion of my PhD.

I would like to thank my husband, the recipient of my constant complaining, for his support, love and an interest in a subject so contrasting to his own field of work. I am thankful for my parents for supporting me to take opportunities which they have never had, my in-laws for their constant praise and appreciation of my hard work and lastly my younger siblings for their love.

A big thanks to Cailean Clarkson and the Purity and Calibration team at LGC (past and present) for their support and motivation, Jean-Marie from Kingston University for the technical support and lastly LGC for the sponsorship!

Abstract

After decades as a niche analytical technique, quantitative NMR (qNMR) has recently gained mainstream attention largely due to its implementation as a primary ratio measurement method with SI traceability to determine the amount of substance. This method enables rapid and inexpensive value assignment for high-purity, organic small-molecule materials. However, the method is inconsistently applied, particularly in the analysis of high order reference materials; therefore a more comprehensive evaluation of its uncertainties is required for use in certification. Industries such as the pharmaceutical and nutraceuticals are increasingly seeking alternative methods for the measurement of large, structurally complex molecules that are unsuited to standard 1D proton qNMR due to spectral overlap.

Increased resolution can be achieved through employment of spectral editing and multi-dimensional experiments, such as heteronuclear single coherence spectroscopy (HSQC). However, the inherent direct proportionality of proton content and signal intensity of ^{1}H qNMR is lost through signal attenuation due to various chemical phenomena. Despite this complication, these 2D approaches can be calibrated and optimized for quantification of select analyte species within complex matrices and chemical mixtures. The additional biases seen, such as those arising as a result of imperfect pulses, variations of J-coupling constants and inadequate relaxation delays can be in many cases compensated for.

Although such calibration approaches can never be as accurate as ^{1}H qNMR, they provide significant advantages over competing analytical approaches as it is a primary ratio method and therefore does not require a reference material/standard for the analyte. In order to provide value assignments with the highest degree of measurement science, the total uncertainty of the measurement method must be evaluated in a manner, which is both comprehensive and metrologically sound. Presented are well documented approaches to validating ^{1}H qNMR methods and understanding and quantifying biases and uncertainties seen in 2D HSQC qNMR.

Contents

Figures

Tables

Acronyms

AA	Amino Acid
AAA	Amino acid analysis
ADC	Analogue to digital converter
AMP	Adenosine monophosphate
BIPM	International Bureau of weights and measures
BNP	Brain Natriuretic Peptide
CCQM	Consultative committee for amount of substance
CE	Capillary Electrophoresis
CGPM	The General Conference of weights and measures
CIPM	International committee for weights and measures
COSY	Homonuclear correlation spectroscopy
CRM	Certified Reference Material
CT-HSQC	Constant Time Heteronuclear Single Quantum Coherence
D1	Relaxation time
DI	Designated institute
DMT	Dimethyl Terephthalate
DSC	Differential Scanning Calorimetry
GMP	Guanosine monophosphate
GUM	Guide to the expression of uncertainty in Measurement
HETJRES	Heteronuclear J resolved spectroscopy
HSQC	Heteronuclear single quantum coherence spectroscopy
HSQC0	HSQC-Time Zero
NMI	National measurement institute
NMR	Nuclear magnetic resonance
NUS	Non Uniform sampling
O1P	chemical shift offset

PANIC	Practical applications of NMR in industry conference
PMMA	Para-Methoxy methamphetamine
PULCON	Pulse length based concentration measurements
qNMR	Quantitative nuclear magnetic resonance
RG	Receiver Gain
RM	Reference Material
RSD	Relative standard deviation
SI	International system of units
SRM	Standard reference material
S/N	Signal to noise ratio
TOCSY	Total correlation spectroscopy
T1	Longitudinal relaxation
T2	Spin-Spin relaxation
URM	Universal reference material

Preface

Chapter 1 is an introduction to qNMR, it's applications and what has been reported so far in literature.

Chapter 2 looks at the sources of errors affecting internally and externally standardised qNMR. 1D qNMR biases are documented and the method is validated via participation in international studies.

Chapter 3 focuses on the applicability of 2D qNMR. 2D qNMR is a niche, state of the art approach allowing wider applications for complex samples or samples in complex matrices. However, a thorough validation of 2D qNMR is yet to be established. Chapter 3 focuses on validating 2D qNMR for use with complex samples, focusing on SI traceability and calibrating for additional biases seen.

Chapter 4 shows how 1D and 2D qNMR is being utilised in industry and gives real time results from studies across the world, and how work from this PhD has made an impact in international comparison studies.

Chapter 1 Introduction

1.1 Background

The theory of nuclear magnetic resonance (NMR) was first reported in 1924 by Wolfgang Pauli, who theorized that when a nucleus is placed in an external magnetic field splitting of their energy levels occurs due to the nuclear spin properties of an atom, which causes them to align with or opposed to the magnetic field. However, advancements to this theory only occurred later in 1946 when Bloch and Purcell demonstrated that nuclei absorb electromagnetic radiation in a strong magnetic field [1].

Initially NMR spectrometers were continuous wave types and only able to detect the most sensitive nuclei (^{1}H and ^{19}F). The sample is irradiated with one frequency at a time, however, this results in lengthy experiment times and samples of low concentration can be problematic to acquire. There was a revolution in NMR experiments when Fourier transform (FT) NMR instruments were reported in 1966 by Richard R. Ernst and co-workers [2]. In FT NMR all frequencies are irradiated simultaneously with a radio frequency pulse making it faster and analysis of dilute samples is possible.

NMR is one of the most versatile methods of analysis and advantageous over traditional analytical techniques with faster sample preparation and experiment times to providing a non-destructive method of analysis [3]. High performance Liquid Chromatography (HPLC), differential scanning calorimetry (DSC) and Capillary Electrophoresis (CE) are used commonly for characterisation of compounds and quantitative applications. However, they have regularly shown their pitfalls when in use as principal techniques in that they cannot extend their capabilities to provide direct traceability [4].

NMR is commonly used for structural elucidation and characterisation of compounds, but in the last decade there has been an upsurge in its quantitative practises. It's functionality as a

primary method of quantification makes it extremely appealing in comparison to HPLC (an indirect method of quantification), where isolation of impurities is usually required as well as response factor calculations to correct for the difference in UV absorbance making the processing of results time consuming [5]. With recent advances in instrumentation and pulse program development NMR has also in some instances been more advantageous than mass spectrometry (MS) techniques [6]. Although MS sensitivity is still higher than NMR where typical sample volumes are 10-50μL compared to the 200-400μL for NMR, sample preparation, reproducibility, quantitative applications and generally cheaper due to higher throughput gives NMR a stronger presence in the analytical world. All techniques have benefits and limitations and are usually used in conjunction with each other to fulfil the end users' needs.

1.2 Applications

Since its discovery NMR applications cover a range of disciplines within the physics, chemistry, biological and medicinal industry. Due to the range of advantages offered by quantitative NMR (qNMR), its application is widespread. Figure 1 shows some of the common applications for NMR.

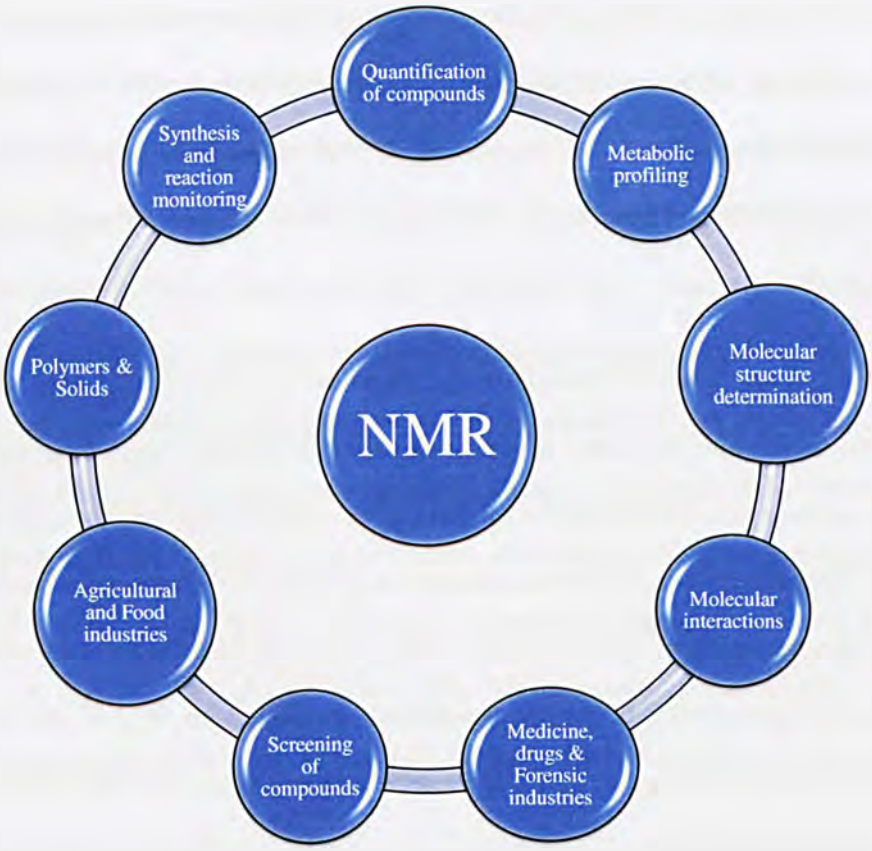

Figure 1.1 – Some common uses of NMR

NMR has been used in the detection of counterfeit products to the identification of impurities and drugs. Within the pharmaceutical industry, NMR is commonly used for structural elucidation, determination of the composition of drug products and impurity profiling *etc* [7]. More recently drug counterfeiting has become a major issue globally with the number of cases the FDA deals with in the US increasing every year [8]. Besides counterfeits sold without any active APIs, the counterfeit drug related deaths has also been a cause for concern. NMR has provided an orthogonal, robust and quick method of detecting counterfeit drugs where changes to production and stereo conformers has made standard approaches difficult and time consuming to perform. NMR provides a method adaptable to the fast pace drug production market. With one method many experiments can be performed on a suspected counterfeit drug such as; residual solvent determination, impurity determination [9], drug characterization, isomeric composition and many more [10].

In the foods industry NMR has been utilised in a range of applications; from characterising Italian garlic to determining the quality and authenticity of wild sea bass lipids [11,12]. Knowing the chemical composition of foods is vital in retailing foods by law and for ethical reasons, and NMR has been at the forefront for the foods industry in achieving fast, simple experiments.

In the petroleum industry NMR is used extensively to assess the quality of materials and products, determining the purity of materials to identifying and classifying crude oils. Portella and co-workers have researched the quantification methods of biodiesel in diesel blends by ^{1}H qNMR, they discuss two calibration approaches showing the advantages of analysing a full ^{1}H spectrum compared to using only part of the ^{1}H spectrum [13]. Cunha and co-workers determine the physical and chemical properties of petroleum fractions with emphasis on measuring the T_2 relaxation times. They found NMR to preserve costs, sample and time when classifying the petroleum distillates [14].

More recently qNMR has had an upsurge in the applicability in large molecules, analysing amino acids, peptides and macrolides. Where conventional approaches to these would be mass spectrometry or chromatography techniques, NMR has shown valuable advantages with simple sample preparation and the ability to perform simultaneous experiments increasing throughput. In the determination of purity of amino acids, conventional methods i.e. HPLC can be very laborious with initial derivatisation of the compound required. A lack of chromophore and difficulties in resolving impurities make this technique undesirable [15]. With no prior extensive sample preparation needed, and from one single experiment valuable data can be extracted using qNMR. qNMR also provides direct traceability to the SI and impurity standards are not needed. However, even with qNMR there are still issues with finding suitable reference standards for purity determinations of compounds, which display a complicated spectrum especially for large molecules such as peptides and macrolides.

There are currently shortcomings in the traditional model for purity assessment for proteins, as the identification of all impurities can prove to be difficult and where identified, reference materials are needed for quantification. It is also difficult to claim traceability to the international system of units (SI) with current HPLC and MS methods, the traceability chain breaks down with limited reference standards available and techniques employed, which provide no SI traceability. Therefore, different techniques are needed to address this. For quantitative analysis there are fundamental complications associated with protein quantification. Proteins are constantly undergoing conformational changes in solution [16]. These dynamic changes make it difficult to assign all protein peaks accurately and may be distinguishable in a spectrum when broad peaks arise, indicating conformational changes occurring or that the protein is just unstable or heavily folded [17]. The applicability of qNMR for protein quantitation needs to be investigated so that it can be exploited to its maximum potential.

A range of techniques, ranging in resolution, have been used for the routine analysis of protein structure. Protein quantification is generally achieved using mass spectrometry, liquid chromatography, x-ray crystallography (XRC) and cryo electron microscopy (EM). XRC is regarded as the gold standard technique in structural biology owing to the atomic detail it provides. However, the analysis requires the protein or complex in a solid crystalline state, which can be challenging to achieve for some proteins e.g. intrinsically disordered proteins and membrane proteins. Alternatively NMR provides similar atomic resolution but avoids solid state sample requirements, although often requires an isotopically labelled protein [18].

For small molecules qNMR provides a faster and cheaper alternative, for peptides and larger molecules qNMR can offer traceability to the SI, however prior method validation is required. A group of researchers in Switzerland (Wider and co-workers) investigated the determination of protein concentrations using the PULCON (pulse length based concentration determination) method, where the correlation of the external radio frequency signal at a specific pulse length is used as the reference signal and is based on the Lorentz principle of reciprocity [19]. The concentration is determined after perfect matching and tuning has been executed and the 360° rf

pulse determined, this rf pulse is then used to calculate the concentration of the sample. However, there are fundamental prerequisites, which have to be met in order to achieve accurate concentration determinations. As the quality of the matching and tuning depends heavily on the instrument hardware connecting the amplifier to the probe (i.e. rf cables) any issues with the devices (i.e. stability of the amplifier) can lead to inaccurate measurements. The tuning and matching of samples is usually an automated process, and the accuracy of this process needs to be investigated to confirm the use of PULCON in quantification of proteins. To establish a simple and reliable qNMR protocol for proteins the fundamental instrument parameters need to be scrutinised and the tools required for quantification need to be improved.

1.3 Introduction to Metrology

Metrology stems from the Greek word of 'measure' and is described by the International Bureau of weights and measures (BIPM) in Paris as the science of measurement, embracing both experimental and theoretical determinations at any level of uncertainty in any field of science and technology [20]. It is an ancient concept dating back to the Egyptians who standardized the measurement of buildings such as the great pyramid to the Egyptian cubit.

Comparability of data is a pre-requisite for any measurement undertaken. In 1875 a treaty was formed, the Convention du Metre, to recognise the need for accurate measurements across time, different locations and other varying parameters all relative to the international system of units (SI) and tracing back to the seven base units of the SI. The SI was established by the general conference of weights and measures (CGPM) which describes the need for a standard system of measurement to ensure worldwide harmonisation of measurements to support today's complex society. In 1977, recognizing the lack of international consensus on measurement, the world's highest authority in metrology, the Comité International des Poids et Mesures (CIPM), requested the BIPM to harmonise measurement with the aid of national standards laboratories [21]. They were to give recommendations on measurement processes and protocols for measuring and regulating the standards worldwide.

Metrology ensures results can be replicated within another system in another part of the world. Today there are 55 member states involved in the Metre convention set up in 1875, along with national measurement institutes (NMIs) and designated measurement institutes (DIs) who are responsible for providing reference standards for measurements. Good measurement allows the UK to remain competitive against other economies. It gives industries confidence in data to support crucial decisions within government and general business infrastructures.

Traceability is a core concept of metrology and primary methods such as NMR represent a cornerstone for achieving traceability. A primary method not only in principle guarantees traceability, but also ensures a method of high metrological quality; hence there is a close relationship between metrology, traceability and NMR. Metrological traceability is defined by the Guide to the expression of uncertainty in measurement (GUM) as the property of a measurement result whereby the result can be related to a reference through a documented unbroken chain of calibrations, each contributing to the measurement uncertainty [22]. These references are usually in the form of standards, which end user's use for calibration purposes. Standards and reference materials are produced by NMIs and DIs who assign reference values to standards, which have full traceability to the SI, in doing so they provide measurements with associated uncertainties.

NMIs and DIs such as BIPM (France), NIST (USA), LGC and NPL (UK) are just a few from the 55 institutes worldwide. Their primary roles are to maintain measurement properties within the country they originate from but they are also involved with providing traceable measurements, traceable reference standards (which is regarded as their core technical competency), research new measurement techniques and making sure their country has the most current tools to meet global needs with respective to measurement.

In order to maintain credibility the NMI's and DI's take part in CCQM studies (consultative committee for amount of substance: Metrology in chemistry and biology). The CCQM is responsible for developing, improving and documenting national standards (certified reference materials and reference methods) for chemical and biological measurements. It provides an

avenue to ensure global comparability of measurements and acts as a forum for knowledge transfer on the research and measurement delivery programmes and ultimately promoting collaboration between institutes.

Measurement uncertainty gives the end user more of a realistic understanding of the trueness of result provided. It ensures measurement results are easily compared. The official definition for uncertainty is described in the VIM series of documents [23].

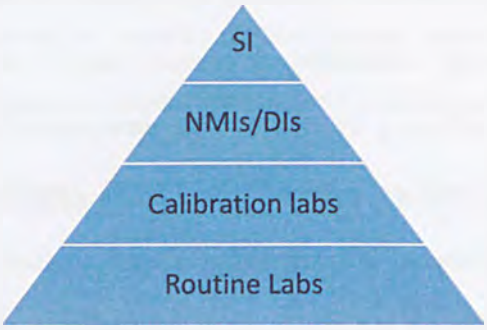

Figure 1.2 – Pathway to achieving SI traceability

Interest in qNMR has rapidly grown in the last few years in the metrological community. Quantification of a compound is conventionally achieved using chromatographic techniques; however these require calibration of the instrument and methods using well-characterised, high-purity standards/calibrants, which distinguish such techniques as a secondary method of quantification. Credibility of the analytical results in chromatographic techniques is only achieved using such reference standards, which may prove costly and time consuming.

Reference standards with stated measurement uncertainties are required within the traceability system. They are most commonly utilised as quality control tools and play an important role in method validation [24]. A reference material (RM) is defined as a material sufficiently homogenous and stable with respect to one or more specified properties, which has been established to be used for its intended purpose in a measurement process. A certified reference material (CRM) is defined as a reference material characterised by a metrologically valid

procedure accompanied by a certificate that states the value of specified properties, including its uncertainty and traceability [25].

Calibration standards for qNMR are currently available from Fluka and Sigma Aldrich, reporting very low uncertainties of between 0.07-0.10 % and claim traceability through referencing against the NIST benzoic acid standard [26].

1.4 Quantitative NMR (qNMR)

Quantification in NMR is achieved by comparing the ratio of the integral of a specific proton absorption at a specific chemical shift directly with another, as the signal intensity is directly proportional to the number of nuclei for that resonance. Hence it is considered a primary analytical technique as there is no need for instrument calibration through reference standards. There are two methods of quantification of a substance by qNMR, a relative method and an absolute method [27]. Purity and concentration determinations are obtained by referencing the area of a signal from the analyte to another signal originating from an internal standard. Malz and Jancke [28] deduced Equation 1.1 for the calculation of purity through NMR.

$$Px = \left(\frac{I_X}{I_{Std}}\right) x \left(\frac{N_{Std}}{N_X}\right) x \left(\frac{M_X}{M_{Std}}\right) x \left(\frac{m_{Std}}{m_X}\right) x P_{Std}$$

Equation 1.1

Px = is the analyte in question, I_X is the signal response of the standard

M_x and M_{std} = molar masses of the analyte and standard

m = weighed mass of the analyte

m_{std} and P_{std} = weighed mass and purity of the standard

N_{std} and I_{std} = number of spins and integrated signal area of the standard in a typical NMR spectra

Whereas, relative quantification is determined by calculating the molar ratio of the two compounds using Equation 1.2.

$$\frac{Mx}{My} = \frac{Ix}{Iy} x \frac{Ny}{Nx}$$

Equation 1.2

Where I and N are the integral area and number of nuclei for the compounds respectively.

1.4.1 One dimensional (1D) Quantitative NMR

As mentioned previously, although qNMR methods are highly advantageous, there are many limitations associated with the method. Many research articles highlight this in detail and the key problems identified with ^{1}H qNMR are;

1. Overlapping of key signal peaks (illustrated in Figure 1.3)
2. Low sensitivity and dynamic range of the instrument (although recently there has been major improvements with the development of cryoprobes and higher field magnets)
3. Very few suitable standards available for qNMR especially at NMI level
4. Volatility of materials
5. Solubility of materials
6. Interpretation of NMR Spectrum (analyst processing of spectrum)

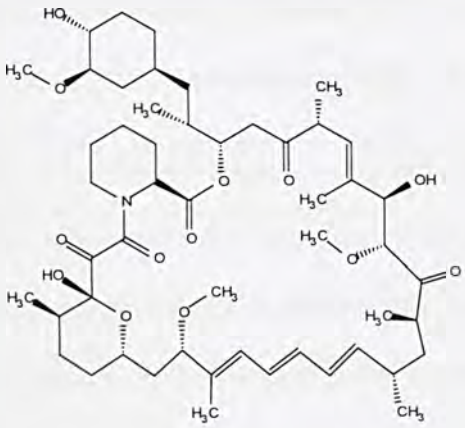

(1)

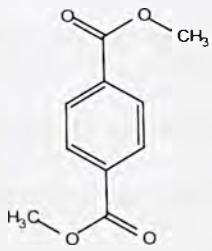

(2)

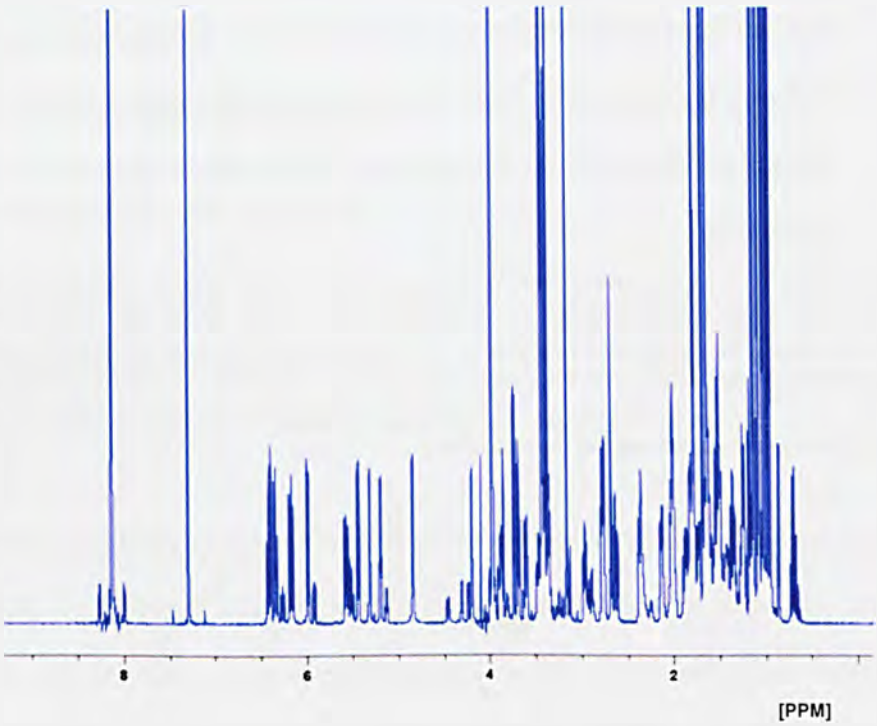

Figure 1.3 – Example ^{1}H spectrum of Sirolimus (1) using Dimethyl Terephthalate (2) as an internal standard, showing the complexity of the spectrum, acquired on a 600 MHz Bruker instrument using $CDCl_3$ NS:16, D1: 60s

Wells and co-workers [29] states the conditions required for successful quantification of a target analyte using an internal standard reference material (SRM). The most crucial parameter being that the internal standard signal must not overlap with any of the signals for the target analyte

and/or impurities. This, although obvious, is very hard to achieve and highlights one of the many limitations to ^{1}H qNMR especially for large complex compounds.

Malz and Jancke [28] investigated the problem of signal overlapping. In complex samples, signals may consist of multiplets due to the coupling with other nuclei. This leads to the problem of inaccurate quantification i.e. impurities and integrations might be over or under estimated. The authors suggested experimental solutions:

1. Having higher magnetic fields that increase the resolution
2. Internal signal integration of several analyte resonances, this can help identify hidden impurity signals under resonances used if values are not consistent
3. Changing the temperature may cause shifts to change isolating further impurity signals
4. Spectral simplification via decoupling of ^{13}C satellites may lead to a simpler spectrum for analysis

Purity and concentration determinations by qNMR are more relevant to the metrological community where NMR can be used as the primary method for characterising a compound or for assigning reference values for standards.

qNMR shows many advantages over traditional approaches to quantitative measurements, and this is also what sets qNMR apart from almost all other metrological techniques used to quantify compounds. The qNMR method only requires that (a) the sample dissolves completely in a solvent (normally fully deuterated), and (b) it contains NMR-active nuclei and that care and attention is paid to data collection and processing. It's a non-invasive technique, capability of providing a primary ratio method of measurement, rapid sample preparation and instrument run time are just a few of the many reasons why NMR is re-emerging as a powerful tool for measurement of sample.

qNMR is significantly affected by various sample specific, experimental and processing parameters. Therefore, each protocol has to be carefully validated to keep consistency between instruments and users.

The experimental factors affecting qNMR are pulse length, relaxation delay, coupling constants, tuning and shimming *etc.* and are detailed further in Chapter 2. The processing parameters affecting quantification are multiplicity and line shape of signal, signal to noise ratio, signal integration and spectral complexity.

Through the utilisation of primary calibrants such as reference materials and standards, qNMR provides a pathway of determining purity or concentrations of solutions via three distinct methodologies;

1. Using internal standards
2. External standards
3. ERETIC (electronic reference signal)

1.4.1.1 Internally standardised qNMR

Using internal standards is the most common method for determining the absolute amount of substances in qNMR. A known concentration of a reference standard is co-dissolved with a known concentration of analyte solution for quantitative analysis (Figure 1.4).

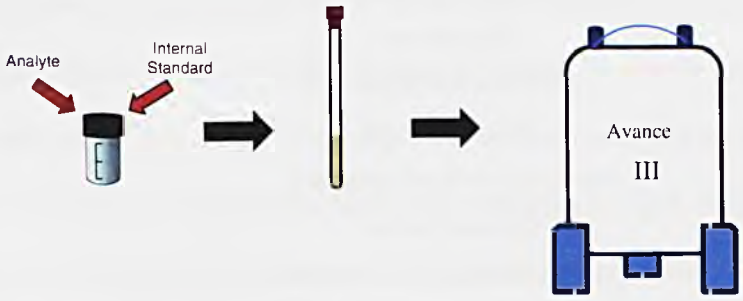

Figure 1.4 – Schematic to show preparation of an internally standardised qNMR assay

The pre-requisites for ideal internal reference standards are that they must be soluble in commonly used solvents, must not overlap with signals relative to the compound under investigation, have a known purity, be inexpensive, readily available in a highly pure form, must not have any chemical interactions with the analyte under investigation, non-volatile and its molecular weight must be in the same region as the compound under investigation. Finding an

internal qNMR standard, which meets those requirements can be time consuming and any compromises will have direct effects on the accuracy of measurements. There is a need for a broad range of internal standards, which can cover a selection of analyte and solvents with SI traceability.

Currently there are three major commercial producers for internal standards for qNMR; Sigma Aldrich, Cambridge isotope laboratories (CIL) and Wako Pure chemical industries LTD. All providing certified reference materials for qNMR. WAKO provide S.I traceable standards via the national metrology institute of Japan (NMIJ) and Sigma Aldrich and CIL claim traceability through referencing spectra to the NIST benzoic acid, which in itself is not intended for qNMR applications. Table 1.1 shows the variety of standards WAKO and Sigma Aldrich sell.

Product Name	Wako	Sigma Aldrich
1,4-BTMSB-d4	☑	
4,4-dimethyl-4-silapentane 1-sulfonic acid	☑	
Dimethyl Sulfone	☑	☑
Maleic Acid	☑	☑
Dimethyl malonic acid		☑
Ethyl 4-(dimethylamino)benzoate		☑
Duroquinone		☑
1,24,5-Tetramethylbenzene		☑
Benzyl Benzoate		☑
Potassium phthalate monobasic		☑
Calcium formate		☑
1,2,4,5-tetrachloro-3-ntrobenzene		☑
3,5-Dinitrobenzoic acid		☑
Dimethyl terephthalate		☑

Table 1.1 – Range of internal standards sold by Wako and Sigma

Sigma Aldrich claim uncertainties of less than or equal to 0.2% for their range of qNMR internal standards, however they claim SI traceability through referencing spectra to the NIST benzoic acid (BA) standard and one historical issue is that several of the ultrahigh purity materials such as this benzoic acid are not certified for purity of the analyte itself, but

certified by titrimetric methods and thus the uncertainty of the measurement is not directly applicable to its subsequent use as a qNMR standard.

Cambridge Isotope laboratories offer a range of solution state ready to use internal and external standards for qNMR (Table 1.2), aiming to minimise sample preparation time and uncertainties associated to weighing out of sample.

Internal reference Solution
5 mM Benzoic acid in DMSO-d_6
15 mM Benzoic acid in DMSO-d_6
External reference solution
5 mM Benzoic acid in DMSO-d_6
15 mM Benzoic acid in DMSO-d_6

Table 1.2 – Range of solution state NMR standards produced by CIL

Several papers have been published [30] highlighting the need for qNMR specific standards. Standards produced for the intended use for qNMR would be invaluable for NMR spectromotrists, more so, standards with traceability and high quality of analytical output. Currently there is a pressing need for qNMR CRMs and RMs for the metrological community.

Rundlof and co-workers investigated the use of 25 potential compounds to be used as internal standards for qNMR, however only 8 were considered suitable for qNMR applications when referenced to a pure acetanilide sample [31]. All materials used lacked traceability to the SI. DSC was used as an orthogonal method for purity determinations of the 8 compounds selected. The paper emphasises the obvious black hole in literature advising of suitable internal standards for qNMR applications and an even more prominent absence in any SI traceable standards. Another paper by Rundlof and co-workers discuss the production of an in-house primary reference standard using secondary reference standards by qNMR for the use of determination of drugs and pharmaceutical products [32]. Many laboratories have to resort to producing in-house qNMR standards due to the lack of commercially certified standards available.

A group of researchers investigated the use of *p*-toluenesulfonic acid (TsOH) as a possible reference compound for qNMR experiments [33]. The advantages of using TsOH as an internal standard is that it has high water solubility, it is commercially available in its pure form and can be removed easily afterwards due to its physical properties. Its application has been seen to be beneficial in calibrating DNA methods.

Saed and co-workers report the use of internal standards to quantify the purity of agricultural chemicals using ^{1}H and ^{31}P qNMR spectroscopy [34]. The purity of a glyphosate and profenofos was determined using sodium acetate and sodium phosphate as the internal standards respectively. Again these standards were chosen due to their solubility in the chosen solvent and their non-overlapping with the NMR signals with the compound under investigation.

Wells and co-workers used dimethylsulfone as a single universal reference material (URM) to which all organic materials may be referenced to. In this research article, a comparison between chromatographic methods and NMR methods was carried out [29]. Both methods are considered to be problematic when dealing with very complex molecules, however in the case of NMR, internal standards are used to overcome this issue.

Watanaby and co-workers used tert-butanol as an internal standard for determining concentrations of paralytic shellfish toxins (PSTs) which is a contaminant of shellfish and crabs consumed by humans [35]. PST contaminated shellfish can lead to paralytic shellfish poisoning, therefore determining it's concentration to ultimately verify toxic levels is crucial in the food industry.

1.4.1.2 Externally standardised qNMR

External calibration methodologies have been used for quantification experiments in instances where an internally standardised assay is either not possible or not desirable. Such circumstances include those where the sample reactivity or spectrum complexity may prohibit addition of a standard or the material is so limited or expensive that it cannot be contaminated with other material. In these cases an externally standardised NMR assay can be employed.

However, due to inaccuracy of the method its application has been limited, where the accuracy of using external standards rarely exceeds 5 %. However, the use of external standards still holds great advantages by enabling quantification experiments without directly contaminating the sample. Hazardous materials can also be safely handled as they can be kept in sealed tubes throughout the experiment. The problem of overlapping signals is also eradicated and the problem of inaccuracy can be reduced by improving the preparation of samples and investigating systematic errors to reduce them further.

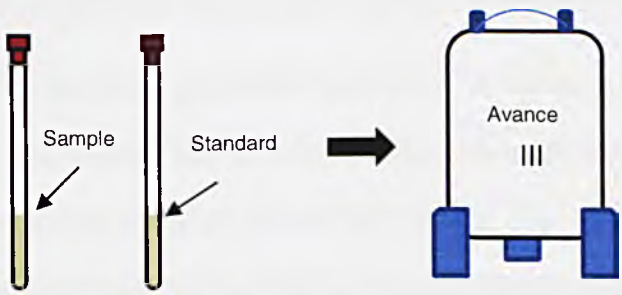

Figure 1.5 – Schematic of sample preparation for externally standardised qNMR assay

There has been a decrease in the utilisation of externally standardised qNMR evident from the decline in the number of publications produced; this may be attributed to the issues discussed above especially the high inaccuracy, which is problematic in the metrological community. However, if all relevant parameters are optimised and corrected for it can produce results with acceptable uncertainties. Chapter 1 of this thesis investigates how to optimise qNMR for use for external standards reducing its uncertainty thus providing a way it can still be accepted within the metrological community.

Burton and co-workers [36] investigated the potential sources of error for externally standardised qNMR and the estimated contribution to % RSD was presented. Experiments were run on a 500 MHz instrument and it was concluded that if all the influencing parameters were controlled then a 1% RSD would be obtainable with the biggest source of error coming from

sample preparation, however a complete breakdown and example has not been given to demonstrate the individual contributions to obtain that 1% RSD.

Liu and co-workers compare the difference in results between HPLC assessments of an antibiotic for purity compared to an externally standardised qNMR assay, differences of no more than 2% were reported [5]. The mass balance approach by HPLC included many indirect methods for the quantification of purity of main components and impurities. Techniques such as GC-FID and Karl Fischer were used to get a full purity assessment, whereas the qNMR technique provides information of main component and impurities all within one experiment.

A paper discussing the use of the external referencing methodology using internal reference standards or residual protonated solvent signals as the external peak has shown how the two methods can work concurrently [37, 38]. Pre-calibration of the internal reference standard or solvent signal is required using an external reference standard. The internal reference peak only serves as a reference point for data acquisition and processing, and the purity of the external standard is used for all calculations. If using the solvent peak, the pre-calibration is found to be batch specific and not applicable to volatile solvents. This pre-calibration of the reference peak requires additional time, sample preparation and optimisation processes but is imperative to make the method quantitative.

1.4.1.3 Eretic qNMR

ERETIC NMR (Electronic Reference to access *in vivo* concentrations) is where an electronic device provides a reference signal for the determination of concentrations and was developed by Akoka and co-workers [39]. The ERETIC signal is produced using a different RF channel to the channel used for observation and the signal also needs initial calibration against a solution of known concentration using Equation 1.3, after which for subsequent analyses the electronic signal can then be used for quantification purposes.

$$[ERETIC] = [REF]A_{ERETIC} / A_{REF}$$

Equation 1.3

The main advantages of ERETIC NMR is that no contamination of the sample is required, preliminary work is avoided as initial relaxation determinations do not have to be made and the position of the eretic peak can be moved in the spectrum overcoming overlapping issues. Akoka and co-workers explore the Eretic method with the internal referencing method using trimethylamine hydrochloride (TMA). They demonstrated that the difference in precision and accuracy for the two methods was insignificant with only a small variation in the ERETIC signal with time observed due to spectrometer instabilities. Later in 2004, Akoka and co-workers evaluate the use of the ERETIC method in 2D qNMR applications for the first time [40]. However, they report issues when using symmetrisation to improve spectral quality for COSY and J-resolved spectra, where the ERETIC peak gets eliminated. To overcome this two ERETIC signals are needed resulting in the need of three RF channels, which limits its application. Other limitations are that the method requires modification to pulse programs and additional spectrometer hardware and set up.

1.4.1.4 Other qNMR methods

Improvements to the above three referencing methodologies have been described in literature where the methods have been adapted to increase its applications. An adaptation to the ERETIC method, Amplitude-corrected referencing through signal injection (ARTSI) was developed by Mehr and co-workers, where the power correction of the reference signal is made accordingly to the pulse width used for the experiment [41]. The group found the quality of probes to affect the ERETIC method but by utilisation of ARTSI probe receptivity and reference signal intensity fluctuations can be controlled giving better quantitative results. This method is also applicable to samples in different solvent or salt compositions, where the ERETIC method had limitations in certain sample compositions.

Since the development of ERETIC NMR, instrument manufacturers (Bruker Biospin) have incorporated functions into their software that enables the simulation of the reference signal, which requires prior calibration for quantitative measurements. This gives an added advantage by being able to compensate for any systematic changes made during acquisition.

Pulse length based concentration determination (PULCON) is an adaptation of the external referencing method, whereby the signal intensity from a sample is inversely proportional to the 90° or 360° pulse length. The method offers advantages like the ERETIC method but doesn't require the need for instrument modifications. Y. Monakhova and co-workers compared the PULCON method to internal referencing methods using 3,5-dintro benzoic acid and although the PULCON method generated higher purity values t-tests found that there was no significant statistical variation between the two methods [42].

1.4.2 2D quantitative NMR

qNMR has predominantly been utilised in the simple One-Dimensional state, and so far only literature concerning the 1D state has been discussed. However, a major drawback of 1D qNMR is the poor resolution of signals in complex spectra, giving poor integration ranges and hindering any quantification. Large or complex molecules such as peptides, macrolides and forensic matrix samples are often not suited to quantitative measurements by 1D qNMR as the signals of interest they generate lack the necessary resolution from adjacent peaks to allow accurate integration, even with external referencing some spectra are so busy that finding a sample peak to integrate may be impossible. Two dimensional (2D) NMR, a technique proposed by Jeener in 1971 [43], gives a higher discrimination of resonances by dispersing signals into the second dimension and exploiting the large carbon chemical shift range. This increases resolution and peak specificity thus allowing for a more precise quantitation method for complex spectra. Figure 1.6 shows the complexity of a small peptide (GFFYTPKA (**3**)) with phenyl glycine (**4**) and shows how well the signals are resolved in the second dimension.

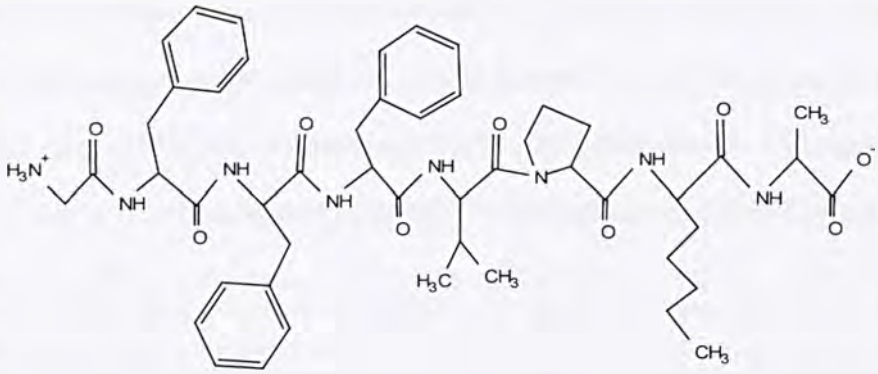

(3)

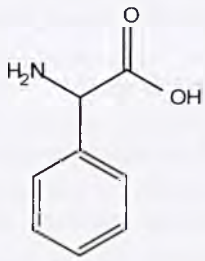

(4)

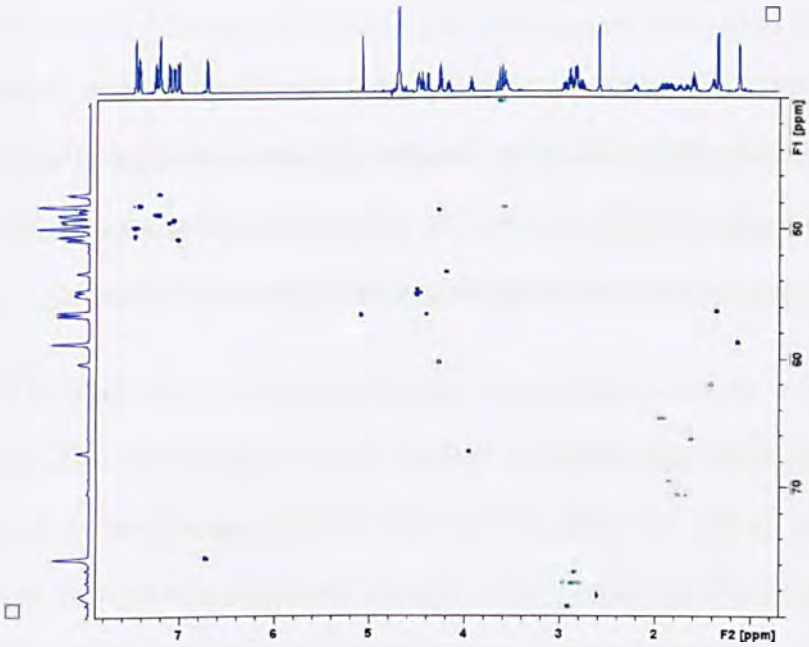

Figure 1.6 – 2D HSQC spectrum of GFFYTPKA (3) spiked with phenyl glycine (4) in D_2O acquired on a 600 MHz Bruker instrument. F1 axis is the ^{13}C dimension whilst F2 shows the ^{1}H dimension. NS: 16, D1:2 sec

Although traditionally used as a qualitative tool, from a quantitative point of view the advantages are substantial. However, there are additional complications that need to be addressed in 2D qNMR. The two fundamental issues of 2D qNMR are the long experimental times required and the signal attenuation during the pulse program.

In 1D qNMR the signal area is directly proportional to analyte concentration (provided correct sample parameters are used) allowing for accurate and precise quantitation, but the intensities of cross peaks in standard 2D qNMR experiments are not directly proportional to the analyte concentration due to resonance specific signal attenuation during the pulse sequence and the non-uniform excitation of the carbon dimension [44, 45]. 2D experiments such as HSQC rely on the polarization transfer through J coupling therefore signal intensity is not only dependent on the delay value of the CH coupling constant for which the experiment is optimised but additional factors such as peak multiplicity, homonuclear coupling constants and T_1 and T_2 relaxation during the pulse sequence.

Another major drawback to 2D qNMR is the long experiment time, caused by the need for multiple FID acquisitions to achieve adequate resolution in the second dimension due to the low natural abundance of ^{13}C. Adding long relaxation delays to account for T_1 effects further lengthens experimental time making the approach extremely undesirable.

However, if optimised appropriately these drawbacks can be accounted for if not eliminated by calibrating them, using optimised methods such as Ultrafast 2D NMR or by adding relaxing agents to shorten the effects of T_1. Many different approaches to 2D qNMR have been investigated over the recent years. J-resolved spectroscopy was one of the very first methods developed in 1976 by Aue and co-workers [46] for achieving quantitative 2D NMR data, where an incremented delay is used to create an indirect time axis for the second dimension. However the peak volumes were no longer proportional to the concentration of individual sample components due to a mismatch of J-coupling constants during the coherence transfer periods. Subsequently, q-HSQC methods were developed where the wide chemical shift of the carbon

dimension introduced problems to quantitivity but could be corrected for by amending the integration results using hypothetical offset dependence values or by using composite pulses, which already have a good offset compensation [47]. Although this makes it possible to correct for the non-linearity of the carbon dimension it is a complicated method to apply for routine experiments. A $HSQC_0$ method developed by Hu and co-workers [48] seems to alleviate the problems mentioned above by extrapolating a series of HSQC spectra acquired with different repetition times. The principle is that of a calibration curve and the extrapolated time-zero HSQC spectrum ($HSQC_0$) produces data where the signal intensities are proportional to the concentrations of individual sample components. This technique has been proved successful in quantifying metabolite mixtures such as alanine, glucose and hydroxybuterate and a separate study quantifying thiocoraline [49,50]. Another possibility explored by Michael and co-workers is applying the ERETIC signal approach to 2D spectra [51]. Michel's group proved that ERETIC signals can be obtained for a 2D COSY spectrum however would need multiple RF channels, limiting its use. Although this proved highly advantageous real quantitative data is yet to be acquired to prove that the method would work for quantitative analysis. Ultrafast 2D qNMR analysis uses a single scan technique to acquire 2D data reducing the experimental time significantly however this technique has not been evaluated for quantitative measurements other than for TOCSY and J-resolved methods, which have highlighted its low sensitivity as being a key issue [52, 53].

The use of non-uniform sampling (NUS) methods has also been documented recently highlighting its ability to significantly reduce 2D experimental time by acquiring only parts of the FID and then using novel reconstruction methods during processing to complete the dataset with the missing parts of the FID [54]. The method can save up to 75% of acquisition time without compromising spectral quality as shown in Figure 1.7. Traditional data acquisition for 2D experiments is collected in a linear fashion, whilst NUS depends on random sampling to minimise artefact effects.

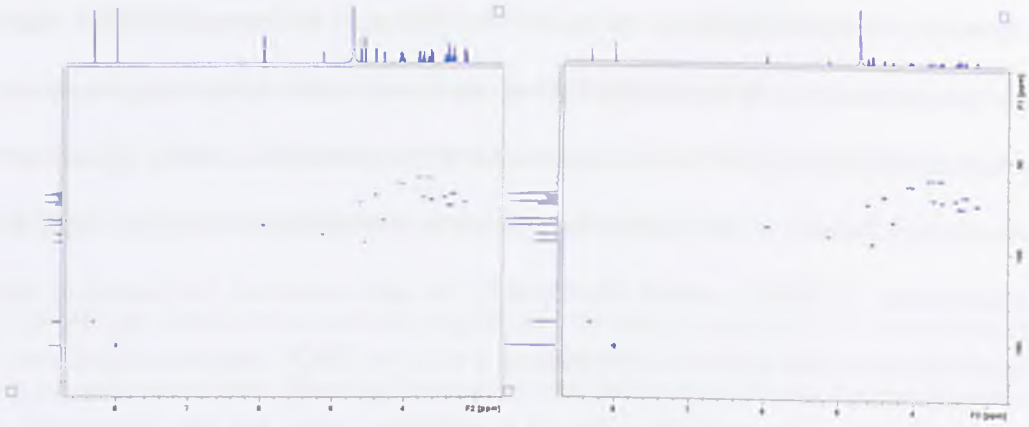

Figure 1.7 – Left: traditional HSQC experiment of glucose and AMP, NS: 8, D1: 2s, Experiment time: 2hr 24min. Right: NUS spectrum using 25% sub sampling, NS: 8, D1: 2s, Experiment time: 36min. F1 axis is the ^{13}C dimension whilst F2 shows the ^{1}H dimension, both acquired on a 600 MHz Bruker instrument using D_2O

1.5 NMR measurement uncertainty

Measurement uncertainty defines the dispersion or spread of results and underpins the quality and accuracy of the measured result. All measurements have errors associated with the end result; these errors can be taken into account by assigning uncertainty estimations to the measurement made, establishing these components in the first place can help reduce or eliminate the overall uncertainty towards the measurements [55].

The uncertainty value enables an analyst to assess the reliability and 'fitness for purpose' of the result. An uncertainty of the measurement explains all significant factors, which cause the results to vary. It is widely used in metrology where the uncertainty value provides a method to unify the evaluation and comparability of results worldwide. It helps gain international confidence in results, manufacturer's specifications, quality assurance and accreditation of systems [56]. Results can ultimately be used by other laboratories based on the value assigned and its uncertainty of materials intended for calibration or testing purposes.

Accuracy and precision measures are often used to indicate how reliable results are. Accuracy is defined as the degree of closeness of experimental measurements to its true value (taken from

the certified value of a reference material). Precision is defined as the degree to which repeated measurements show the same results, the standard deviation of measurements is an indicator of precision.

In qNMR the main source of uncertainty is from sample preparation and reproducibility of qNMR measurements associated with weighing [57]. Another source of uncertainty, as discussed in the article by Rizzo and co-workers, is operator to operator variation i.e. phasing of the baseline, adjusting peak integrations *etc* [58]. Shu-Yu Liu and co-workers compare qNMR to mass balance methods in an uncertainty study of macrolides. They found that the uncertainty derived from qNMR measurements are smaller in general than the traditional mass balance approaches, as the mass balance approach has many sources of uncertainty making the expanded uncertainty relatively large, they recommend using qNMR as a complimentary method to the mass balance approach [59].

A fishbone diagram has been generated (shown ion Chapter 2) to encapsulate sources of bias and uncertainty in regards to quantitative measurements in qNMR [60]. There are two main types of uncertainties in qNMR, Type A uncertainty and Type B uncertainty.

Type A uncertainties include the error coming from the precision of the measurement and standard deviation of replicate analyses. Type B uncertainties are based on scientific judgement and information available either from previous data or manufacturer's reports *etc*. Chapter 2 focuses on the uncertainties arising from both Type A and Type B uncertainties.

1.6 Scope of thesis

The key aims of this thesis are:

- Achieving traceability to the international system of units (SI) for qNMR measurements, this has never been done before for 2D qNMR. NMR at the moment is inconsistently applied and for this reason doesn't yield the unbiased result as assumed it would.

- The NMR community within the metrological field operates at the highest level of measurement science and therefore these biases need to be understood and quantified.
- Explore applications of 1D and 2D qNMR methodologies from simple molecules to complex mixtures providing uncertainty budgets for each type of analyses and compensating or calibrating for any bias observed.
- Investigate type A errors and document methods to reduce or account for them.

Many research papers have mentioned the high number of sources of errors associated with externally standardised qNMR measurements, however, an in depth comparison between the two common referencing methods has not been made. This thesis will make a detailed comparison between internally standardised and externally standardised qNMR measurements and which instrumental factors contribute a substantial source of error for these two methods of quantification, with the aim of achieving low uncertainties.

Chapter 2 1D qNMR

2.1 Background

In order to achieve qNMR measurements of high accuracy and quality, many factors influencing the end result need to be optimised and accounted for.

The accuracy, precision and reliability of any qNMR data relies on the fundamentals of the instrument, manipulation of spectral data and most importantly sample preparation. There is currently no standardised protocol for sample preparation for quantitative analysis. Many instrumental acquisition parameters need to be optimised to give quantitative results of high accuracy and to keep systematic errors to a minimum, however, this is a time consuming process. It has already been established that a relaxation delay of $5xT_1$ must be used to achieve full relaxation from a 90° pulse angle where T_1 is the spin-lattice relaxation time [61]. It is therefore necessary to measure the T_1 for each analyte prior to any qNMR analysis, as insufficient relaxation will give a reduced signal intensity output. Many instrumental parameters, which can have variable settings on the instrument have been established by research papers as having profound influences on the overall measurement results. Figure 2.1 shows the sources of uncertainty associated to ^1H qNMR analysis [62]. The main contributors are then classified into four categories which are considered as fundamental components to qNMR analysis. This chapter will investigate how significant the contributors to bias are and ways to reduce or compensate for them, in all instances a Bruker Avance III 600MHz instrument with a TXI probe was used for all experiments.

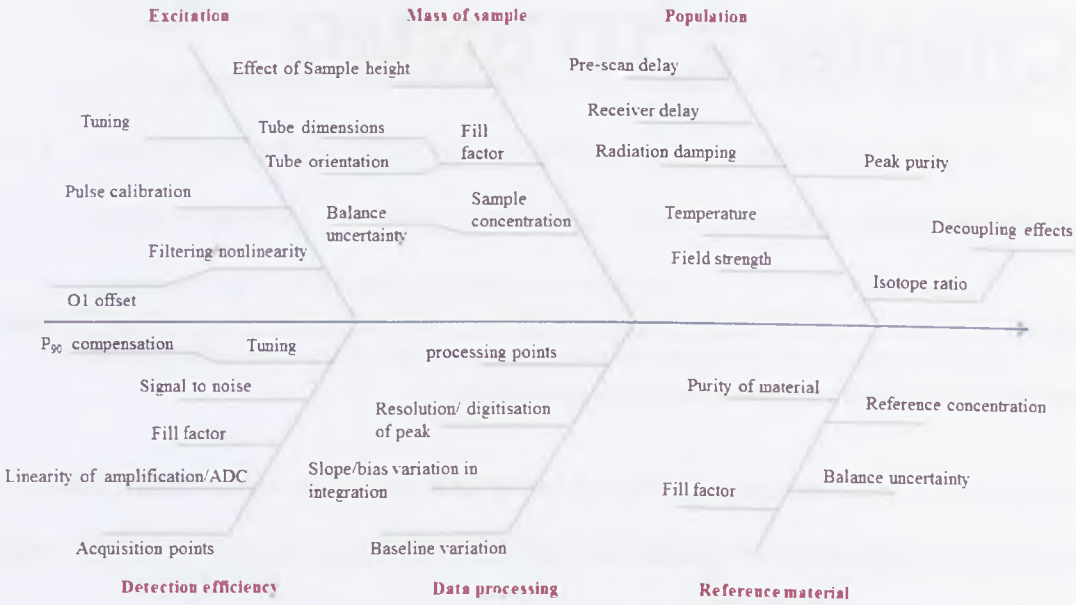

Figure 2.1 A fishbone diagram of all the possible sources of uncertainty arising from qNMR experiments.

Table 2.1 shows how each contributor to uncertainty correlates to the different types of qNMR.

Parameters affecting uncertainty budget	Internally Standardised	Externally Standardised	2D Approaches
Pulse calibration*		x	
Receiver Efficiency*		x	
RGA calibration *		x	
Digitisation	x	x	x
Lineshape & Multiplicity	x	x	x
Signal to Noise*	x	x	x
Sample prep (weighing uncertainties)*	x	x	x
Temperature		x	
Receiver Delay*	x	x	x
Tube volume*		x	
Sample height *	x	x	
Operator variation in processing	x	x	x
Intermediate precision - orientation *	x	x	
T1 & T2 relaxation in pulse train			x
Coupling constant			x

Table 2.1 Parameters contributing to bias and uncertainty for internally and externally standardised experiments and 2D qNMR experiments

The contributors to error and bias mentioned in Figure 2.1 all fall under the following four main categories which will be discussed in this chapter;

- Molecular properties (Population)
- Sample preparation (Mass of sample, Reference Material)
- Acquisition parameters (Excitation, Detection efficiency)
- Processing parameters (Data processing)

2.2 Molecular properties

The sources of error and bias discussed under this category are attributable to the molecular properties of the sample and standard. Such properties will determine the experimental conditions and affect the absorption of the radiofrequency, ultimately affecting the qNMR results. A series of experiments have been implemented to see the extent of the impact caused by these properties.

- Effect of relaxation time
- Isotopic ratios
- Chemical shift

2.2.1 Effect of relaxation time

The contribution of this parameter, which is sample dependant has to be pre-determined for best practise in ^{1}H qNMR. Using 7x the longest T_1 will give a maximum bias of 0.09%, however in qNMR experiments it is essential to demonstrate that a minimum of 5x T1 is achieved where D1 + acquisition time = 5x T1 of the longest relaxing nucleus. At 5x T_1 approximately 99.3 % of the equilibrium value is re-established. As the effect of this parameter for ^{1}H qNMR is excellently documented in literature [63, 64] no further work was carried out to determine its bias contribution. The longest relaxing nucleus was identified for all qNMR experiments reported and this condition was met.

2.2.2 Isotopic ratios

Differences in natural Isotope ratios (most commonly ^{13}C and ^{2}H) can contribute to bias within qNMR assay. Natural isotopic ratios are well known molecular markers for qualitative and quantitative analyses. The amount and natural ratio variations of ^{13}C and ^{2}H are different for every signal within an analyte, which has shown to come into particular importance with food authenticity and quality of products [65-68]. More specific to quantitative analyses, the ability to extend integration regions to include the ^{13}C satellites is seldom possible in all but the simplest of systems; the more complex the spectrum the more the analyst is prone to processing errors by having to ensure flatter baseline for larger integration areas. One way to overcome the issue of ^{13}C satellites over complicating spectra further is by running a GARB de-coupled experiment, which cancels out the coupling seen by the ^{1}H-^{13}C interaction. However, this has an effect on the intensity of the ^{1}H-^{12}C peak so can cause an over-estimation in the intensity of the ^{1}H-^{12}C peak. Although this wasn't addressed in this thesis as it adds very little contribution to the uncertainty, it is a factor which can add to experimental bias and should be considered.

2.2.3 Chemical shift

Chemical shift holds important information of chemical structure and is used for the assignment of molecules. The chemical shift range observed in the final spectrum extends from -1/2SW to +1/2SW (where SW is the spectral width set by the user) about the offset (in ppm). Whilst the offset (O1P) defines the centre of the spectrum the range it covers is set by the SW. The impact of chemical shift offset is very important to quantitative measurements as it has an impact on the signal intensity output. Figure 2.2 shows the excitation profile of the RF pulse, as it can be seen that the closer to the middle of the spectrum the signal is the higher the intensity of the signal. Therefore, an incorrect O1P value or chemical shift offset will cause considerable bias to the intensity of the signal. It is also important that the pulses used in the experiment have a reasonably flat excitation profile for the area of interest; this can be problematic if there is a wide distribution of chemical shifts in the spectrum. The application of digital filtering to the

NMR signal is a source of non-linearity across the NMR spectrum. It is known that accurate quantification should not be attempted at the extreme limits of the spectrum.

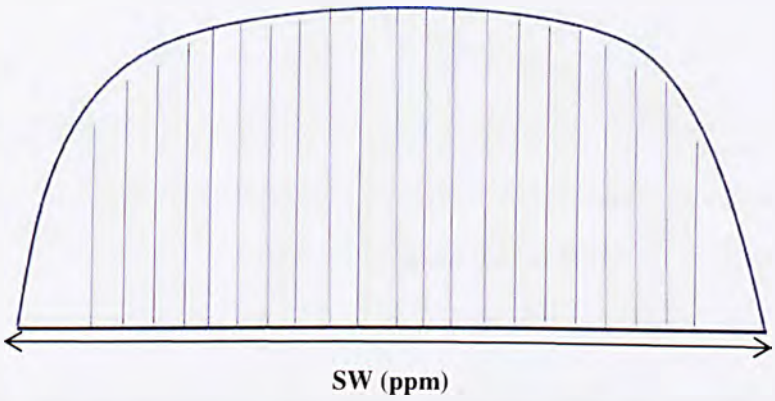

Figure 2.2 – Excitation profile for a shaped pulse, where the flat region is expected to give the highest intensity

2.2.3.1 Material and Methods

A sample of dimethyl terephthalate (DMT (**5**)) in $CDCl_3$ was used to calculate the ratio of the two signals with varying offset (O1P) (-2.0 to 13.0 ppm). The offset was varied in 1 ppm increments with a spectral width of 20 ppm; this enabled the two signals from DMT to move across the spectral window as shown in Figure 2.3. qNMR experiments were run in triplicate in a randomised order for each observation.

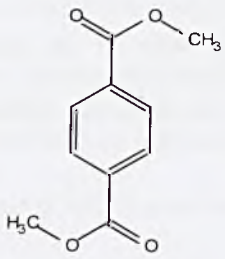

(**5**)

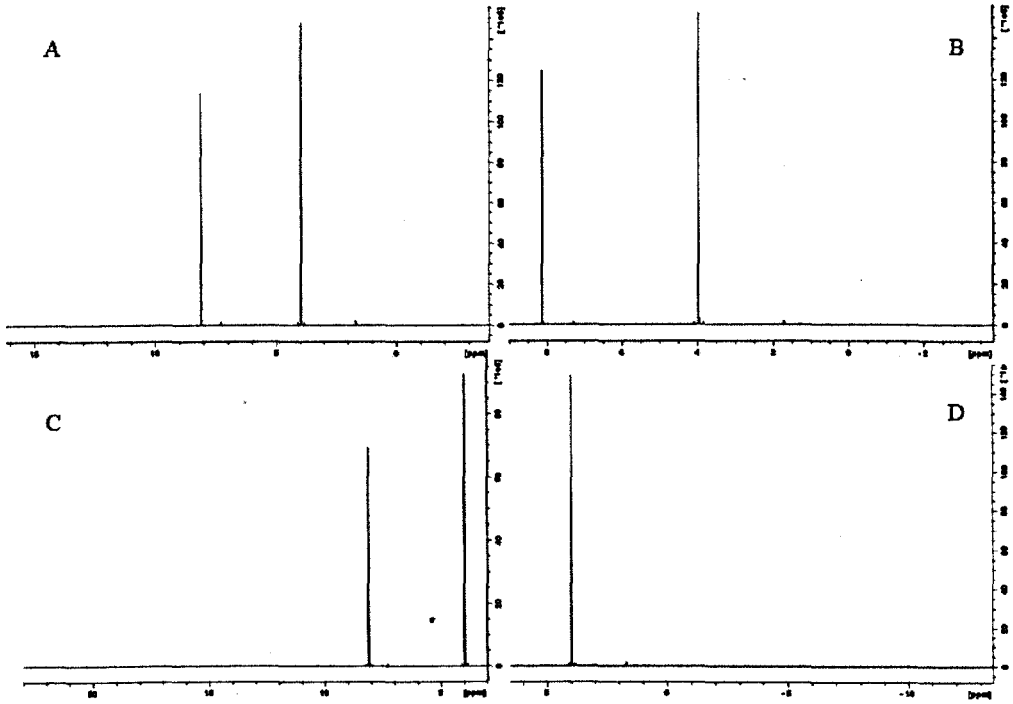

Figure 2.3 – ^{1}H spectra of DMT showing how the peaks move across the spectral window with varying O1P; ran using D1: 30, NS: 16, fixed RGA:

A: O1P: 6.175 (default), B: O1P: -1 , C: O1P: 13, D: O1P: -3.5, all acquired on a 600 MHz Bruker instrument using DMSO-d_6

2.2.3.2 Results

Figure 2.4 below shows that the ratio of the two peaks in DMT, both peaks were integrated at the varying offsets and the relative ratio of the peaks plotted against the O1P below. As predicted the O1P's close to the edge of the spectrum give a lower signal intensity or overestimated signal intensity due to the peaks shifting to the non-flat excitation region during the pulse sequence.

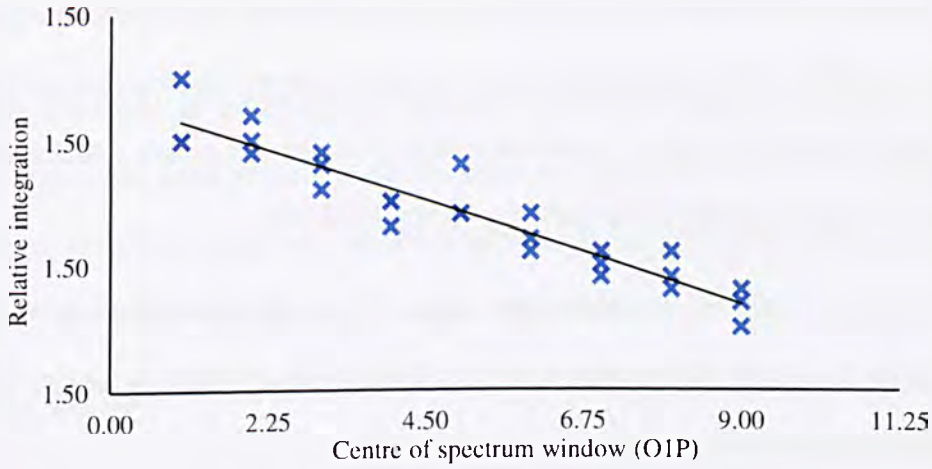

Figure 2.4 – Graph showing change in integration as O1P varies

The results are shown graphically above and show that there is a small but statistically significant bias across the spectrum and calculated at 0.018 % per ppm. It is therefore recommended to use signals close to the centre of the spectrum and peaks with small O1P variation between them for quantification removing bias from the analysis, however this uncertainty is covered within the experimental repeatability error therefore in non-optimal conditions peaks close to the edge of the spectrum may be considered.

2.3 Sample Preparation

Sample preparation for qNMR measurements is one of the techniques most useful advantages, in that it is simple, fast and inexpensive. However, one of the largest sources of error for qNMR measurements comes from incorrect sample preparation, therefore if not done correctly measurements are prone to inaccuracies. Factors such as concentration of sample, sample tube specifications and filling height are some of which were investigated.

2.3.1 Effects of NMR tube inhomogeneity and volume variation

Tube inhomogeneity and the filling volume variation can impact on the quality and reproducibility of NMR spectra. Deviations in internal volume of the NMR tubes will result in a variation in the 'fill factor' and thus directly impact on the absolute intensity of the resultant NMR signal. This latter factor is critical to any externally standardised NMR experiment and

the following experiments have been designed to assess the impact of both the volume of solution added to a tube and the inter- tube variation in internal volume. Sensitivity loss due to RF power dissipation in tubes is also affected by its shape and sample availability. Therefore smaller or a more cylindrical tube can be more beneficial [69].

The excitation and signal detection of the sample is from RF coils situated in the NMR probe toward the base of the NMR tube (Figure 2.5). Traditionally, NMR tubes are filled with enough sample to fill the active volume.

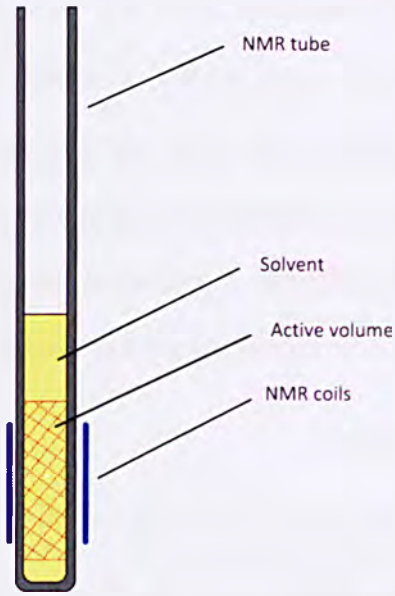

Figure 2.5 - Schematic of NMR tube and active region of coil

Commercially available NMR tubes come in wide range of specifications from cheap disposal tubes at one extreme to precision engineered ones at the other. The tubes are typically specified by the following criteria; internal and external diameters, concentricity and camber. The task of an NMR tube is to hold the liquid sample in the shape of a 'perfect cylinder'. There are three main factors which contribute to having a 'perfect' NMR tube.

1. *Outside Diameter (OD) and Inside Diameter (ID)*

The internal diameter of the NMR tube will directly affect the volume of sample within the active volume of the NMR probe and will thus affect the signal intensity. If the OD is too small the tube may shift in the probe or completely fall through the probe, if the OD is too large the tube may come in contact with the probe causing damage to the probe itself.

2. *Concentricity*

A measure of the lack of wall uniformity, this can be thought of as how perfect the internal cylindrical volume is and how centralised in the outer volume of glass.

Poor concentricity causes a portion of the sample to lie outside the 'perfect cylinder' region, leading to difficulties in shimming. Concentricity is zero for a 'perfect' tube, but tubes which conform to concentricity tolerances between 0.15 mm and 0.013 mm will provide reliable spectral resolution.

Figure 2.6 – Schematic to show lack of wall uniformity in an NMR tube

3. *Camber*

Camber measures the lack of straightness of a tube. Extremely poor camber can lead to probe damage. Tubes with camber deviations below 0.053 mm will give good enough quality spectra.

Poor tube concentricity and camber causes poor spectra quality by reducing the homogeneity of the sample. Stronger magnetic fields require stricter tolerances for tubes, as they enhance the distortions in NMR tubes. These factors affect externally standardised qNMR measurements more where two tubes are required for the sample and standard.

A set of experiments were run to determine the optimal sample volume for an NMR tube and derive the uncertainty associated with tube to tube variation for use in principally externally

standardised NMR assays. Once the tube to tube variation has been determined a correction factor can be applied to calibrate each tube against each other, if the correction factor is deemed significant.

2.3.1.1 Materials and Methods

After a review of the specifications of commercially available NMR tubes, the Wilmad 535-pp8 tubes (Sigma Aldrich P/N: Z274550-1PAK) were chosen as the most suitable tube and 15 tubes from the same batch were obtained. A stock solution of 4.1 mg/mL Dioxane (**6**) in $CDCl_3$ was used for the sample height experiments and analysed by ^1H NMR under standard qNMR parameters with a fixed receiver gain and five replicate analyses.

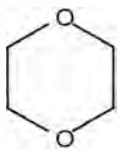

(6)

For the impact of sample height (volume variation), three different filling heights were investigated; 4 cm, 5 cm and 6 cm (measured from the glass bottom of the NMR tube to the meniscus of the sample solution). An additional experiment was run where the tube was filled to 6 cm and then was further displaced by about 3mm in the depth gauge to elevate the sample volume by that amount in relation to the NMR coils, mimicking situations where the auto sampler robot can displace the tube height when returning the sample back to the auto sampler.

For the tube to tube variation experiments using the Wilmad NMR tubes a stock solution of DMT (Figure (**5**) on page 36) in Toluene-d_8 was prepared.

For the tube to tube variation a fixed sample height of 5cm was chosen, which equated to a volume of stock solution of DMT of approximately 680 µL being pipetted into each NMR tube. The same stock solution was used for each of the 5 tubes. The experiment was run over two days, with different run orders.

2.3.1.2 Results for sample height variation

Figure 2.7 shows the mean absolute integrals for the series of experiments run at different fill volumes for Dioxane. It appears that the 6cm filled tube volumes gave the highest signal intensity, whereas the 4cm gave the lowest signal intensity, Figure 2.8 shows that the % RSD is 0.03 % at 5cm compared to 0.15 % at 4cm and 0.05 % at 6cm. This indicates that the optimal filling volume should be at least 5cm or above.

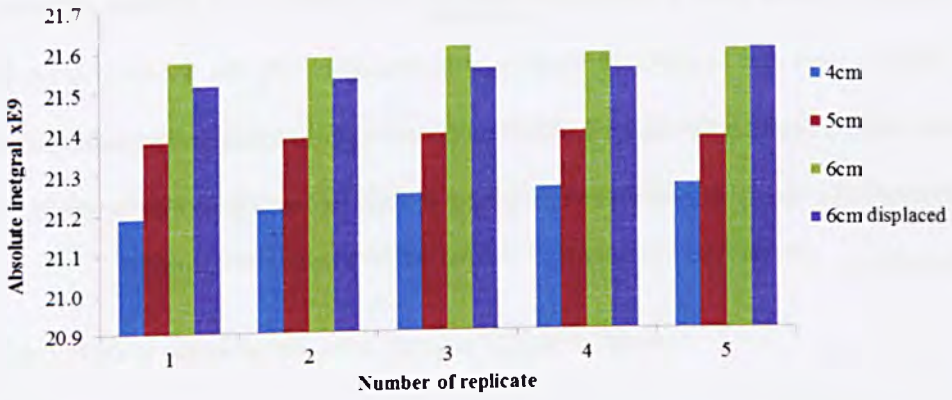

Figure 2.7 – Effect of fill volume on the signal intensity for Dioxane

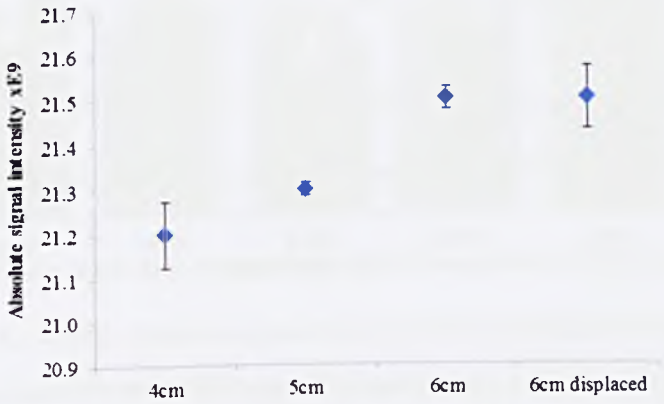

Figure 2.8 – Absolute intensity of signal at different fill levels with associated standard deviations at each filling level

2.3.1.3 Results and Discussion for tube to tube variation

Figures 2.9 and 2.10 show the absolute integrals for 5 NMR tubes run on two different days. On Day 1 the % RSD between tubes ranges from 0.44-0.72 %, whilst on Day 2 the % RSD ranges from 0.27-1.20 %. On Day 2 there is a rogue data point seen for tube two, replicate one. If this point is taken as an anomaly and ignored the % RSD ranges from 0.27-0.73 % on the second day.

From these graphs there is no obvious trend in the sequence, the absolute intensity is different on the two days due to different receiver gain settings set by the automation on ICON. Single factor ANOVA analysis showed there to be no significant bias between the tubes on the different days, see Appendix A. The graph plotted according to run order can be found in Appendix B.

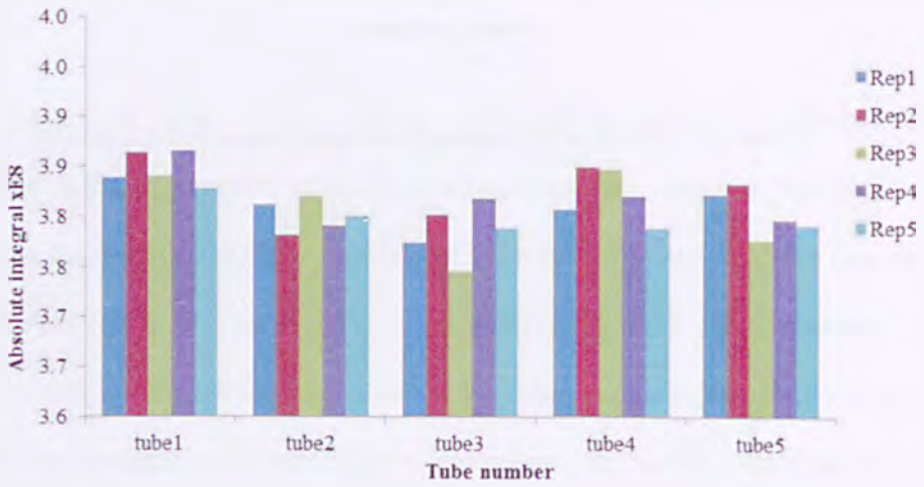

Figure 2.9 - Intensity variation coming from different NMR tubes (Wilmad tubes) for one sample, Day 1 (RG: 32, NS: 4, D1: 60 sec all acquired on a 600 MHz Bruker Instrument using $CDCl_3$)

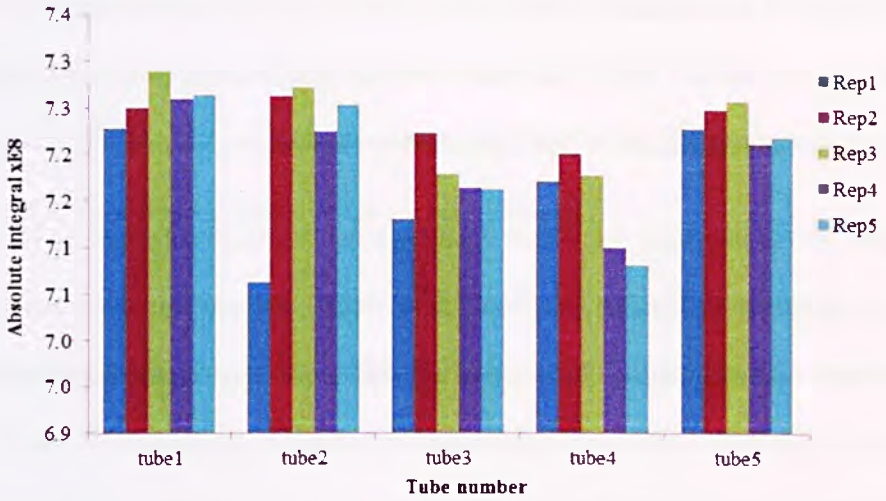

Figure 2.10 – Intensity variation coming from different NMR tubes (Wilmad tubes), Day 2 (RG: 64, NS: 4, D1: 60 sec, all acquired on a 600 MHz Bruker Instrument using $CDCl_3$) *Axis have different integral scaling due to different RG in acquisition parameters

2.3.1.4 Uncertainty associated with sample filling volumes

The experiments indicate that the active NMR region of the coil extends beyond the expected volume even at solvent heights of 6 cm, this is a variable that needs to be accurately reproduced to minimise the uncertainty associated with the NMR measurement.

The standard deviation of the absolute NMR integral without control of NMR sample height, construed from the five replicate tubes analysed was calculated as 0.68 %.

The accuracy in the determination of sample height is estimated to be ± 0.1cm. This equates to a range of 0.20 % for a 5cm filled tube assuming a rectangular distribution using Equation 2.1 below.

$$u(x) = \frac{stdev}{\sqrt{3}}$$

Equation 2.1

Table 2.2 shows the expanded uncertainties attributable for the different fill volumes. The expanded uncertainty at a 95 % confidence limit using a coverage factor of 2 is 0.06 % when filled to 5cm with a maximum of 0.30 % when filled to 4cm.

The larger uncertainty seen for a 4cm depth and the displaced tube can be explained as the volume in which the uncertainty exists will be in a more sensitive part of the active volume than in the other two experiments. The cause of any difference between the uncertainties at 5 and 6 cm depth is most likely within the experimental error for the instrument.

	4 cm	5 cm	6 cm	6 cm displaced
% RSD	0.15	0.03	0.05	0.14
Expanded U	0.30	0.06	0.11	0.28

Table 2.2 – Uncertainties arising from different fill heights

2.3.2 Balance uncertainty

The specification and precision of the balance used plays a significant role in the overall uncertainty measurement of qNMR data. A five figure balance will add a considerable level of inaccuracy to measurement compared to a six figure balance, therefore in all instances a six figure balance will be used for quantitative work.

2.4 Acquisition parameters

There are multiple acquisition parameters accessible for manipulation by the user. These have to be optimised for best practise; this includes pre-calibrating parameters and running initial experiments to determine their optimal operating range. The following parameters have been determined to influence qNMR measurements.

2.4.1 Pulse Calibration

The length of time the radiofrequency pulse is applied to a sample is called the pulse width, and is usually given in flip angles. For an optimum spectrum a 90° flip (pulse) angle is used which corresponds to the length of a pulse giving the maximum response from a given NMR-active

nucleus. To reduce errors associated with the pulse length, its calibration is imperative and can be done manually using most software's, for example the Bruker 'POPT' command. To be able to directly compare the integral from the analyte peak with that of the reference standard peak, the magnetisation of NMR signals must be in equilibrium.

Figure 2.11 shows the sample being 'flipped' 90 degrees so the nuclear spin is changed from the z axis (spin at equilibrium) to the x-y plane. This 90° pulse angle typically corresponds to a 7-13 μs pulse width. In some cases, alternate pulses such as a 30° pulse angle can be applied instead of the optimal 90° to minimise relaxation time and allow for faster pulsing; however this results in a decrease in absolute signal from the sample.

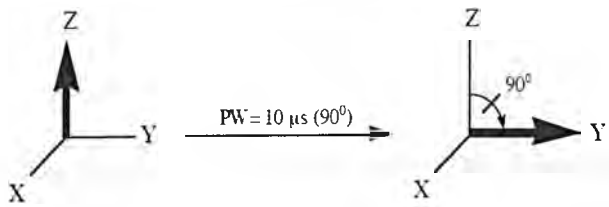

Figure 2.11 – Magnetisation being 'flipped' 90°

The 90° pulse is set as a combination of the pulse length and power level. Different samples will have a different length of 90° pulse angle, therefore it is essential to determine this experimentally beforehand.

The length of the 90° pulse is dependant of 4 major factors:

- The probe – depends on the configuration, quality and condition of probe.
- The power of the pulse – the higher the power the shorter the pulse will be.
- The tuning – if the tuning is poor the 90° will be longer due to power losses.
- The solvent – Changes in the dielectric constant arising from changing solvents and varying salt levels will impact significantly on the tuning.

To accurately determine the 90° pulse angle, a sequence of experiments was recorded with incrementing pulse angles to enable one of the signal maxima or null points to be determined as

shown in Figure 2.12. Null points are used preferentially for pulse determination as they are easier to determine accurately. The 360° pulse angle is then divided by 4 (or 2 if a 180° pulse angle is used) to give the 90° pulse.

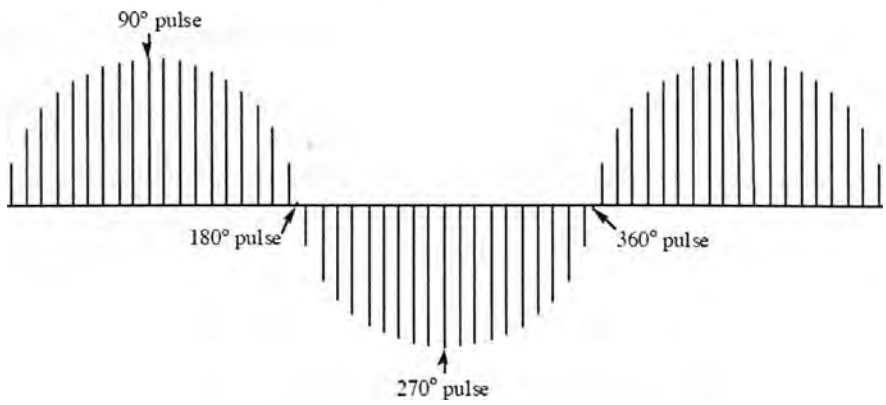

Figure 2.12 – Spectrum of a POPT experiment showing 360 null point and how the 90° pulse is calculated

The aim of these experiments is to investigate the accuracy of the instrument in delivering its 90° pulse and to calculate the uncertainty associated with it.

2.4.1.1 Material and Methods

Initially a pulse angle of 30° was compared to a pulse angle of 90° to determine the impact on the signal response. After which a series of experiments were run to experimentally determine the 90° pulse using an Ethyl Benzene (**7**) sample in deuterated chloroform spiked with 0.1% dioxane. An accurate 90° pulse angle was determined manually using the command 'POPT' and a calibration was performed on a single peak from the sample. From this the pulse width was determined as 7.1 μs at 90° at a constant power level of -12.20 -dBW. Subsequently a variable pulse list was generated so the experiments could be conducted under automation, which incremented the pulse width non linearly from 6.5 – 7.5 μs. Nine spectra were collected each at the different pulse angles (85-95°) in replicates of 5.

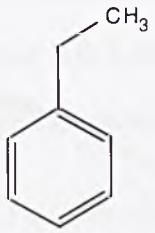

(7)

2.4.1.2 Results & Discussion

Experiments comparing the 30° and 90° pulse angles were run using the ethyl benzene solution. From Figure 2.13 it can be seen that the 90° pulse does give much higher signal intensity when compared to the 30° pulse angle as expected and therefore recommended to use a 90° pulse angle for all quantitative work.

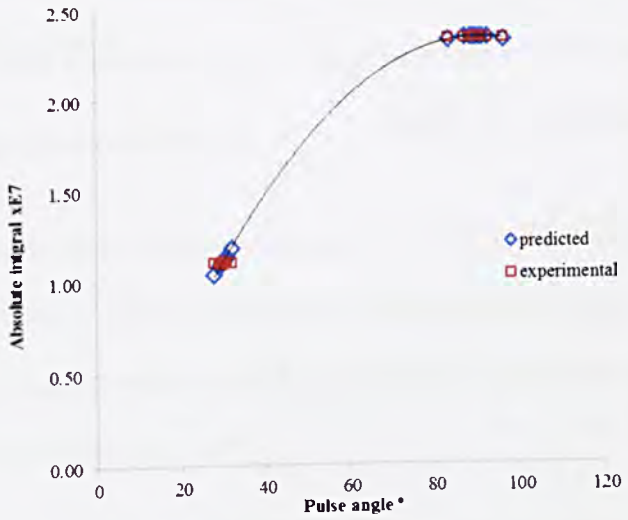

Figure 2.13 – Signal intensities at a 30° pulse angle compared to a 90° pulse angle of ethyl benzene solution acquired on a 600 MHz Bruker instrument using $CDCl_3$ NS: 1, D1: 60 sec

Figure 2.14 shows the observed absolute integrals for the series of nine incremented pulse widths investigated (pink) compared to the theoretical signal intensity (in black). As it can be seen from Figure 2.14 the observed signal plot shows a similar trend to the theoretical signal plot as expected.

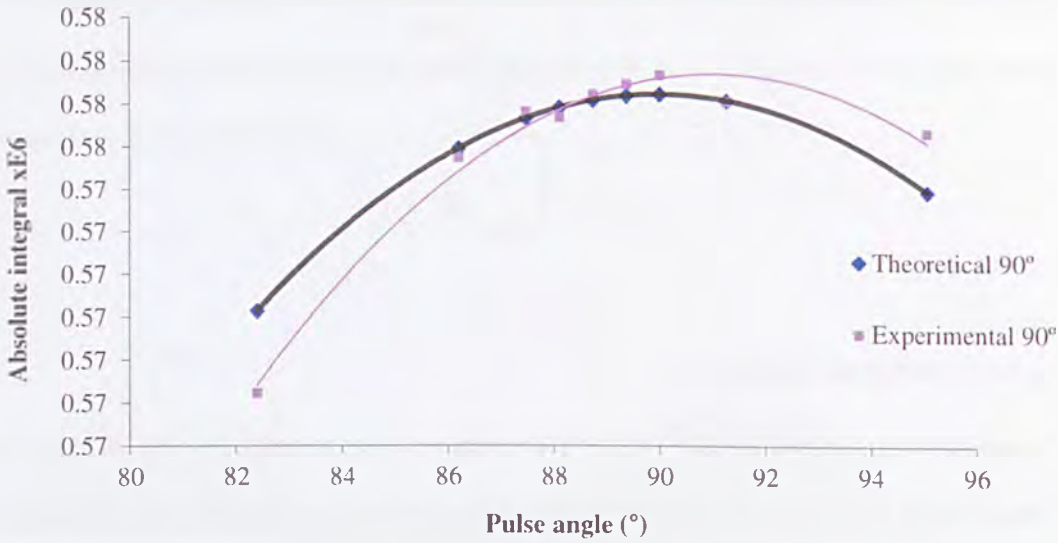

Figure 2.14 - Theoretical vs experimental signal intensity at different pulse angles

2.4.1.3 Uncertainties associated with pulse generation

Figure 2.15 shows the % RSD at each pulse width determined from the average of the five replicates at the different pulse angles.

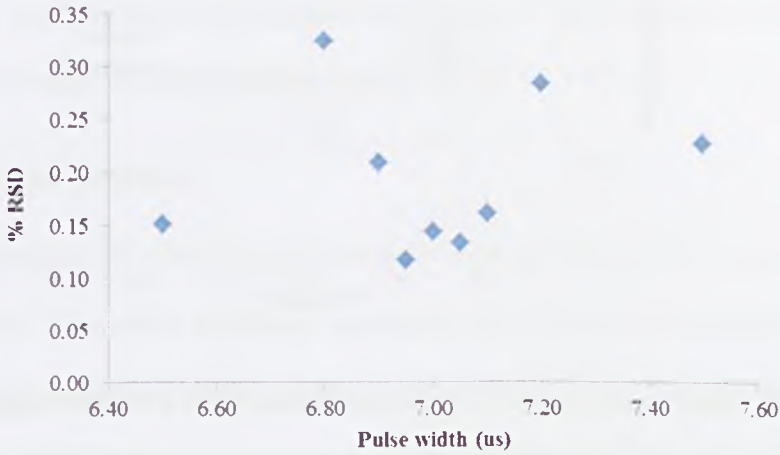

Figure 2.15 – % RSD from the use of different pulse widths and how they impact integral intensity. Pulse width around 7 us gives the most consistent and lowest % RSD

The average % RSD from the precision data was 0.19 % which incorporates the maximum error associated with tuning of the sample and position effects. The maximum error associated with calibrating the 90° pulse is 0.06 % and is calculated in the following way.

An uncertainty of ± 0.2 μs is assumed with determining the 360° null point via the POPT experiments, since pulse angle determination is to 1 decimal place (a 0.1 μs error is too small to assume), this translates to an error of ± 0.05 μs with the 90° pulse determination.

The typical 90° pulse on this system is 7.1 μs, therefore the uncertainty associated to this is 7.1 ± 0.05μs. By tuning the spectrometer on insertion of each new sample, the pulse angle delivered by the spectrometer should be consistent. This is typically done under automation by the ATMA function. The effectiveness of this routine is monitored by the reproducibility of the 90° pulse. All calibrations of the 90° pulse on this system at this power level have fallen in the range 7.00-7.25 μs. From this, the uncertainty of the 90° pulse in a tuned system without pulse calibration is taken to be ± 0.25 μs, this equates to a ± 3.5 % error in the 90° pulse angle and an associated error in signal intensity of ± 0.11 %. Assuming a rectangular distribution, the standard uncertainty is $0.11/\sqrt{3} = 0.06$ %.

2.4.2 Receiver Tuning and Calibration

Tuning and matching is often performed on every individual experiment. Its function is to ensure accurate execution of pulse angles in the NMR experiment, which minimise losses on signals of the required magnetisation and reduces unwanted signals and artefacts that the pulse programs are designed to filter out.

Complex pulse programs require the delivery of accurate pulse angles to select or filter out different phases of magnetisation and allow coherence transfer between nuclei. The tuning of an NMR probe involves varying the capacitance of the tuning and matching capacitors in the NMR probe. The tuning capacitor allows tuning of the circuit to match the Larmor frequency of the NMR experiment whilst the matching capacitor changes the efficiency of the band pass filter (to match its response against a built in 50 ohm (Ω) reference load) [70].

Any imperfections in the tuning and matching of the probe would manifest themselves in a lengthening of the experimentally determined 90° pulse. Mismatch conditions lead to longer 90 pulses, loss of signal and inefficient Broad Band decoupling, leading to increased residual line

broadening. The work below has shown that imperfections in the tuning can be identified via the experimentally determined 90° pulse and compensated for in the receiver circuit by applying a suitable correction factor. By investigating the effects of non-optimally tuned instruments, a suitable compensation factor could be determined and the impact on the uncertainly budget, which would be most relevant to externally standardised quantitative experiments.

2.4.2.1 Materials and Methods

Using the same sample of ethyl benzene spiked with dioxane, the instrument tuning was deliberately offset using the ATMM function over a range of frequencies and then the 90° pulse experimentally determined using the Bruker command 'Popt' at that offset frequency. A quantitative ^{1}H NMR experiment was then recorded and the absolute integration of the peak at 3.73 ppm (see Figure 2.16) in the spectrum was calculated.

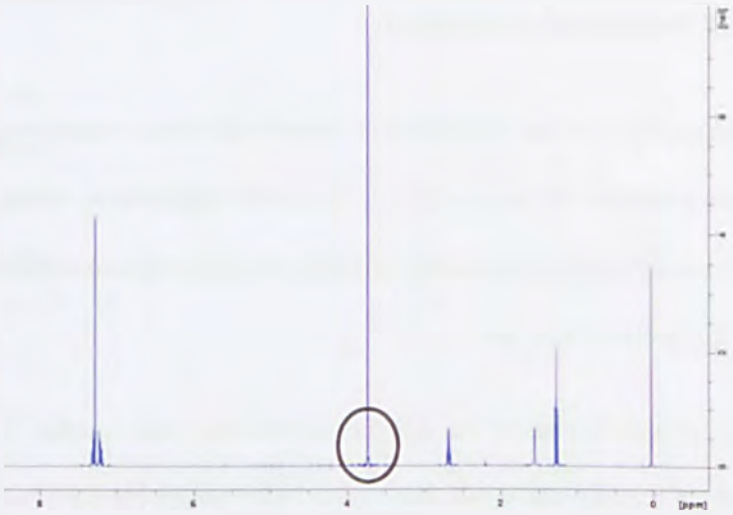

Figure 2.16 – Spectrum showing dioxane peak (circled) chosen for investigating effect of detuning of probe on signal intensity, acquired on a 600 MHZ Bruker instrument in $CDCl_3$ NS: , D1: 60 sec

2.4.2.2 Results and Discussion

Table 2.3 and Figure 2.17 show the results from the ethyl benzene (7) sample where the instrument was detuned over a range of frequencies and then the corresponding 90° pulse experimentally determined. It can be seen that a detuned instrument at 602.01 MHz

corresponding to a pulse width of 13 μs gives the lowest signal intensity as expected. The highest signal observed comes from a pulse width of 9.38 μs at a frequency of 596.56 MHz. Even at a detuned pulse width of 11 μs gave a higher signal intensity than that of the optimal 7.13 μs.

Frequency (MHz)	Pulse width (μs)	Absolute integral
600.13	7.13	212442130.16
600.22	7.38	218377268.08
600.41	8.38	234401931.36
596.56	9.38	237724357.20
596.65	9.50	235267066.22
596.96	10.00	229860876.08
597.16	11.00	222944319.63
602.37	13.00	85660826.08
602.01	13.00	64817403.15

Table 2.3 – Integral intensity at frequency offset at day 1

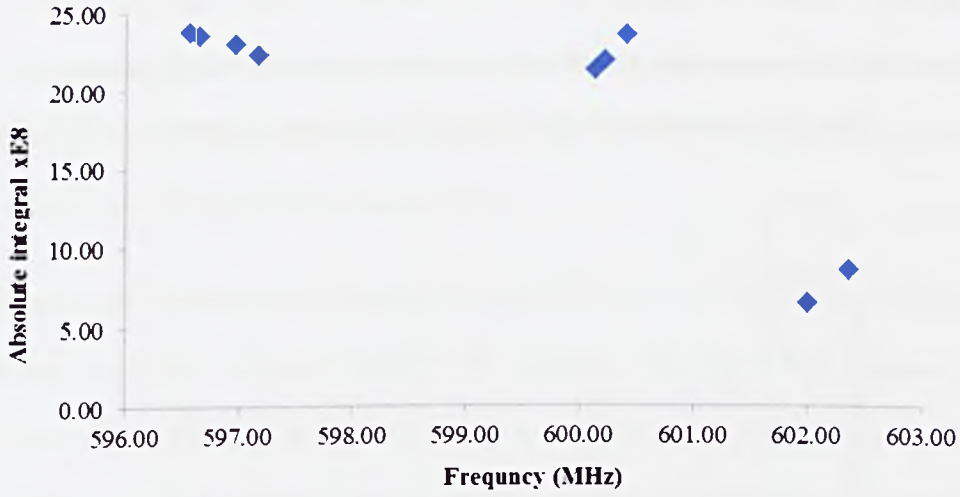

Figure 2.17 – Dioxane signal integral variation when running experiments at offset frequency, acquired on a 600 MHZ Bruker instrument using $CDCl_3$ NS: 1 D1: 60 sec

The assumption before these experiments were run was that a detuned instrument would lead to a longer 90° pulse and would result in a lower absolute integral due to the signal loss in the mistuned receiver circuit. The data clearly shows that the efficiency in the receiver circuitry does not match that in the transmitter circuitry and that even at a longer pulse width (above the

optimal 7.125 μs) maximum signal is still being achieved. The experiments were repeated again to confirm the effects seen. Figure 2.18 shows the same experiment ran on a different date, however a smaller number of data points over the frequency range was used. An additional experiment using a sample of TSP in $DMSO_{d6}$ was also run to see if the effects were seen in another solvent too (Figure 2.19).

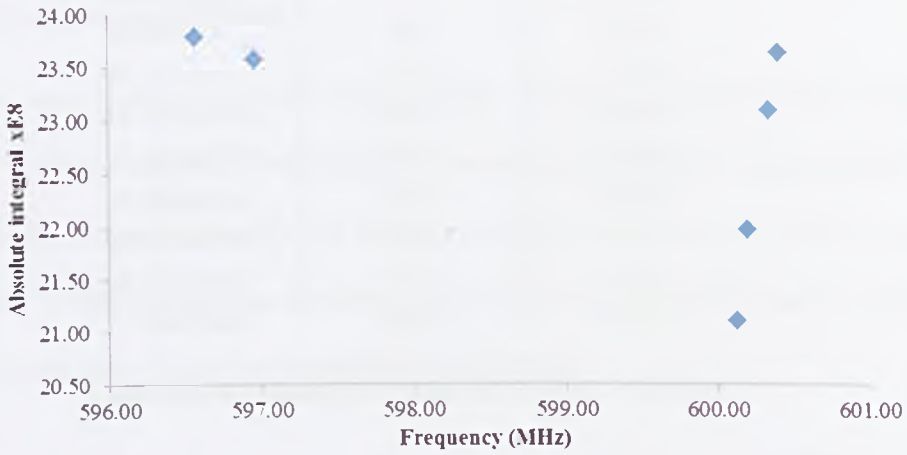

Figure 2.18 – Dioxane integral variation when running experiments at offset frequency; day 2, less data points acquired over the frequency range (same parameters as Fig 2.17)

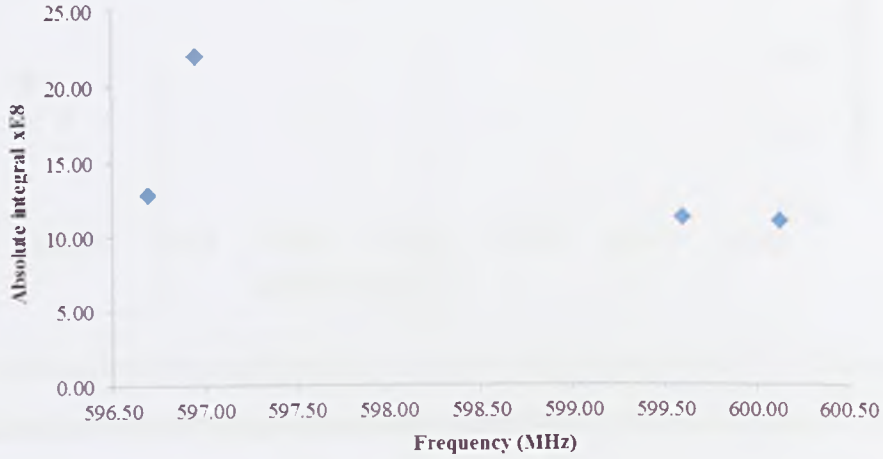

Figure 2.19 – Effect of offset in a different sample and solvent: TSP in DMSO-d_6. Acquired on a 600 MHZ Bruker instrument NS:1 D1:60 sec. Both showing running at an offset frequency can still yield maximum signal intensity

The data shows that the maximum tuning efficiency for the pulse transmission does not coincide with maximum efficiency in the receiver circuit. The NMR experiment set-up can maximise

efficiency for the transmitter circuit and recalibrate the pulse if required but no such tuning or compensation routines are available for the receiver. The data shown suggests that for these particular systems, a compensation factor for the receiver tuning could be made based on the experimentally determined P1 values but the general applicability of these graphs across other solvents and analytes would need to be investigated further. Without extensive additional work to map the interrelationship between the tuning and receiver circuits, the pragmatic solution is to run a Quality Control to ensure that the experimentally determined 90° pulse falls within a tight range and so removed the need to apply a correction factor.

2.4.3 Receiver Gain efficiency

The receiver gain (RG) is a parameter that corresponds to the amplification applied to the radiofrequency signal. This RG setting has to be optimised to the strength of the analytical solution to maximise the signal to noise ratio [71]. For solutions of a weak concentration the RG has to be set higher to increase amplification, and for a concentrated solution the RG has to be set to a low value to prevent overload of the receiver. Improper use of the RG can contribute to a significant error of the qNMR measurement.

The analogue radiofrequency signal detected by the RF coils in the NMR probe is digitised via an analogue to digital converter (ADC). The receiver gain (RG) is a measure of the amplification of the analogue signal coming from the NMR probe; the higher the gain, the larger the amplification used. The receiver gain is normally adjusted automatically to allow the signal to fill the range of the receiver without being truncated. An optimal filling of the receiver will allow full use of the dynamic range and thus maximise the signal to noise.

The RG parameter isn't as significant when running internally standardised qNMR experiments, as the ADC amplification applied will be the same for the sample and reference peak. It only really becomes of importance when running externally standardised qNMR experiments. In externally standardised qNMR a series of additional factors are required in the assay calculation

(see equation 2.2) and an array of additional factors come into consider for the uncertainty budget.

$$P_{meas} = \left(\frac{I_{meas}}{I_{ref}}\right) x \left(\frac{N_{ref}}{N_{meas}}\right) x \left(\frac{M_{meas}}{M_{ref}}\right) x \left(\frac{m_{ref}}{m_{meas}}\right) x \left(\frac{R_{ref}}{R_{meas}}\right) x \left(\frac{v_{ref}}{v_{meas}}\right) x \left(\frac{T_{ref}}{T_{meas}}\right) x \left(\frac{V_{ref}}{V_{meas}}\right) x P_{ref}$$

Equation 2.2

The additional terms being

R_{ref} & R_{meas} the receiver gain compensation factors for the referand and measurand

T_{ref} & T_{meas} the receiving efficiency for the referand and measurand

v_{ref} & v_{meas} the active volumes for the referand and measurand

V_{ref} & V_{meas} the solvent volumes for the referand and measurand

The Bruker CORTAB function partially addresses the issue of the nonlinearity in the amplification, however the nonlinearity is still reported to be an issue by users. The aim of the following set of experiment is to determine correction factors and associated uncertainties, which need to be applied when running externally standardised qNMR experiments in the three following methods:

1. Using different RG values but not compensated for
2. Using different RG values but compensated for
3. Using the same RG values

2.4.3.1 Materials and Methods

Six solutions of dimethyl terephthalate in deuterated acetonitrile were prepared over a range of concentrations ranging from 0.2 mg/mL to 30 mg/mL (see Table 2.4) to allow testing over the range of receiver gains that would typically be employed for quantitative NMR work. Each

sample was analysed 5 times at receiver gains of 1, 2,4, 8, 16, 32, 64, 128 and 256 (the more concentrated samples could not be used at high receiver gains as this overloads the ADC rendering any quantitation invalid).

	Concentration (mg/mL)
DMT solution 1	31.87
DMT solution 2	1.67
DMT solution 3	0.52
DMT solution 4	6.69
DMT solution 5	1.73
DMT solution 6	0.26

Table 2.4 - Range of concentrations of DMT in CD_3CN analysed for varying RGA experiments, acquired on 600 MHZ Bruker instrument, NS:16

2.4.3.2 Results and Discussion

Figure 2.20 shows the normalised values for the nine RG values used for the different solutions.

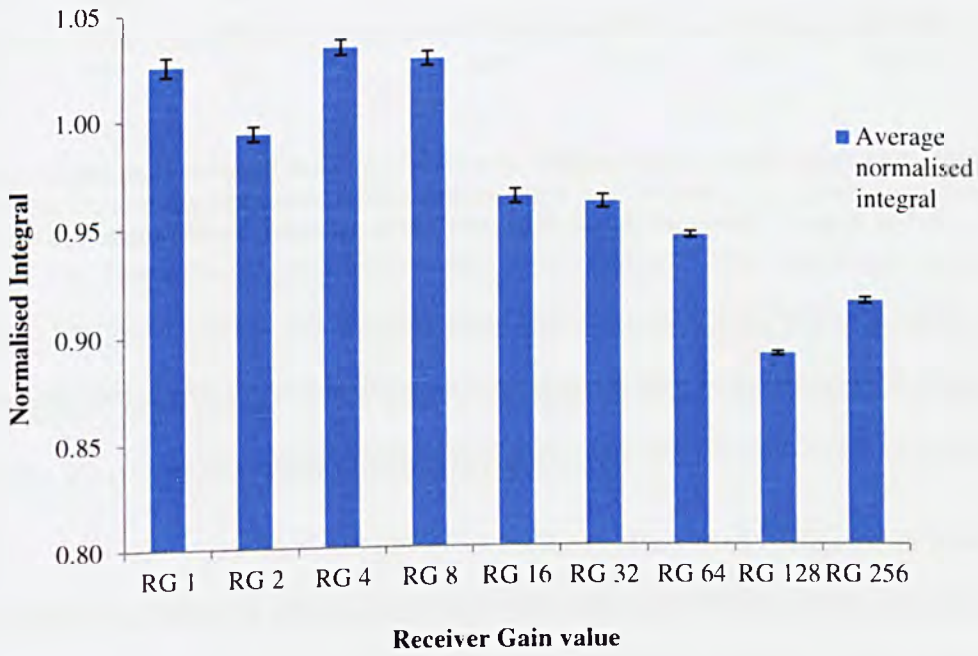

Figure 2.20 – Average Normalised values for 6 solutions of DMT using 9 different RGs, with 4 replicate analyses of each solution at a certain RG value (normalised against the average of 6 solutions. NS: 16 in CD3CN all acquired on a 600 MHz Bruker instrument)

Figure 2.20 shows as anticipated that the amplification is not linear and therefore one cannot compare data from one solution to another without incurring significant bias. Ideally the above graph should show all signal to be normalised at 1.00 of the relative integration but in fact shows that for RG's of 1, 4 and 8 you are consistently applying more than the set receiver gain. The data was obtained on three non-consecutive days but due to insufficient randomisation in the order of analysis, no between day effects have been determined.

	Full data			Excluding SS1		
	F	*P-value*	*F crit*	*F*	*P-value*	*F crit*
RG1	3.289	0.023	2.661	2.360	0.090	2.895
RG2	6.322	0.001	2.661	4.599	0.009	2.895
RG4	3.289	0.023	2.661	0.494	0.740	2.895
RG8	2.129	0.100	2.661	1.965	0.141	2.895
RG16	4.318	0.007	2.661	2.823	0.054	2.895
RG32	4.694	0.005	2.661	2.638	0.066	2.895
RG64	1.496	0.243	2.895	1.496	0.243	2.895
RG 128	0.335	0.579	5.318	0.335	0.579	5.318
RG 256	0.101	0.759	5.318	0.101	0.759	5.318

Table 2.5 - Single Factor Anova analysis of replicates for each Receiver Gain shows that above an RG of 32 the F crit value is larger than the F value indicating significant bias in the results

A correction factor for samples analysed under different RG values was derived from the mean of each RG normalisation with its associated standard deviations, which could be used for a set of specific NMR tubes for externally standardised NMR assays.

Three uncertainties have been extracted from the experiments, which need to be applied according to how the RG values are used. Table 2.6 shows the expanded uncertainties generated for the three methods of RG utilisation used for this experiment.

	RG uncorrected	RG corrected	same RG used
Relative std u	0.075	0.004	0.003
Expanded U	0.15	0.007	0.005

Table 2.6 – Uncertainties derived for the different methods of using RG to be applied to externally standardised qNMR

For example the relative uncertainty associated with using different RGs is calculated using Equation 2.3. The standard deviation of the average normalised integral values from the full range of RG was used, which was calculated as 0.053 %.

$$\sqrt{0.053^2 + 0.053^2} = 0.074\ \% \qquad \textbf{Equation 2.3}$$

This equates to an expanded uncertainty at the 95% confidence limit using a coverage factor of 2 as 0.15 %.

For the corrected RG uncertainty calculation, the 'worst case' standard deviation (RG1 = 0.0026) from the different RG values was used to derive a relative uncertainty. This gave a relative uncertainty associated with using different RGs of 0.004% (shown in equation 2.4).

$$\sqrt{0.0026^2 + 0.0026^2} = 0.0037\ \% \qquad \textbf{Equation 2.4}$$

This equates to an expanded uncertainty at 95% confidence limit using a coverage factor of 2 of 0.07%.

The relative uncertainty associated with using the same RG for externally standardised assays is based on the 'worst case' standard deviation (RG1=0.0026). This uncertainty contains a significant contribution from sample repeatability and should be regarded as a maximum value and is therefore taken directly as the relative standard uncertainty. Which gives an expanded uncertainty at the 95% confidence interval (k=2) of 0.005%.

The experiments conducted during this study have demonstrated the extent and consistent nonlinearity of the receiver gain function. The compensation factors for a series of receiver gains have been determined along with the associated uncertainties. The uncertainty generated by the use of two different receiver gains for the reference and measurand was found to be higher than that from the use of a single, non-optimal, fixed receiver gain.

2.4.4 Resolution of spectrum

The digital spectral resolution is dependent on the number of time domain data points (TD) acquired by the instrument. This property can be controlled by the user during data acquisition. The length of the experiment is directly proportional to the size of the TD used.

Equation for digital resolution:

$$\text{Digital resolution} = SW\ (Hz) / TD \qquad \textbf{Equation 2.5}$$

2.4.4.1 Materials and Methods & Results

Ten replicate analyses were carried out using a solution of benzoic acid (350b, NIST) and Maleic acid (Sigma Aldrich) to determine the impact of TD on spectral resolution. Four time domain data points were selected; 8K, 16K, 32K and 65K. Table 2.21 shows that with increasing TD, although experimental time increases, the % RSD of the 10 replicate analyses decreases. Therefore by default a TD of at least 32K should be used for all quantitative measurement to minimise uncertainty.

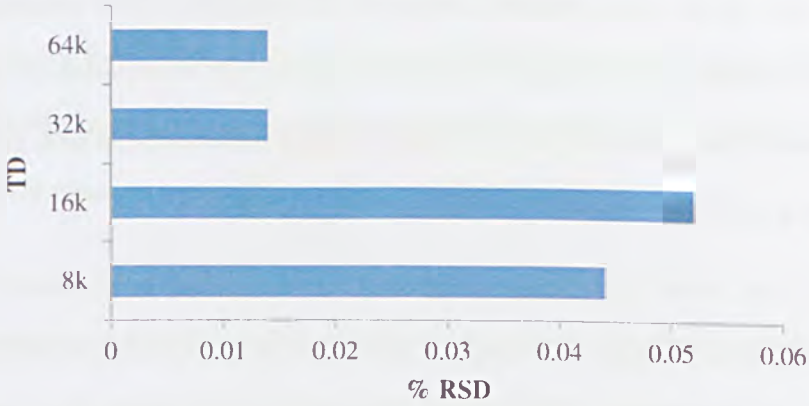

Figure 2.21 - % RSD from acquisition using different data points (TD) on a sample of Benzoic acid and Maleic acid in DMSO-d_6 acquired on a 600 MHZ Bruker instrument NS: 16

2.4.5 Assessment of Environmental Field Noise

The principle characteristics of the instrument's field are its magnetic induction value, its homogeneity across the sample and its stability. The stability of the magnetic field is, however, a combination of the magnet's inherent stability and the impact of the environment, in which it is placed. It is well known that older NMR instruments are very sensitive to building vibrations and electrical interferences, which can cause deleterious effects on the spectra. For quantitative work, this poses a problem as the artefacts around the base of the resonances may interfere with the accuracy and reproducibility of the NMR measurements.

The 600 MHz NMR facility at Kingston University sits on an anti-vibration system with dampening equipment integrated into the supporting legs which will minimize, although not completely eliminate, vibrational interference. This section investigates the sources of field noise effects arising in the vicinity of the NMR.

Analyses of historical spectra obtained on this instrument have shown apparently random occurrences of artefacts at fixed frequencies around the base of peaks.

Field noise effects in NMR spectroscopy can come from many sources including:

- Magnet system components - Shims lock system, field gradient *etc*
- Instrument console related - Power wiring, transformers, relays *etc*
- Environment - Electric wiring, transformers, motors, stabilizers
- Sample motion - Vibration or sample rotation
- Random vibrations caused by moving chairs, doors, tables, rooms adjacent to the magnet room, elevators *etc*.
- Periodic vibrations i.e. caused by machinery or air vibration caused by ventilation systems and fans.
- External vibrations i.e. cars, trains, aeroplanes, building sites nearby *etc*.

The main source of the observed artefacts is suspected to be the air compressor unit located within the laboratory, which starts and stops periodically through the day and produces a very discernible hum whilst operating. The unit is free-standing on rubber wheels, about 1.3 metres from the magnet. The periodic running of the air compressor unit could affect the field noise through either induction from the electric wiring or through vibration via the dampened legs (or a combination thereof).

2.4.5.1 Materials and Methods

A series of 10 replicate experiments were performed during times with the air compressor either exclusively on or exclusively off. The ethyl benzene/dioxane sample was used.

2.4.5.2 Results and Discussion

All the spectra obtained with the air compressor on showed artefact peaks at 46 Hz either side of the main peak (Figure 2.22) – these peaks were not observed in any of the spectra with the air compressor off (Figure 2.23). The integrations (Figure 2.24) from these peaks show the standard deviation of the integrals to be significantly higher for those obtained with the air compressor on (0.48% RSD compared to 0.09% RSD).

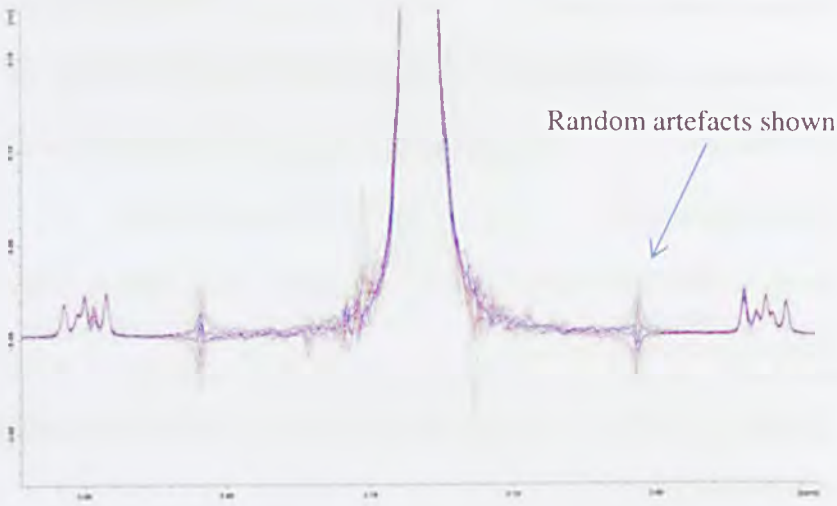

Figure 2.22 - Overlaid NMR spectra with air compressor unit on

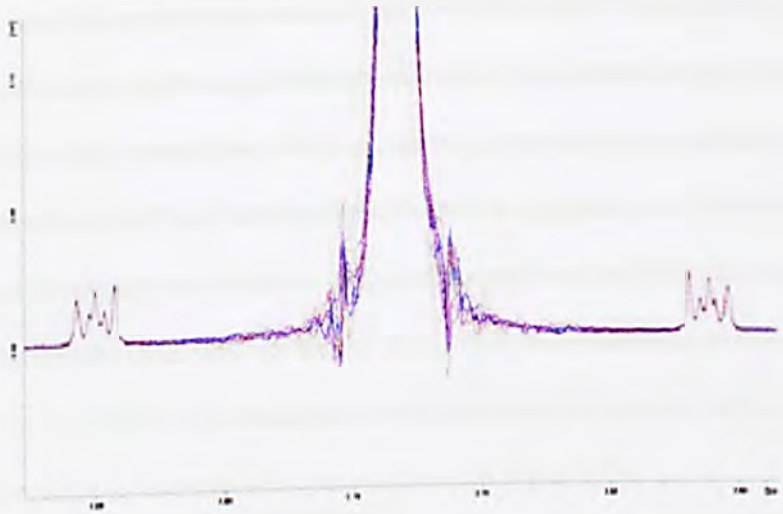

Figure 2.23 - Overlaid NMR spectra with air compressor unit off

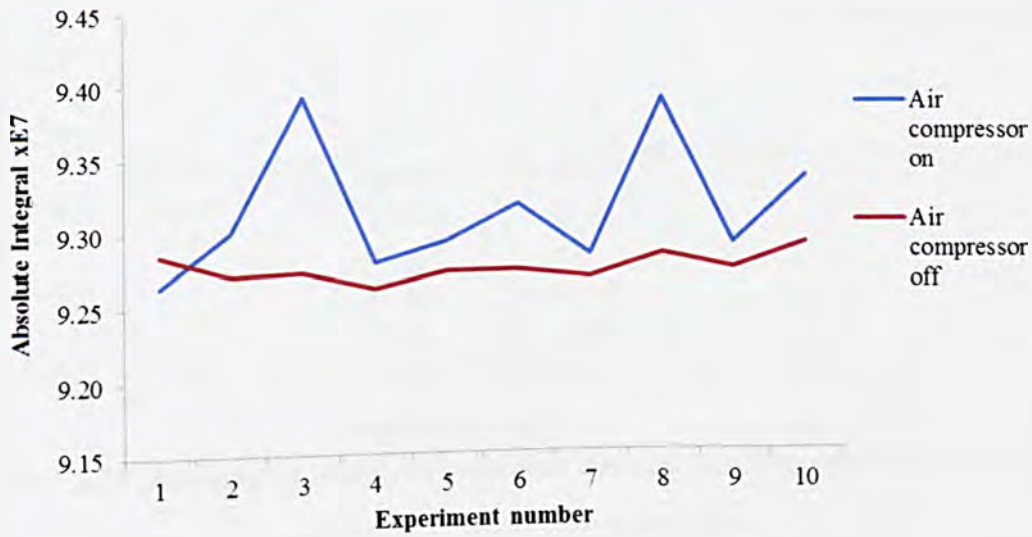

Figure 2.24 - Integration Values of replicate analyses which shows the variation of when the Air compressor is on to when it is off

To ensure full integration of the peak (>99.9%), an integration window of 76x the peak width is required. In this instance, with a peak width of approximately 1Hz, an integration window of approximately 150Hz is required which would extend into the ^{13}C satellites so would practically be reduced to just before these satellites (approximately 130Hz). The two artefacts at +/- 46Hz therefore fall within this band and, due to random phasing can distort the baseline and make the integration less reproducible.

Spectral deconvolution was investigated as an alternate processing tool to see if it gave a more robust quantification method when faced with the challenge of the artefacts and was carried out on the 10 experiments run with the air compressor unit on. Deconvolution of the spectra in this case involved the curve fitting of a theoretical lorentzian line. The standard deviation and % RSD is compared with the non-deconvoluted data to determine whether processing the data in this way would reduce the error. Table 2.7 shows the area derived from the deconvolution processing and the two standard deviations are compared.

Exp no.	Deconvolution area
10	127.35
11	130.93
12	135.30
13	134.94
14	136.28
15	135.50
16	135.47
17	136.06
18	135.51
19	135.86
Average:	134.32
Std dev:	2.88
RSD:	**2.15**

Table 2.7. Deconvolution areas derived for when air compressor is on

The de-convoluted data gave a % RSD of 2.15 %, whilst the non de-convoluted % RSD was 0.48 %, In this case, deconvolution of the peak did not improve the % RSD of the data set and so this approach was discontinued.

The experiments conducted during this study have demonstrated that the air compressor unit is giving rise to the principal periodic field noise seen in ^{1}H experiments on this 600MHz instrument. Whilst theoretically it could be due to electrical inductance or vibration, the latter is thought more likely. Initial work is underway to confirm the exact nature of the interference to minimize its effect. An anti-vibration system with radiation dampening equipment is already in place and further embellishment of this system is not seen as a cost effective solution. Changes

to the unit's positioning and dampening of the vibration effects caused by it will be made subsequent to this investigation and its impact will be monitored. The uncertainty associated with longer acquisition experiments that last for multiple air compressor cycles will be covered by repeatability determination therefore there is no need to add an additional uncertainty to measurements. The change in position of the air compressor unit and also the change in the direction of the blades from the air conditioning vents significantly saw a reduction in the artefacts seen in ^{1}H qNMR experiments and subsequent analyses gave % RSD's less than 0.2 % which was acceptable for repeatability data as shown in Figure 2.25.

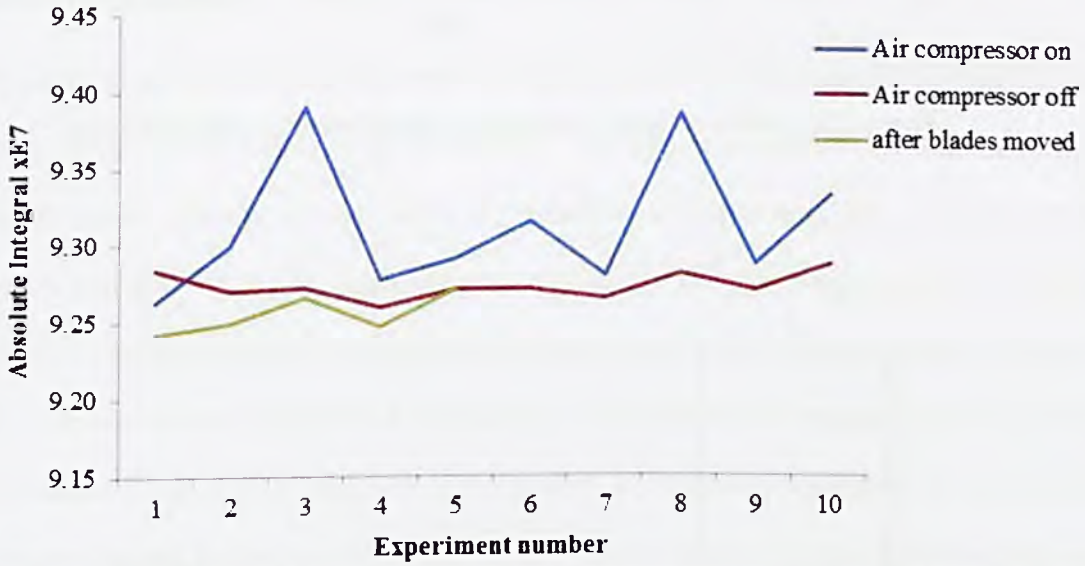

Figure 2.25 – Additional data after blades from air compressor unit was moved, showing five replicates with an RSD of less than 0.2 %

2.4.6 Signal to noise

Two solutions of DMT in different concentrations were used to assess the impact of signal to noise on the intensity of signal. On the basis that at the 90° pulse the signal intensity is at its highest, the variable changed in these experiments was the pulse width and the consequent intensity observed. The pulse angle was varied to the sample from 7μs to 0.05μs and also through dilution of the sample with additional $CDCl_3$. Signal to noise (S/N) was calculated through the Bruker Topspin feature found in the software.

The ratio of the two signals in a sample of DMT in $CDCl_3$ solution was monitored over a wide range of signal to noise. Figure 2.26 plots the ratio of the two signals over the various S/N achieved. Each measurement was carried out five times.

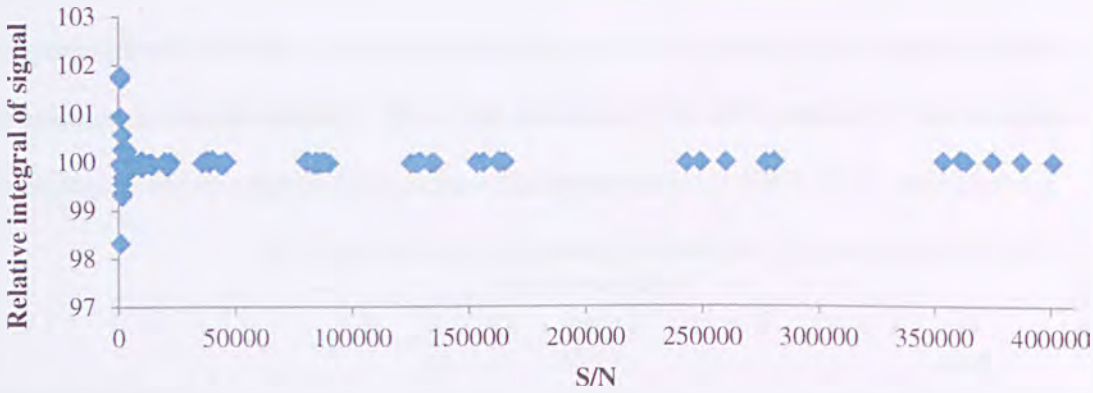

Figure 2.26 – Effect of signal to noise on the signal intensity of the DMT peak

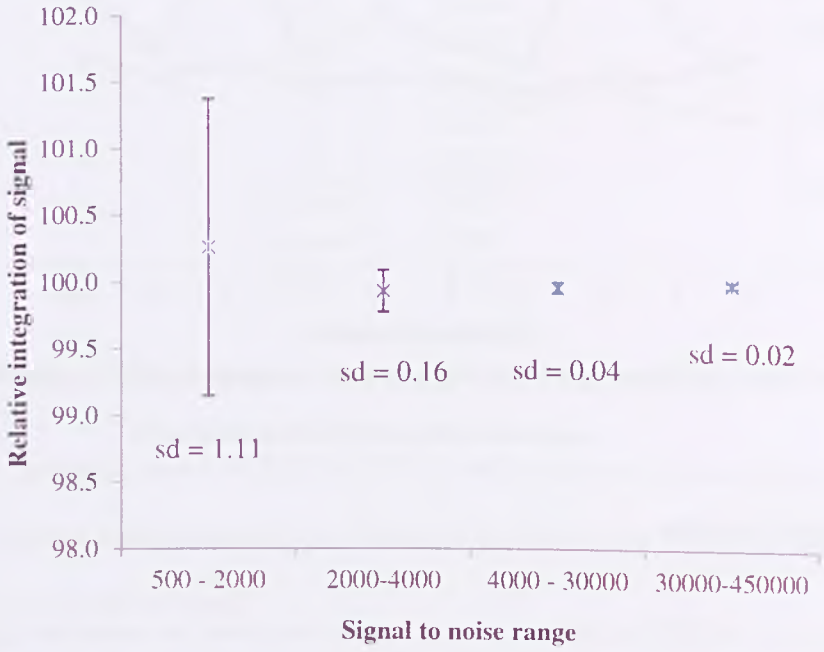

Figure 2.27 – Graph showing effect of S/N on signal intensity at different levels of S/N ratio

The data in Figure 2.27 shows, as expected, that the uncertainty of measurement increases at low signal to noise and it is recommended that a signal to noise ratio of >4000 be used to minimise the uncertainty due to signal to noise variation.

The signal to noise of the two signals for integration will potentially affect the accuracy of the measurement. The predominant effect will be to increase the standard deviation of the measurements but also has the potential to increase a slight bias where there is a significant difference in signal intensity.

2.5 Processing Parameters

There are many processing parameters, which can influence and manipulate the data but as long as the user is consistent this can add significant benefit to quantitative measurements.

2.5.1 Operator Bias

To establish the variability coming from user bias a dataset of maleic acid **(8)** and benzoic acid **(9)** in DMSO-d_6 was processed by two analysts. The dataset included 10 replicate analyses of the 10 mg/mL solution, and integration of the benzoic acid aromatic peak at 7.9 ppm and the maleic acid peak at 6.2 ppm. Processing included transforming the data, phasing and applying baseline correction and finally integrating the signals used for quantification. Figure 2.28 shows the variation between integration of both analysts. The % RSD of the integration of 10 replicates for analyst 1 was 0.62 % and 0.60 % for analyst 2. Processing appears to be reproducible between analysts, furthermore the within analyst variation appears to be low. However, between lab variation needs to be investigated and is discussed further in Chapter 4 where data from a recent pilot study confirms the high variability coming from user dependent processing protocols between labs and emphasises the need for a more stringent processing protocol

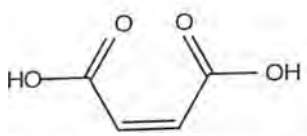

(8)

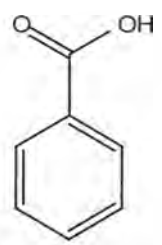

(9)

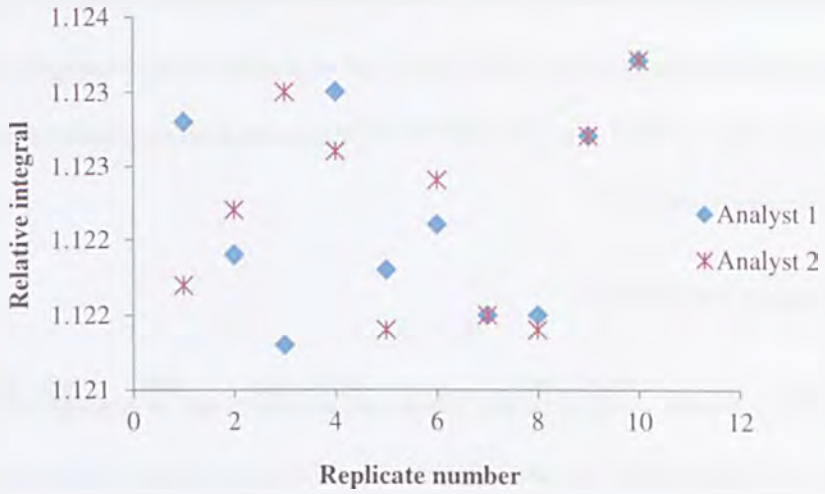

Figure 2.28 – Variation in relative integrations for data processed by two analysts on the same sample set of maleic acid and benzoic acid in DMSO-d_6, all acquired on a 600 MHZ Bruker instrument NS:16 D1:60 sec

2.5.2 Software impact

Three assay solutions of MA and dimethyl sulfone (**10**) were used to determine the impact of different processing platforms. The two common commercial processing platforms; Bruker Topspin (pl6) and MestReNova (v9.0) were used.

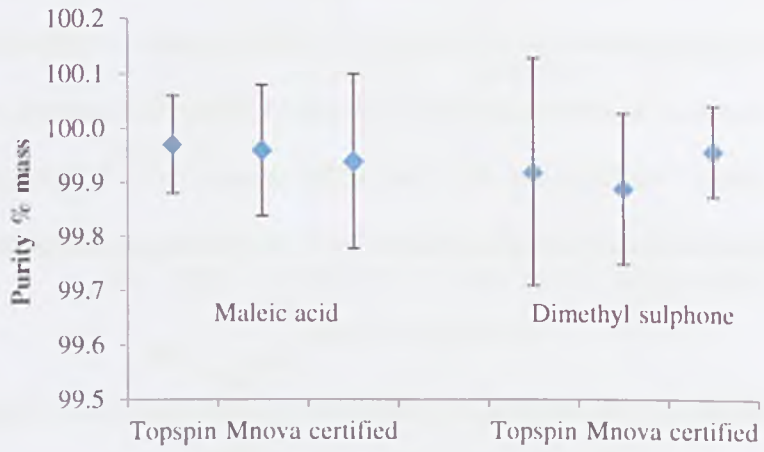

Figure 2.29 – % Purity determined using two software platforms and compared to 'certified' value, error bars determined using standard deviation of replicate analyses and uncertainty reported on certificate of analysis

The assay results of the two materials were seen to be comparable and thus both deemed suitable for processing qNMR results.

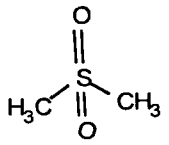

(10)

2.6 Conclusion

The experiments and calculations in Chapter 2 show the impact of the major instrument and sample related sources of uncertainty for internally and externally standardised NMR assays. Instrumental and processing parameters have been scrutinized with an output of optimum parameters detailed. Through careful calibration and compensation the effect of instrumental, sample specific and processing parameters can accounted for in quantitative measurements ensuring bias and errors are kept to a minimum. As qNMR widens its application to larger, more complex molecules, the factors investigated in this chapter can become more significant and correction for them in the assay is recommended where high accuracy is required. To complete the validation of 1D qNMR measurements eight reference materials purchased from Sigma Aldrich (Fluka TraceCert qNMR standards) were assayed against each other and the results compared to the certificate of analysis provided by Sigma Aldrich.

Analyte	Internal standard	Solvent	Experimental result % mass	Certified value % mass	Difference from certified value % mass
Maleic Acid 1	Benzoic acid	DMSO-d_6	99.97 +/- 0.09	99.94 +/- 0.16	0.03
Maleic Acid 2	Benzoic acid	DMSO-d_6	99.79 +/- 0.03	99.79 +/- 0.07	0.00
Dimethyl Malonic Acid	Benzoic acid	DMSO-d_6	99.52 +/- 0.11	99.49 +/- 0.12	0.03
Dimethyl Malonic Acid	Maleic Acid	D2O	99.50 +/- 0.37	99.49 +/- 0.16	0.01
DMMA	BTFMBA	DMSO-d_6	99.46 +/- 1.06	99.49 +/- 0.12	0.03
DMT	TMB	$CDCl_3$	99.92 +/- 0.12	99.99 +/- 0.16	0.07
DQ	TMB	$CDCl_3$	99.39 +/- 0.34	99.31+/- 0.14	0.08

Table 2.8 – Summary of validation using various certified reference materials from Sigma-Aldrich and comparing them to the 'certified' value

The results (Table 2.8) show a mean difference between the experimental qNMR assay values to the certified purity values of the reference materials of 0.04 % mass with a maximum

difference of 0.08 % mass which can be attributed to integration effects. The data shows excellent correlation to the certified values and justifies the use of protocols described to minimise uncertainty in Chapter 2.

Chapter 3 2D qNMR

3.1 Background

Multidimensional NMR was first introduced in 1971 by Jeener [72] and is used routinely for structural identification work, it is only now starting to emerge as a quantitative method, predominantly for small molecules. For large, complex molecules, the application of ^{1}H qNMR will not be generally applicable, due to the complexity of the NMR spectra impeding accurate quantification, ^{1}H qNMR experiments for large compounds give limited resolution and poor integration ranges this highlights the need to develop 2D qNMR approaches. By dispersing the NMR signals into the second dimension and exploiting the wide spectral width in the heteronuclear dimension, signals in complex spectra can be more readily resolved to give specificity of analyte signals. In 1D qNMR the peak area is directly proportional to analyte concentration (provided correct sample parameters are used) allowing for accurate and precise quantitation, but the intensities of cross peaks in standard 2D NMR experiments are not directly proportional to analyte concentration due to resonance specific signal attenuation during the pulse sequence. The fundamental problem with the use of 2 dimensional approaches is that the biggest advantage of qNMR, it's uniformity of response across analytes is lost and care must be taken to minimise these deviations and account for them where possible. HSQC experiments rely on the polarization transfer through J coupling and is typically one bond CH coupling, therefore signal intensity is not only dependent on the delay value of the CH coupling constant for which the experiment is optimised but additional factors such as peak multiplicity, homonuclear coupling constants and T_1 and T_2 relaxation during the pulse sequence also have an impact that needs to be addressed if precise quantitative measurements are to be obtained in such 2D experiments. Another major drawback to 2D qNMR is the impact of adding long relaxation delays to already long experimental times due to the low natural abundance of ^{13}C and need for multiple FIDs to achieve adequate resolution in the 2nd time domain. This inhibits

the use of long relaxation delays as required for 1D qNMR experiments (typically 5 x T1 [73]). The impact of the effects seen from J coupling, T_1, T_2 relaxation times and resolution need to be accounted for to derive an uncertainty budget for the application in 2D qNMR. Conventional 2D experiments such as COSY, TOCSY, J-resolved NMR, HSQC can be used but have generally been limited to qualitative measurements due to high sensitivity to pulse imperfections and instrumental parameters [74]. Many 2D quantitative advances have already been made in the last decade largely in metabolomics and more recently methods for overcoming the limitation set out by the non-uniform magnetisation transfer due to variation in J_{CH} values. Heikkinen and co-workers discuss the importance of using non-optimal polarization transfer delays for quantitative measurements, highlighting that if the range of heteronuclear coupling constants is large between the two chosen signals, the corresponding peak volumes will be significantly reduced [75]. Rai and co-workers propose an approach for quantification of metabolites by correlating measured cross peak volumes with the concentration of metabolites in urine samples using internal standards with known concentrations [76]. Alternatively Gronwald and co-workers use calibration curves to determine the concentration of metabolites with the need to calibrate each individual signal for quantitation [77]. Hu and co-workers present a method of extrapolating peak intensities from a series of constant time gradient selective HSQC experiments to obtain a gradient selective $HSQC_0$ spectrum, from which concentrations of metabolites can be determined [78]. All of the above methods have shown precision of around 3% or higher but have not been optimised for experimental parameters such as relaxation delays and variation in J_{CH} coupling constants. The lack of reporting on how the parameters affect the uncertainty of the measurements for quantitative work, mean that the above reported methods are not applicable to the metrological community as they have no SI traceability. There is also a pressing need in proteomics and metabolomics to be able to quantify large molecules (conventionally analysed by amino acid analysis) with a great deal of accuracy and realistic, cost effective experimental times. Hence accurate, reliable analysis using heteronuclear 2D NMR experiments, require an evaluation of additional sources of error and represent a

fundamental step in producing more efficient, traceable quantitative methodologies by 2D qNMR, that have broad application to a variety of key industry sectors.

The work in this chapter evaluates the application of HSQC methods to perform quantitative analysis with minimal bias. The variation between experimental and theoretical bias is discussed and approaches to determine the measurement uncertainty with a minimum of method validation is investigated. By validating a typical 2D qHSQC experiment for complex molecules a more accurate protocol can be achieved within the NMR community. This standard approach provides optimal experimental conditions and achieves SI traceable qNMR measurements with smaller uncertainties for large complex compounds, exploring the major uncertainty components attributable to different qHSQC methods. After initially assessing the suitability of the standard Bruker HSQC pulse program compared to 1D protocols, the various sources of bias were investigated to compose a comprehensive uncertainty budget for qHSQC experiments. Following this different complex sample systems were investigated in various solvents to determine effects on quantitation.

Non uniform sampling methods are also investigated to determine its feasibility with qHSQC methods in reducing experimental time and assessing its accuracy for quantitative measurements.

3.2 Experimental plan

To be able to validate and investigate the bias in 2D HSQC methods various organic molecules were selected to assess the variability coming from the additional sources of bias. The following sample systems were chosen to carry out the work;

- Simple model systems using glucose, adenosine monophosphate and guanosine monophosphate
- A commercially sourced food syrup for real sample type in complex non-deal matrix analysis
- A reference material (Digoxin) with a known purity value
- A small peptide - GFFYTPKA (3000da)

The main focus on trying to achieve SI traceable quantitative methods using 2D NMR was to facilitate protein and large organic molecule measurements within the metrological community. Currently protein quantification relies on traditional methods such as amino acid analysis, where the peptide is hydrolysed to its amino acid components and then either run using matrix assisted laser desorption/ionisation (MALDI) techniques [79] or LC-MS or derivatised for GC-MS analysis [80,81]. This method can take up to a week to carry out all of the steps making it tedious and laborious. Furthermore SI traceability is achieved by buying in expensive standards which must endure the hydrolysis step of the method. Therefore a technique which can reduce sample preparation time and can provide direct SI traceable measurement is very appealing.

A small peptide of GFFYTPKA was sourced and the feasibility of quantitative HSQC methods assessed. However, running validation experiments on peptides proved to be costly with limited sample availability and therefore the method was validated on simple molecule model systems, a certified reference standard (sourced from LGC) and a commercially sourced date nectar product for validating a real sample in a complex matrix all which have an abundance of sample size. Figure 3.1 shows the approaches used to validate 2D qNMR in this chapter.

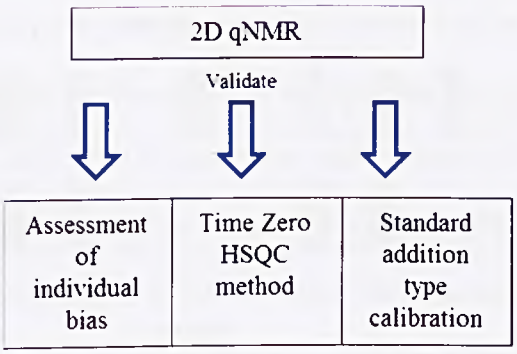

Figure 3.1 – Experimental plan for validating 2D method

The major sources of bias coming from 2D qNMR have been identified in this chapter and the two main approaches to correct for the biases were;

1. If reference standards are available the biases can be calibrated using a calibration curve. This calibration will eliminate the errors seen from differences in T_1/T_2, coupling constant variation and signal attenuation. Two main calibration type approaches are investigated in this chapter; standard addition and time zero HSQC.
2. If there are no standards available, to achieve traceability and account for signal attenuation and biases the maximum errors associated from the biases have to be applied. Therefore pre-determination of T_1/T_2, optimum coupling constant values and tailoring of the analysis is required. The maximum errors from biases can be extracted from validation data.

As previously mentioned, Markely and co-workers describe a method to account for signal attenuation during the pulse sequence of a HSQC experiment to make the method quantitative known as $HSQC_0$. This protocol was evaluated and it's ability to account for all the errors associated with the method. Figure 3.2 shows a simplified schematic of the standard Bruker HSQC (hsqcedetgpsp.3) experiment along with a simplified $HSQC_0$ pulse sequence developed by Markley's group which consists of a series of constant time Bruker HSQC experiments. Default HSQC parameters on a Bruker 600 MHz instrument are; NS:4, DS:16, TD in F1: 256, F2: 1024, SW F1: 165ppm, SW F2: 6.6 ppm, D1: 1.5 sec.

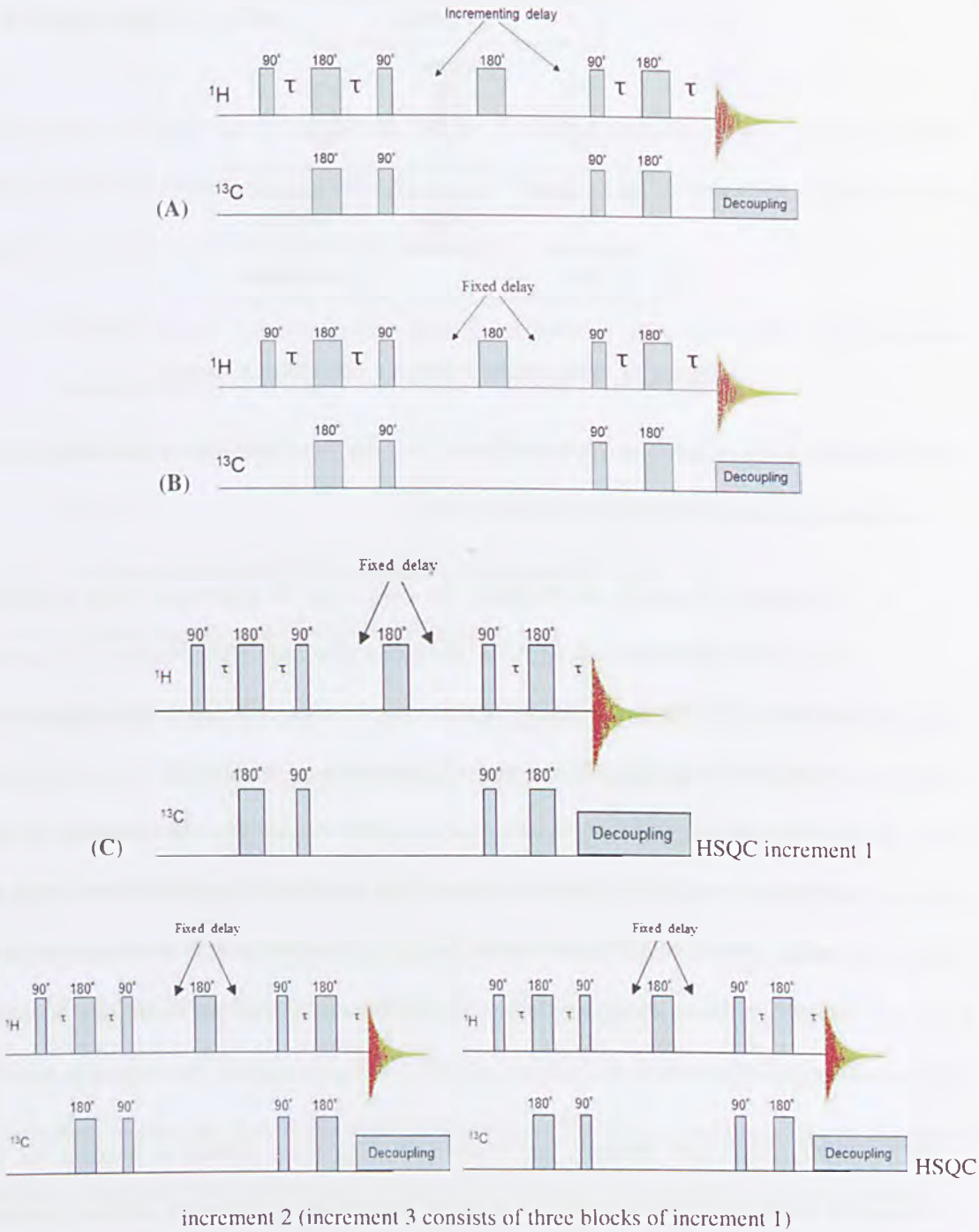

Figure 3.2 – (A) A simplified Bruker standard HSQC experiment (hsqcedetgpsp.3), (B) A simplified Bruker constant time (CT) HSQC experiment, (C) A simplified adaptation of Markley's $HSQC_0$ experiment

The $HSQC_0$ method consists of three increments of the Bruker constant time (CT) HSQC experiments with additional phase adjustments to account for rephocusing and defocusing of spins. Increment one is the standard Bruker CT HSQC experiment, increment two involves two

CT HSQC experiments, however data from the first iteration is not recorded and increment three involves three CT HSQC experiments with data from the first two iterations not recorded. By back extrapolating the data a $HSQC_0$ time point value is achieved which is equivalent to the peak volume before any signal attenuation occurs. Although $HSQC_0$ spectra can give enhanced sensitivity, spectral noise especially T_1 related noise limit the applicability of the method, therefore T_1 and coupling constant effects should be considered. Typically, it is agreed that by integrating reference peaks and analyte peaks from the same region of the spectrum negates issues caused by variation from coupling constants *etc.*, however this will be further investigated.

For the standard addition type calibration spiking in the internal standard at different levels will determine a correction/response factor measuring the difference observed in the reference signal to analyte signal over the different concentrations. The resultant calibration curve is extrapolated to a point where no bias is observed.

A maximum error calculation for T_1 variation and coupling constant variation was determined using validation studies to account for individual biases.

3.3 Materials and Methods

- GFFYTPKA peptide sourced from Thermo Fischer
- Digoxin (LGC ERM AC200a)
- Benzoic acid (NIST 350b)
- Glucose (Sigma Aldrich)
- Phenyl Glycine (P3 Biosystems)
- Adenosine monophosphate (AMP) (Sigma Aldrich)
- Guanosine monophosphate (GMP) (Sigma Aldrich)
- Dimethyl terephthalate (DMT) (Sigma Aldrich)
- Aldosterone (Sigma Aldrich)

- Deuterated D_2O and DMSO-d_6 (Sigma Aldrich)

All solutions were gravimetrically prepared using a five figure and six figure balance at a concentration of 10-20mg/mL unless stated. Once prepared the solutions were sonicated and transferred into 5mm Norrell NMR tubes sourced from GPSE scientific.

Data was processed on TopSpin 3.2 and automatic baseline optimisation was applied after automatic phasing on all 2D data. All 1D data were phased manually with a 0.3 Hz exponential apodization applied to the FID. A polynomial baseline correction was manually applied to the peaks of interest before manual integrations were applied.

3.4 Initial screening of peptides

Three peptides were screened to assess the feasibility of quantifying peptides by NMR. 1D and 2D experiments were run on the peptides which were spiked with an internal standard (maleic acid and trioxane, Sigma Aldrich). A standard Bruker HSQC experiment was used for the 2D qNMR. The peptides analysed were angiotensin I, angiotensin II and bradykinin (also sourced from Sigma). For these sizes of peptide, the application of qNMR will not be generally applicable, but reliant on fortuitous NMR spectra (with specific amino acid residues such as histidine giving well resolved resonances in the 1D spectra). Limited resolution, giving poor integration ranges makes finding a suitable integration peak difficult in the 1D spectrum. 2D NMR helps to resolve these peaks so that the integration is made easier. Figure 3.3 shows a typical un-spiked 1D NMR spectrum of bradykinin **(11)** to show its complexity and how the signals were better resolved in the 2D HSQC experiment.

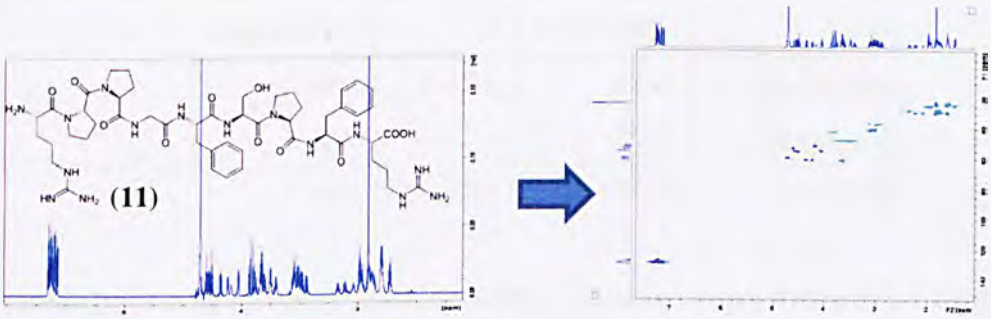

Figure 3.3 – Left: ^{1}H spectrum of bradykinin: NS:16, SW:10ppm, D1:1sec,

Right: 2D HSQC spectrum of Bradykinin: NS:4, SW:165ppm, D1:1sec, F1 TD: 256, F2 TD: 1024, all acquired on a 600 MHz Bruker instrument using D_2O

The qNMR purity obtained for the three peptides as determined by 2D internally standardised qNMR (using maleic acid and trioxane (**12**)) as the internal standards) are shown in Table 3.1. These values were compared to their certificate of analysis purity as provided by the supplier (Sigma Aldrich) which were determined by HPLC analysis. From Table 3.1 it can be seen that there is a significant difference between the obtained results and the expected 'certified' results as expected since the certified value was determined by HPLC analysis only. The results show that the uncertainty obtained are in the order that we need however standard 2D experiments are not optimised to do quantitative analyses and further work and method development needs to be carried out to fine tune the method. The lack of certified materials available commercially and the limited sample size of materials impede the validation of the method using peptides, but the need for understanding the biases and methods for calibration become unavoidable. The rest of this chapter aims at showing ways to improve the accuracy of 2D quantification by NMR using calibration methods or accounting for biases using a combination of approaches.

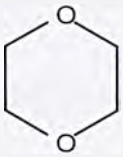

(12)

Peptide	qNMR Purity	U	Certified purity
Angiotensin I	88.8%	± 1.0 %	90%
Angiotensin II	84.3%	± 1.0 %	93%
Bradykinin	89.5%	± 2.0 %	98%

Table 3.1 – ^{1}H qNMR purity compared to HPLC 'certified' purity for three small peptides

3.5 HSQC validation to determine individual biases

Validation was performed on the 2D Bruker HSQC experiment to determine biases coming from chemical shift, T_1 and coupling constants. Repeatability, precision and linearity was also captured in the validation study.

Due to the expensive nature of peptides the HSQC method could not generate many replicate analysis data for validation work and therefore small simple molecules such as glucose, AMP and GMP were used. Once trends and biases were established the method was implemented on a complex reference material before implementing it on the peptide GFFYTPKA to confirm similar trends were seen.

3.5.1 Bias from peak selection

Using adenosine monophosphate (AMP (**13**)) and guanosine monophosphate (GMP (**14**)) as the internal standard bias from the selection of peaks used for quantification was assessed. Figure 3.4 shows a typical spectrum for AMP and GMP.

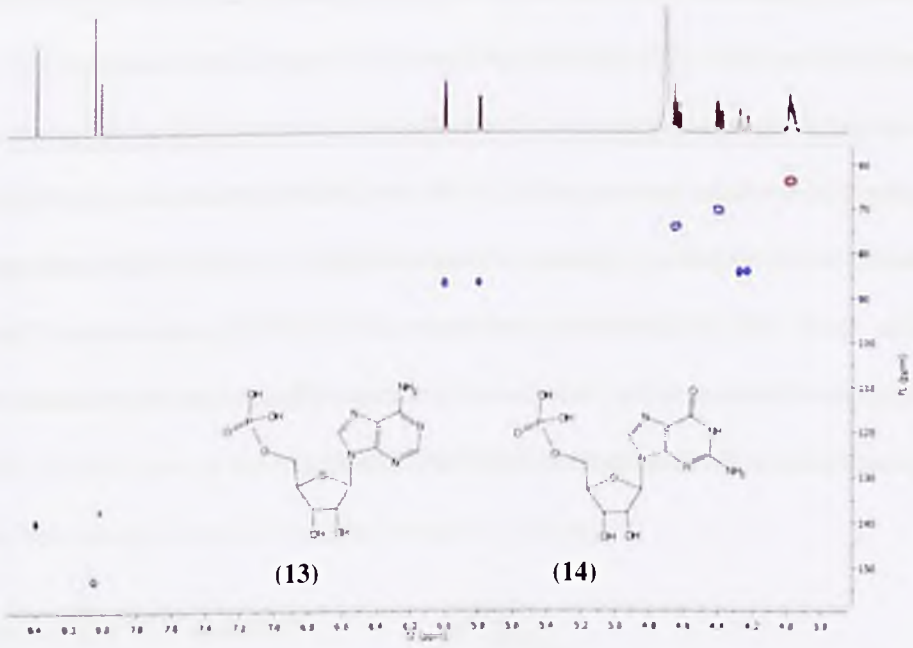

Figure 3.4 – 2D HSQC spectrum for a solution of AMP and GMP in D_2O acquired on a 600 MHZ Bruker instrument NS:4, D1:2sec

Signals with similar chemical shift, multiplicity, coupling constants or functional groups are thought to be well matched signals for quantitative analysis as these parameters are dependent on the hybridisation and electronegativity of the atoms. Therefore, coupling constant of peaks are related to its chemical shift and neighbouring peaks will have similar coupling constant values making the selection of peaks for integration critical in 2D analysis.

This was investigated by analysing a solution of AMP and GMP and comparing the ratios of signals based on chemical shift. The anomeric signals and aromatic signals of AMP and GMP were used to determine the bias arising from selection of peaks.

For evaluation of integral ratios of signals in similar regions of the spectral window, one data set compared the anomeric signal of AMP to the anomeric signal of GMP which would represent a well matched internal standard signal to the analyte signal (both in the same chemical shift region). The second data set compared the anomeric AMP signal to that of the aromatic GMP signal which would represent a poorly matched internal standard signal to that of the analyte

signal (both in significantly different chemical shift regions). Four sets of experiments were run in the following way, a ^{1}H qNMR experiment which would represent the 'true' gravimetric value (gravimetric meaning the use of a certified reference material so the gravimetric value is the value corrected for mass as stated on the certificate) furthermore, there are fewer errors associated to ^{1}H qNMR experiments, a standard HSQC experiment (hsqcedetgpsp.3), HSQC constant time (CT) increment 1 experiment and a $HSQC_0$ experiment. The HSQC CT experiment will show whether there is a significant difference in the standard Bruker HSQC experiment and the Bruker constant time HSQC experiment.

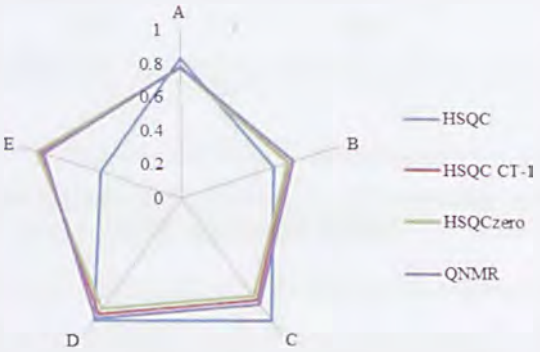

Figure 3.5 – Assay showing well matched signals used for integration. Five solutions (A-E) used to assess the repeatability by plotting the relative signal intensity for each different experiment

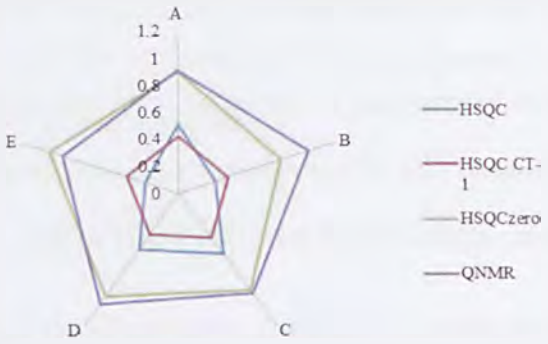

Figure 3.6 – Assay showing poorly matched signals used for integration. Five solutions (A-E) used to assess the repeatability by plotting the relative signal intensity for each different experiment

Figures 3.5 and 3.6 clearly show the impact on signal intensity when using a well matched internal signal compared to a poorly matched internal signal. For Figure 3.5 where a well matched resonance for the internal standard was used, it can be seen that other than the standard Bruker HSQC experiment, the $HSQC_0$ and HSQC CT agree well with the ^1H qNMR assay signal intensity values. Figure 3.6 shows that when using a poorly matched resonance for integration there is a larger deviation between the standard HSQC and HSQC CT values therefore using well matched resonances is beneficial to quantitative measurements as anticipated. In the case of the ^1H qNMR and $HSQC_0$ experiments resonance chemical shift appears to have insignificant bias towards integration of signals.

3.5.1.1 Bias from O1P and O2P

The same solution of AMP and GMP was used to assess the impact from variation of O1P and O2P. Section 2.2.3.2 showed that in 1D qNMR analysis there was a small but significant bias (0.018% per ppm) due to the variation of O1P therefore the effect of O1P and O2P was investigated in the heteronuclear dimension. It would be interesting to investigate the bias in 2D experiments where there are other complex pulses involved and how this affects the signal intensity and ratios of signals. The outcome should confirm if peak intensity is robust across the spectrum or is only consistent in the middle of the spectrum.

The default HSQC spectrum had an O1P set to 4.7 ppm and the O2P set to 75.0 ppm, with the spectral width of 16 ppm in the proton dimension and 165 ppm in the carbon dimension. The peaks used were the anomeric AMP and GMP signals at 5.8 PPM and 6.0 PPM respectively, giving them a central location within the spectral window of the default HSQC spectrum. The O1P and O2P were varied from the default O1P and O2P as shown in Table 3.2.

	Distance from default O1P (ppm)	Distance from default O2P (ppm)	New O1P (ppm)	New O2P (ppm)	'Graphical' O1P	'Graphical' O2P
Default	0	0	4.7	75	1.1	11.65
	+2	0	6.7	75	-0.9	11.65
	-2	0	2.7	75	3.1	11.65
	+3	0	1.7	75	4.1	11.65
	-3	0	7.7	75	-1.9	11.65
	0	-50	4.7	25	1.1	61.65
	0	+30	4.7	105	1.1	-18.35
	-2	+30	2.7	105	3.1	-18.35
	+2	-50	6.7	25	-0.9	61.65
	-2	+30	2.7	105	3.1	-18.35
	+3	+30	7.7	105	-1.9	-18.35
	-3	+30	1.7	105	4.1	-18.35
	+3	0	7.7	75	-1.9	11.65
	-3	0	1.7	75	4.1	11.65

Table 3.2 – Experiment schematic to show how O1P and O2P were varied from default values, the 'Graphical' O1P and O2P indicates the positioning of AMP peaks for Figure 3.7 below

The above variations generated peaks moving around the spectral window as shown in Figure 3.7. The AMP anomeric signal is 1.1 ppm away from the default O1P centre of spectrum of 4.7 ppm and 11.65 ppm away from the default O2P of 75 ppm. By changing the O1P and O2P as described the signals shift across the spectral window as shown in Figure 3.7. The theory is that the more of a central location the signals used for integration are, the higher the signal intensity and lower the standard deviation in results.

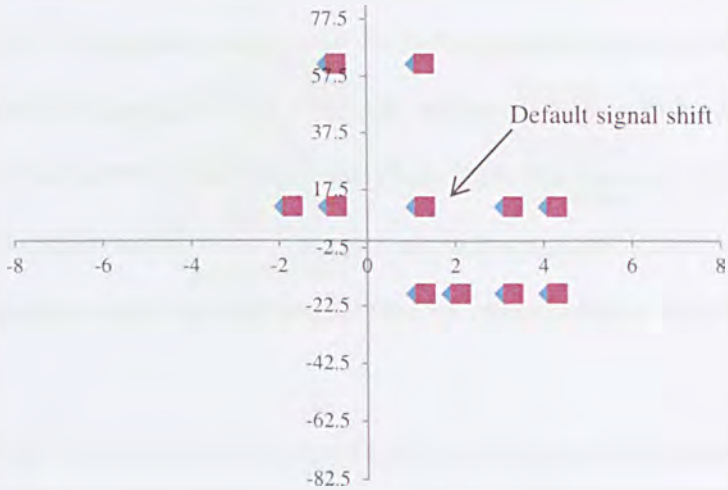

Figure 3.7 – A schematic to show were signals would fall in the spectral window by changing O1P and O2P as described in Table 3.2: Red: GMP signal, Blue: AMP signal

Figure 3.8 shows the relative ratio of the AMP to GMP anomeric signal at the different O1P and O2P settings, this was repeated over two days. In both days the lowest standard deviation came from when there was no variation in O1P or O2P from the default settings. The difference seen in relative integral ratios is insignificant and the standard deviation coming from results is well within the reproducibility of the experiment (with the largest % RSD of 0.014%). It is shown that the O1P bias is consistent with the trend seen in Chapter 2, indicating a small but significant bias coming from O1P variation in 2D qNMR. There is a less obvious trend seen in the results from O2P variation, in instances where only the O2P was varied by -50 ppm and 30 ppm away from the default O2P and no O1P changes were made. It is clear that O1P variation has a larger impact than O2P variation for 2D qNMR analysis. The bias for in O1P variation was calculated to be 0.42 % per ppm for a heteronuclear experiment and 0.03 % for O2P variation.

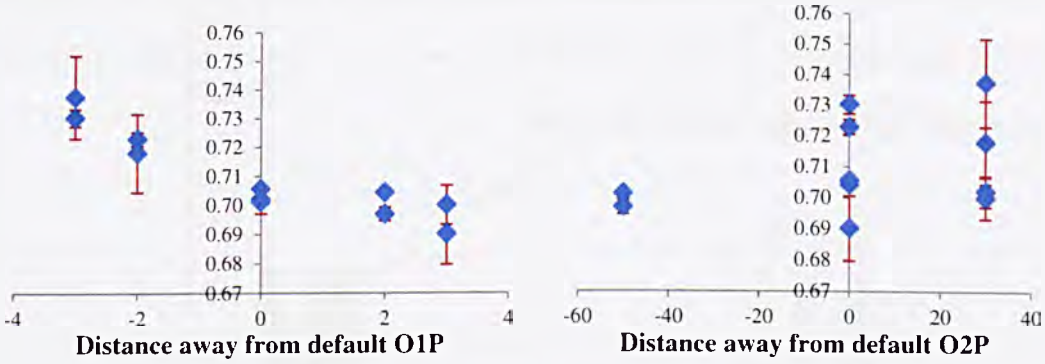

Figure 3.8 Left: Results of how varying O1P affects the relative ratio of AMP to GMP

Right: Results of how varying the O2P affects the relative ratio of AMP to GMP

3.5.2 Linearity and repeatability using Glucose and AMP

Solutions of glucose and AMP as the internal standard were used to assess the repeatability, linearity of experiments and stability of solutions giving a better idea of biases arising from different experiments and concentration effects and the impact of interconverting forms of glucose in solution.

A series of experiments to determine the variation in 1D and 2D experiments were initially performed. Four solutions of glucose and AMP were prepared at varying concentrations were prepared (indicating if there were any concentration effects for the different experiments) ranging from 2.6 – 0.26 mg/mL. A 'gravimetric' value (a theoretical calculated value derived by dividing the mass of both analytes with their molecular weight) was compared to the ^{1}H proton qNMR result, the ^{1}H proton water suppression (saturation transfer) result and a standard Bruker 2D HSQC result. A water suppression experiment was chosen as it was clear that a calibration of the attenuation factor applied to quantitative measurements would need to be done, it was also interesting to assess quantitivity of peaks close to the saturation peak. The gravimetric value used the weights used for sample preparation. Figure 3.9 shows that the ^{1}H water suppression results (^{1}H sat trans) are consistently low for each solution potentially due to the glucose anomeric signals of interest being close to the water reference peak used for the saturation transfer of signal. The glucose anomeric peaks on either side of the water are most likely being suppressed to a degree as well as the water peak. The ^{1}H proton and HSQC value agree fairly well with the 'gravimetric' value.

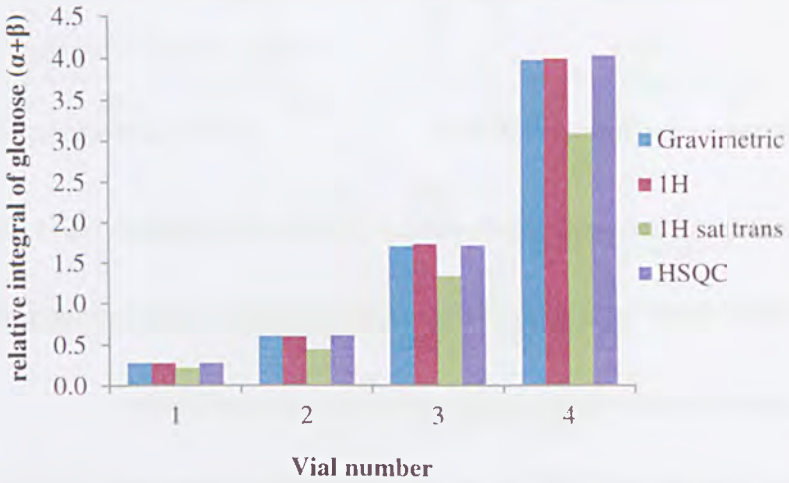

Figure 3.9 – Relative signal intensity shown for both alpha and beta forms of glucose for three different experiment types, comparing them to the 'gravimetric' value. Four solutions of different concentrations were used in D_2O. Vial 1 - 2.5 mg/mL. Vial 2-1.1 mg/mL, Vial 3 – 0.6 mg/mL, Vial 4 – 0.25 mg/mL, all acquired on a 600 MHZ Bruker instrumnet

Using solution 1 from the four sets of solutions, repeatability was assessed on increment 1 and increment 2 of the $HSQC_0$ constant time (CT) experiments. Six repeatability experiments were

run and the % RSD showed acceptable repeatability for the $HSQC_0$ experiments. The increment 1 CT-HSQC experiment gave a % RSD for the six replicates of 0.89 %, and the increment 2 CT-HSQC experiment giving 1.30 %.

Linearity is a fundamental component of method validation. The linearity of an analytical procedure is its ability to obtain results which are directly proportional to the concentration of the sample. Four solutions of the glucose at different concentrations ranging from 2.6 – 30.0 mg/mL were used to assess the linearity of the three different experiments. Each experiment showed to have excellent linearity across the concentration range shown by the high regression values, for a validated HPLC method the linearity must be above 0.995 to pass. It was reassuring to see that the 2D solutions also showed excellent linearity across the concentration range.

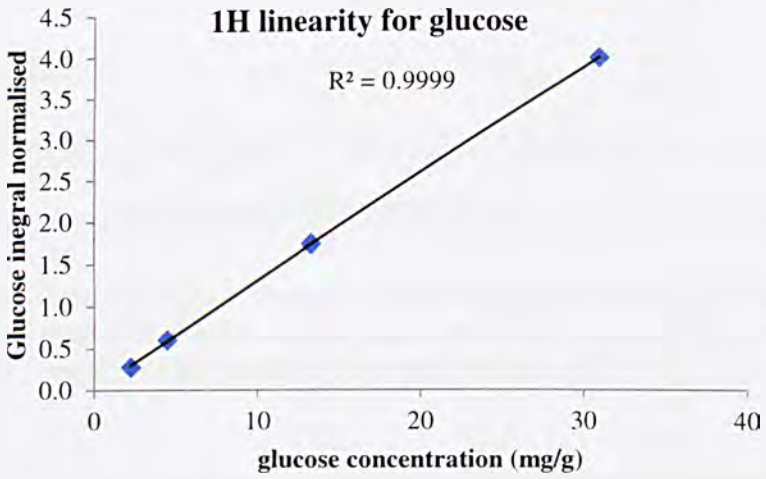

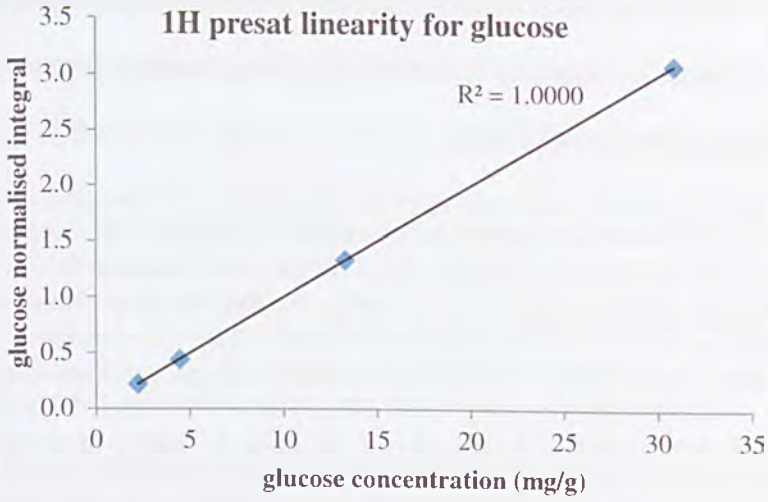

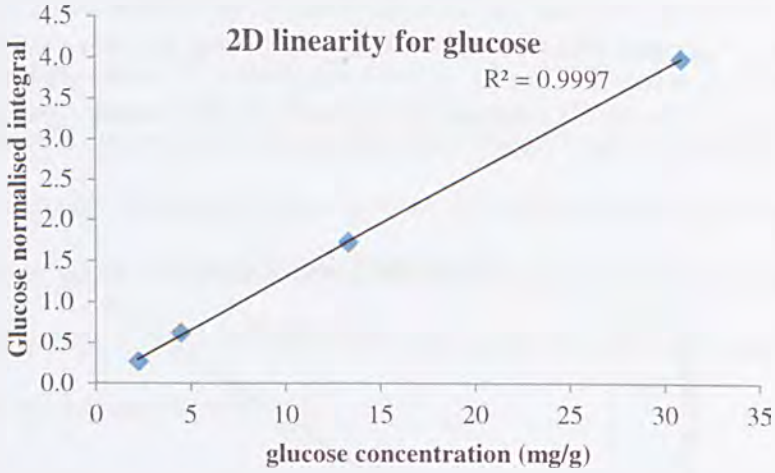

Figures 3.10, 3.11, 3.12 – Linearity for three experiments using the same solutions showing good linearity with R^2 of greater than 0.995, all acquired on a 600 MHz Bruker instrument using D_2O. The Glucose is normalised against the AMP signal

Since the linearity and repeatability experiments were run over a period of time, stability was assessed to see how if at all the ratio of alpha to beta glucose had changed. An interday repeatability experiment (along with an assessment of the solution stability of sample) was conducted on solution four by assaying on three different days, and the levels of alpha to beta glucose were found consistent over a period of one month this was a good indication of the robustness of the method.

Date:	Alpha glucose	Beta glucose
08/05/2015	0.7126	1.1788
15/05/2015	0.7139	1.1618
18/06/2015	0.7200	1.1840
Average	0.7155	1.1749
Std dev	0.004	0.012
% RSD	0.55	0.99

Table 3.3 – Stability data for solution Four, showing consistent levels of alpha and beta glucose

3.5.3 Variation in T_1

Spin-lattice relaxation (T_1 relaxation) is the rate of relaxation of the spins in the sample to go back to equilibrium after a pulse. Each signal from a sample will have different T_1 rates therefore this is very much a sample and concentration dependant phenomena and is determined by the relaxation delay (D1) instrumental acquisition parameter.

3.5.3.1 AMP and GMP

Using the AMP and GMP solutions the T_1 for the anomeric signals were determined experimentally and showed to have little variation across the solutions (Table 3.4).

		T1 (s)				
	Peak (ppm)	solution1	solution2	solution 3	Solution 4	Solution 5
GMP	5.7	1.82	1.72	1.67	1.72	1.66
AMP	5.9	1.57	1.53	1.49	1.53	1.49

Table 3.4 – Experimentally determined T_1 values (in seconds) for the anomeric signal of AMP and GMP peaks across the five solutions

By default all HSQC experiments are set up with a D1 of 1.5 seconds. Clearly this does not meet the requirement of 5 x the longest T_1 in the sample as stated in many research papers for the relaxation delay. Experiments to determine the impact of using a small D1 showed that a relaxation of 3 seconds was sufficient for the anomeric peaks. Any less than that then there would be a significant bias coming from insufficient relaxation of signals. The ratio of the two anomeric peaks are plotted in Figure 3.14, which shows that using a D1 of 1.5 seconds gives the

lowest signal intensity for both signals. By assessing the D1 implications across the range of peaks in a solution it is obvious a similar trend is observed. This time recording the absolute signal intensity of each peak at a D1 of 1.5s and 25s, the latter produces results with much higher signal intensity (Figure 3.14). The peak at 8.4 ppm shows that the signal is fully relaxed at 1.5 seconds already so using a higher D1 would be covered by the experimental error of the experiment.

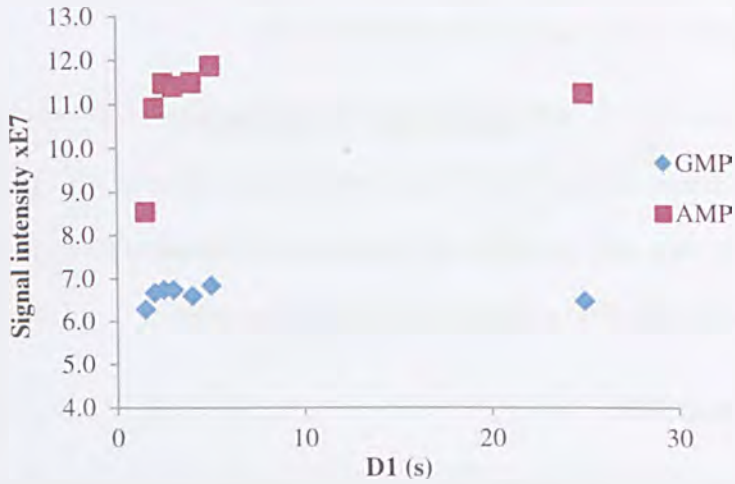

Figure 3.13 – Ratio between AMP and GMP signals are compared to increasing relaxation delays. Acquired on a 600 MHz Bruker instrument using D_2O

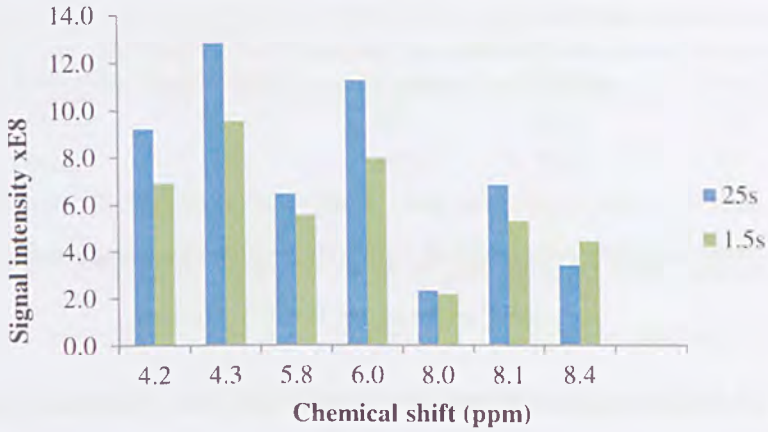

Figure 3.14 – Effect of relaxation delays at two extremes are compared for various peaks from the same solution

3.5.3.2 Digoxin

Digoxin (**15**) is a well-established reference material certified by LGC was chosen as one of compounds to further validate the method on because of its spectral complexity.

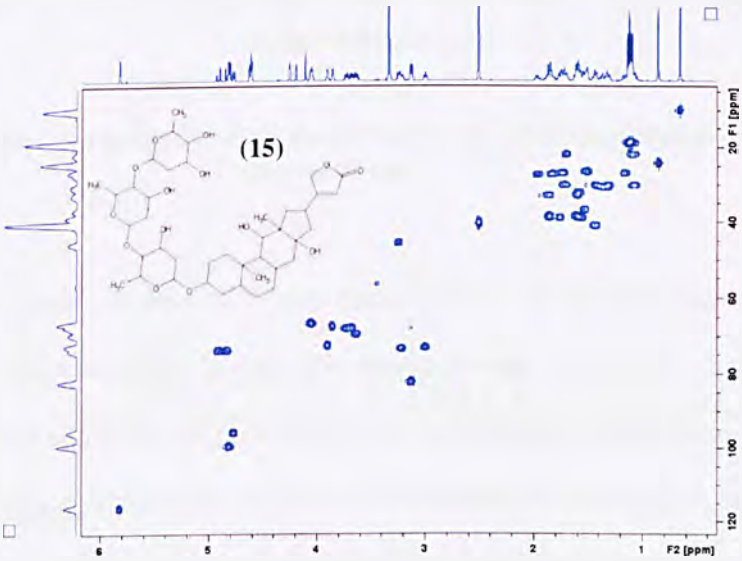

Figure 3.15 – Structure of Digoxin and its corresponding 2D HSQC spectrum, acquired on a 600 MHz Bruker instrument using DMSO-d_6

Currently Digoxin is certified for purity using chromatographic techniques in-house at LGC and 1D qNMR analysis; it is certified at 98 %. Experiments using different D1 values were run to assess the impact on signal intensity. As anticipated a default D1 of 1.5 Seconds was too short for Digoxin. A D1 of 2, 5 and 10 were used to see the impact on relative signal intensity for HSQC experiments, with the D1 of 2 seconds generally giving lower signal intensity (Figure 3.16).

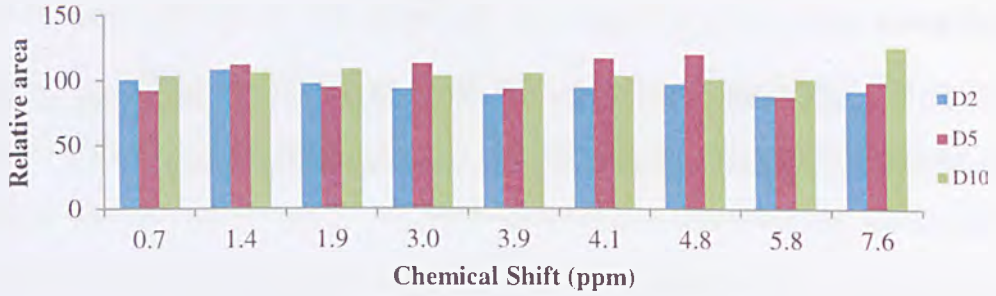

Figure 3.16 – Relative intensities shown for Digoxin peaks when run at a relaxation delay of 2, 5 and 10 seconds

Repeatability was assessed on a few signals over four replicate analyses using the HSQC experiment and a maximum standard deviation of around 9 % seen which is a lot higher than seen for the simple model molecules, however, spectral processing and integration methods are likely to cause a significant contribution to the analysis of complex molecules and could be the reason why the standard deviation is so high for these replicate analyses.

Chemical shift (ppm)	STD dev
1.11	8.47
1.71	6.20
3.00	1.91
4.77	7.54
7.51	8.89

Table 3.5 – Repeatability data showing standard deviation of five peaks ran four times

Further work needs to be carried out on Digoxin to try and reduce the standard deviation between replicate analyses by optimising and standardising interpretation of 2D data.

3.5.3.3 GFFYTPKA Peptide

A small peptide, GFFYTPKA (**16**) sourced from Fisher Scientific was used to validate the 2D qNMR work for peptide applications.

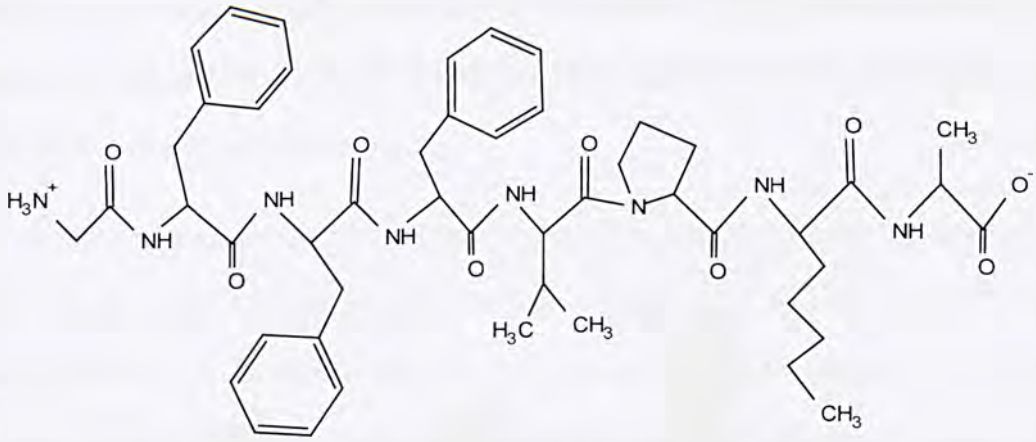

(16)

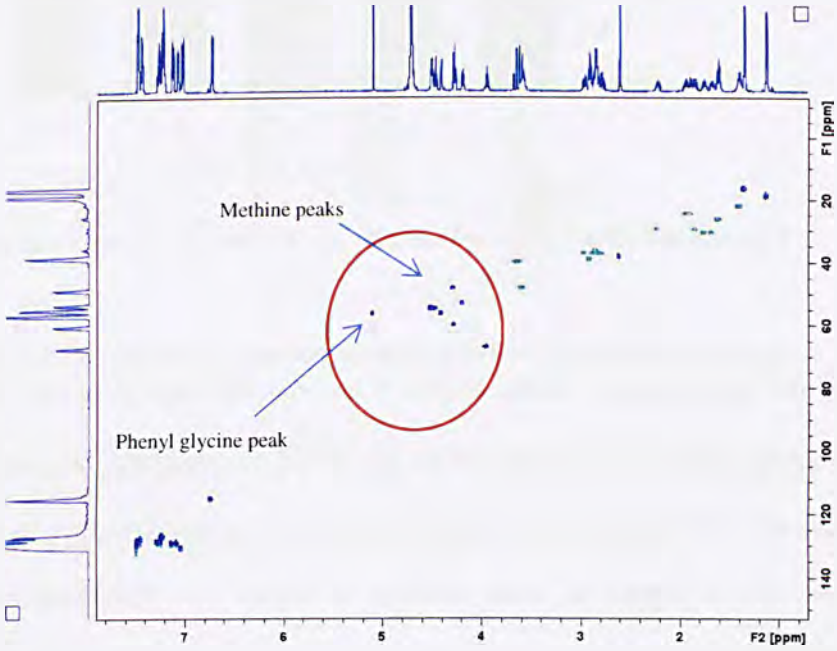

Figure 3.17 – 2D HSQC spectrum for (16), peaks used for integration are shown in the red circle. With the internal standard phenyl glycine (PG) methane peak at 5.09 ppm and the methine cluster of peaks from 3.96- 4.8 ppm. Acquired on a 600 MHz Bruker instrument using D_2O

The effect of relaxation delay was investigated on the methine peaks of the GFFYTPKA peptide, with a D1 of 1.5, 5 and 10 seconds being analysed. An initial T_1 experiment was used to determine the longest T_1 in the sample which was attributable to the phenyl glycine internal standard and gave a T_1 of 2 seconds. Therefore the default D1 of 1.5 seconds would have been insufficient; however looking at Figure 3.18 it shows that for the phenyl glycine peak, the 1.5

second relaxation delay gave the largest absolute signal area, with the smallest error indicating that a 1.5s D1 was sufficient. Further work will need to be done to fine tune the T_1 effects on this peptide,

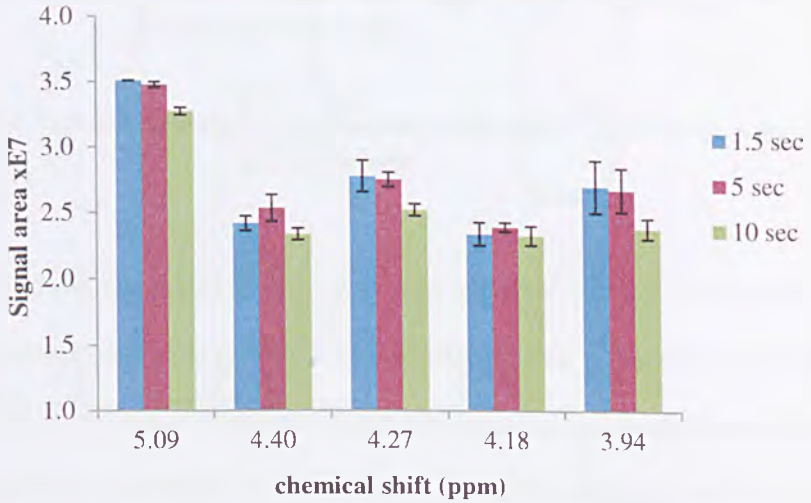

Figure 3.18 – Effect of relaxation delay on the internal standard and peaks of GFFYTPKA (17)

Using the three model systems, reference material and peptide it was shown that T_1 has a considerable impact on the bias seen in 2D qNMR as expected. However the trends were not transferrable and showed to be sample dependant. It is therefore best to use a minimum of 5 seconds D1 to reduce T_1 error making its impact less significant on the measurement uncertainty.

3.5.4 Variation in ^{13}C-^{1}H coupling constants

Coupling constants are a measure of bond distance and angles and provides key information about the chemical shift, connectivity and the multiplicity of the molecule. Each signal will have a unique coupling constant value and if this isn't optimised there may be some attenuation of signal. Running a ^{13}C-^{1}H J-resolved (HetJRES) experiment (also developed by Ernst in 1976) the coupling constants (J values in Hz) for each signal in a sample can be experimentally determined.

The variation in C-H coupling constants was investigated using the reference material digoxin and the peptide GFFYTPKA. The default coupling constant value used 2D experiments is 145 Hz for a Bruker AV600 instrument.

A HetJRES experiment can resolve both homonuclear and heteronuclear multiplicities in the two dimensions of a 2D spectrum whilst also providing chemical shift information. A spin echo sequence is used as shown in Figure 3.19. After the initial 90° pulse there in an evolution period where evolution of chemical shifts and coupling constants occur, followed by a 180° pulse and second evolution period which refocuses the spin.

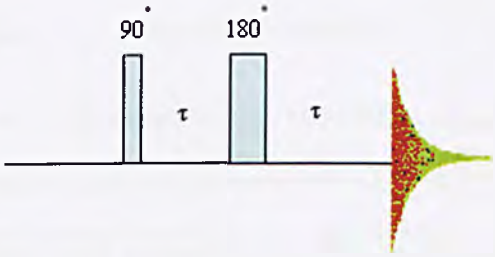

Figure 3.19 – Standard pulse sequence for a Bruker HetJRES experiment

Figure 3.20 shows the signal intensity of a few signals for digoxin when run over 125 – 165 Hz showing little impact from the coupling constant variation for most peaks.

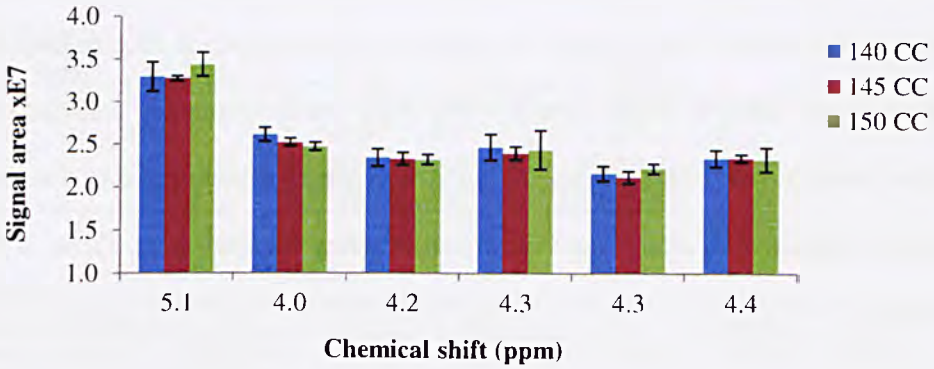

Figure 3.20 – Absolute signal intensity for some peaks in digoxin ran using coupling constant of 125, 145 and 165 Hz

For the GFFYTKA peptide the methine peaks were used to collect a HetJRES experiment (Figure 3.21) to determine the following J values listed in Table 3.6;

Chemical shift (ppm)	3.95	4.19	4.27	4.28	4.40	5.09
J value (Hz)	142	146	150	137	146	145

Table 3.6 – Experimentally determined coupling constant values for the internal standard phenyl glycine and the GFFYTPKA peptide ran using a HetJRES experiment

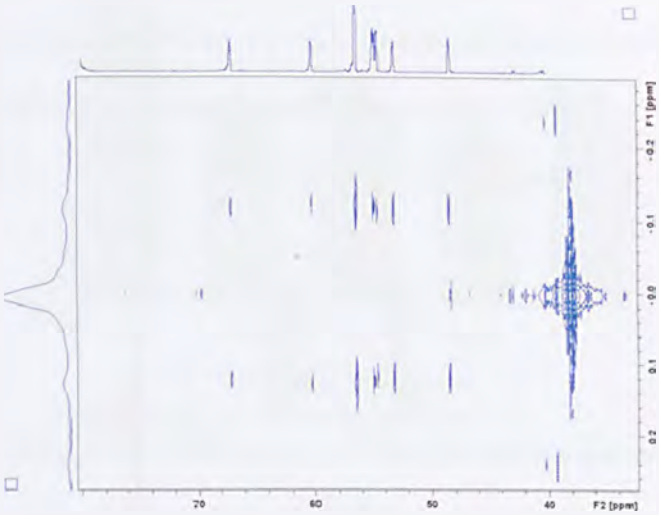

Figure 3.21 – A HetJRES experiment showing the methine peaks of interest for the peptide (16) acquired on a 600 MHz Bruker instrument using D_2O

By default the instrument is set up to run experiments with a J value of 145 Hz, however, as Table 3.6 shows the range varies between 137 and 150 Hz for the methine peaks in the peptide, therefore the default value of 145 Hz is not particularly accurate. Experiments were set up to determine the effect in signal intensity with using variable coupling constant values. Three J values were chosen; 140, 145 and 150 (a much tighter range compared to what was run for the digoxin). Figure 3.22 shows how the signal intensity for each peak varies at the different J values.

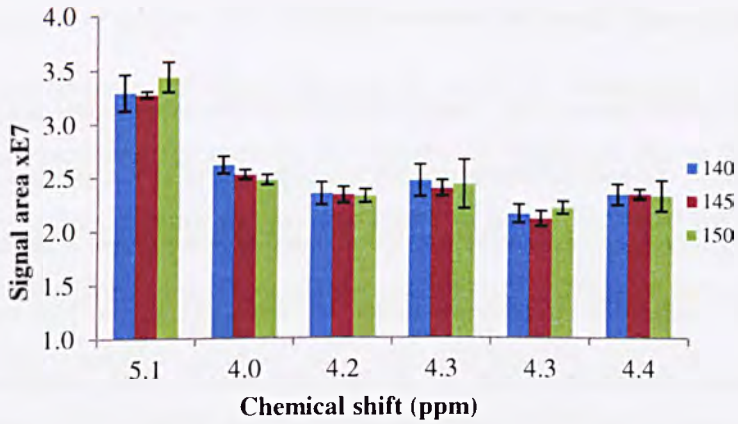

Figure 3.22 – Variation in absolute signal intensities at coupling constants of 140, 145 and 150 Hz for the peptide. Error bars showing standard deviation of three replicate analyses show insignificant variation

There doesn't appear to be a significant change in absolute signal intensity for the methine peptide peaks when varying the coupling constant from 140-150 Hz. However, for the internal standard phenyl glycine there is an obvious increase in signal intensity when using a 150 Hz coupling constant, indicating that the optimal coupling constant for the methine peaks and the internal standard are different and may need compensating for. Single factor ANOVA analysis determined the bias to be statistically insignificant as shown by the small *F crit* value.

Anova: Single Factor

SUMMARY

Groups	*Count*	*Sum*	*Average*	*Variance*
	6	26.2019	4.366983333	0.148555366
140	6	151864667	25310777.78	1.62227E+13
145	6	149464000	24910666.67	1.64216E+13
150	6	151784333	25297388.89	2.05136E+13

ANOVA

Source of Variation	*SS*	*df*	*MS*	*F*	*P-value*	*F crit*
Between Groups	2.85217E+15	3	9.50722E+14	71.53945141	7.20077E-11	3.098391
Within Groups	2.6579E+14	20	1.32895E+13			
Total	3.11796E+15	23				

Table 3.7 – Single factor ANOVA analysis of variation of coupling constants, *F crit* is smaller than the F value indicating insignificant bias

3.5.5 Resolution and signal to noise of spectra

Acquiring 2D qNMR data is time consuming as numerous experiments need to be collected for good resolution in the indirect frequency domain. The GFFYTPKA peptide was spiked with the standard phenyl glycine to assess the impact of signal to noise on the reproducibility of 2D peak integration; the higher the Hz/point the lower the resolution. Figure 3.23 shows the how the % relative standard deviation (RSD) of the methine HSQC peak integrals decreases as the resolution in the ^{13}C dimension increases. A resolution of 50Hz/point or better was shown to be required to consistently generate integrals with a % RSD less than the target of 2 %.

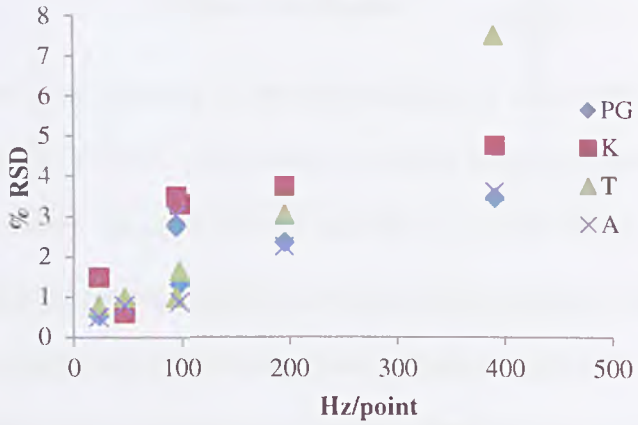

Figure 3.23 - % RSD of replicates plotted against Hz/point for four peaks in the peptide. The number of data points (TD) was varied ranging from 64-512

The impact of signal to noise (S/N) plays a critical role in the uncertainty of qNMR measurements. This is a complex area with impact from a variety of sources including noise, receiver gain amplification, digitisation and radiation damping. Whilst the bulk of the effect will be shown as Type A uncertainty and thus will be contained within the standard deviation of the replicate analyses, some potential bias may be observed between peak of significantly different line shape at low S/N and by proximity to other signals at high S/N (radiation damping).

Large S/N ratios are not practical for 2D quantifications due to both the low sensitivity of the experiment and the need to collect multiple FIDs to achieve that large S/N. The repeat HSQC

analysis of a sample of peptide GFFYTPKA was used to assess the impact of S/N on the uncertainty in determination of signal intensity for a HSQC experiment. Five repeat HSQC experiments were recorded, for each set the number of scans and the % RSD of the signal integrations were plotted against the average signal to noise calculated for that set of peaks (Figure 3.24). With a target of < 2% standard deviation, it was seen that for the selected signals a S/N of >100 was required to generate sufficiently reproducible data. For 1D qNMR analysis this would require a S/N of >4000 to generate reproducible qNMR data as seen in Chapter 2.

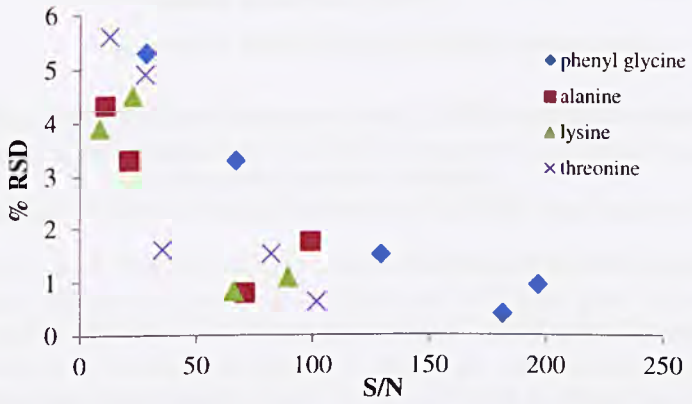

Figure 3.24 – The signal to noise was calculated on experiments ran with 2-128 scans and plotted against the % RSD of five replicate analyses. Peaks used were phenyl glycine, alanine, lysine and threonine

3.6 Time Zero HSQC

The $HSQC_0$ method was implemented on a sample of GFFYTPKA peptide and the value compared to ^1H qNMR and amino acid analysis (AAA) techniques. By back extrapolating the absolute integrals of the three increments the following graph was obtained (Figure 3.25) for the $HSQC_0$ experiment. Using the log of integral the data was back extrapolated to give a time 'zero' intensity, which would correspond to the intensities where no signal attenuation occurs. These $HSQC_0$ intensities are then put into the qNMR equation (Chapter 1 Eq. 1.1) to calculate % purity to determine the amount of peptide present in the sample.

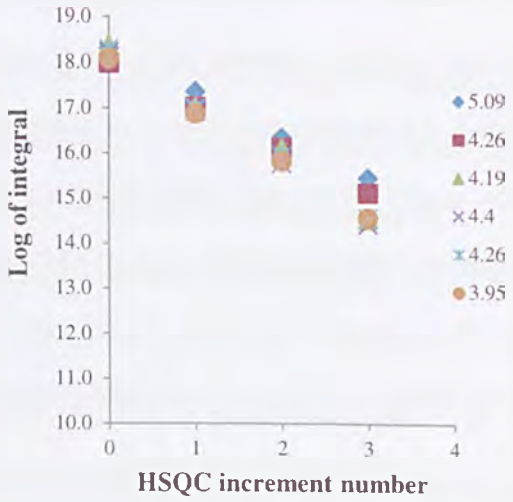

Figure 3.25 – Back extrapolated $HSQC_0$ data for peaks from GFFYTPKA which give rise to signal intensity values at time point zero

Initial experiments showed the peptide to have a purity of 64.4 % by ^{1}H qNMR, 66.0 % when using the standard Bruker HSQC experiment and 73.07 % by 2D $HSQC_0$ qNMR experiment. The AAA analysis yielded a purity of 73.1% which agreed excellently with the $HSQC_0$ results. Clearly without calibration biases are still seen in 2D standard qNMR experiments as expected (66.0% compared to 73.1%). For the NMR analysis only the methine peaks were used from the peptide and the phenyl glycine as the internal standard. The 1D qNMR experiment was already set to its optimal conditions so no further optimisation was required, yet there was nearly a 10% difference in the 1D value compared to the 2D $HSQC_0$ and AAA values, showing the benefit of using 2D $HSQC_0$.

Initially, when evaluating which peak to select from the 2D spectrum for quantification, the % purity value according to which peak was selected for integration was compared against the 1D qNMR value to assess the variation across peaks. This gave a better indication of which of the methine peaks were most suitable to use for quantification in the standard HSQC experiment. Figure 3.26 shows the variance in % purity obtained according to peak selection indicating that the peak at 3.95 ppm or 4.28 ppm most likely had similar physical properties to the internal

standard therefore gave the highest purity/signal intensity. For this reason for the 2D $HSQC_0$ analysis the 3.95 ppm or the 4.28 ppm peaks was used for quantification.

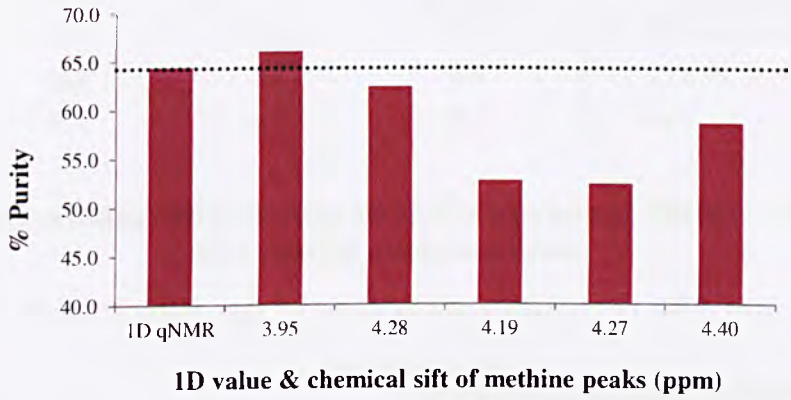

Figure 3.26 - % Purity values obtained by ^{1}H qNMR compared to 2D qNMR based on the different methine peaks selected. Dashed line shows 1H qNMR value result of 64.4 %

Figure 3.26 suggests that the two peaks at 3.95ppm and 4.28 ppm give values closest to the ^{1}H qNMR value. These two peaks correspond to threonine and alanine respectively. Possible reasons for significant variation in % purity according to chemical shift could be due to difference in T_1 values or coupling constant implications. These factors were investigated further to assess their impact. It was obvious that the choice of peaks according to their chemical shift and environment they were in played some role in the results produced.

The repeatability of the three HSQC increments was assessed by running six replicates of each. Table 3.8 shows increments 1 and 2 to have good repeatability however increment 3 gave poor % RSD for the aromatic peaks of AMP and for the anomeric GMP peak.

Chemical shift (ppm)	% RSD		
	Increment 1	Increment 2	Increment 3
5.79	0.69	0.95	3.16
5.99	0.28	0.75	1.11
8.02	1.27	1.51	8.99
8.39	1.29	0.85	7.25

Table 3.8 – Repeatability data for 4 peaks from the AMP and GMP solution using different HSQC increments (shown in Figure 3.2 (C))

3.7 Standard addition calibration

When reference standards are available for calibration of biases, a standard addition type calibration would be the easiest form of calibration. A standard addition calibration would monitor the ratio of sample to the reference internal standard to assign a response/correction factor for the signal and ultimately give a point where no bias is observed. A response factor in this case is the measure of the spectral response of the analyte signal compared to that of the internal standard. The standard addition calibration method was assessed using a simple aqueous model system of glucose and AMP and also with a commercial sample of date nectar for a 'real' sample in a complex natural product matrix.

For the simple model system, solutions of AMP with varying concentrations of glucose were prepared. These solutions were subjected to 1D and 2D standard HSQC experiments to assess if there was any significant difference between the results obtained from the two experiments. The linearity of both datasets was good as confirmed by the high R^2 (Figure 3.27). Table 3.9 shows that the response factors and R^2 values obtained from ^{1}H NMR data and HSQC data are comparable, both showing good linearity and reproducible calculated response factors close to 1. The data points from both ^{1}H and HSQC data are identical that they are indistinguishable from each other on the graph. In this simple case both methods produce similar signal responses and biases are deemed insignificant to correct for.

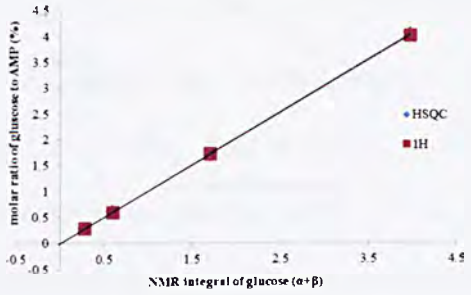

Experiment	R^2	Equation from line
1H	1.0000	y=1.0057x + 0.0005
2D	1.0000	y=1.0159x - 0.0079

Figure 3.27 –^{1}H and 2D HSQC data for simple system of glucose and AMP, Table 3.9 – Regression lines from graph

For a more complex system a commercial sample of date nectar was used to quantify the amount of glucose (α+β) in the sample using standard addition. A sample of 20 mg/mL of date nectar ('Beloved Date Nectar' sourced from a supermarket) and 12 mg/mL of internal standard AMP (Sigma Aldrich) was prepared gravimetrically. A separate stock solution of glucose (Sigma Aldrich) at a concentration of 20 mg/mL was prepared. The date nectar is more interesting as it is a real sample with an unknown concentration of glucose. To determine accurately the amount of glucose in the original sample, different levels of stock glucose was spiked to extrapolate the concentration of glucose in the original sample. An aliquot of the date was taken and spiked with the glucose stock solution at two different levels, and two individual replicate solutions prepared. A ^{1}H proton experiment and 2D standard HSQC experiment was run for each concentration and the un-spiked (Figure 3.28). When processing the 2D data for the date nectar two analysts were used to assess the user contribution to uncertainty arising from processing of data.

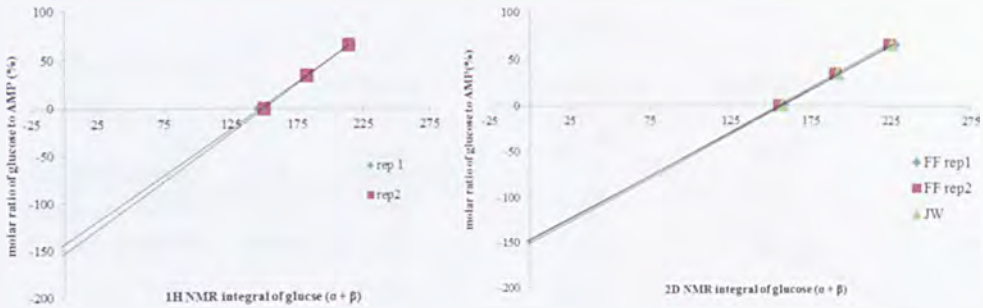

Experiment	R^2	Equation from line
1H rep1	1.0000	y=0.9699x - 143.08
1H rep2	0.9998	y=1.0237x - 153.41
2D FFrep1	0.9962	y=0.9347x - 146.36
2D FFrep2	0.9999	y=0.9537x - 148.36
2D JW	0.9998	y=0.9565x - 151.04

Figure 3.28- Left: ^{1}H data for Date Nectar

Right: 2D data for two analysts for the Date nectar

Table 3.10 -^{1}H and 2D HSQC Regression lines from both graphs

The slope of the line is calculated and represents the response factor of the signal, it indicates whether the signal from the glucose is being under observed or over observed at the different concentrations and ultimately presenting a response factor for the signal. The slope also calculates the 'concentration' of analyte in an unknown sample which has been used to determine the amount of glucose present in the date nectar sample. The ^{1}H and HSQC data are yet again comparable with very good R^2 values obtained (Figure 3.28, Table 3.10). The HSQC gave a value of 50.5% glucose in the sample and the standard addition calibrated value for the ^{1}H qNMR results gave a value of 50.8 % glucose. The uncalibrated ^{1}H qNMR value initially yielded a value of 35 % glucose in the sample confirming that the water saturation experiment was affecting the glucose signals in the spectrum and if uncalibrated would give inaccurate results caused by radiation dampening. This approach confirms that using standard addition type calibration even the standard HSQC experiment can produce accurate results as shown by the

agreement of values yielded from HSQC and ^{1}H experiments. Any variation in the replicates and analysts can be attributed to processing variation of spectra.

The 'typical' sugar content stated on the bottle and the website for the date nectar product quoted a value of 65 % sugars, which will have been determined by non-specific tests and accounted for other sugars as well as glucose. From the NMR spectra 12 other minor sugars were seen but at levels <1% therefore not quantified. Only glucose levels were quantified for these experiments, and the values obtained are reliable since the label and website values would have huge errors associated with the analyses performed. A study conducted by Walker and co-workers in 2015 showed that the nutrition labels of foods and beverages showed actual sugar content determined by gas chromatography were either <10% or >10% of the labelled total sugar quoted on the label [82]. Therefore, the values obtained by the standard addition calibration method above are in the right accurate approximation, further validated by the closeness in results of the 1D and 2D approach. This study highlights the need for accurate and effective methods to analyse components in food which are required for packaging and labelling to adhere to recommended consumption levels.

3.8 Collaborative work

The 2D qNMR validation work received substantial interest from a national measurement institute (NMI) in America; The National Institute for Standards and Technology (NIST). NIST have a similar function as LGC but within the USA. They are a government funded organisation who is mainly involved with the development of reference standards and undertaking government projects. A well-known project NIST has worked on is the report for the 9/11 collapse of the world trade centre's where they had to determine the primary cause of the collapse of the world trade centre's [83]. NIST would like to use qNMR for complex matrices especially to assist the Drug Enforcement Agency (DEA) of the US to find a quicker and simpler method to quantify and identify complex unknown compounds.

I was invited for a one month's secondment to NIST where we tried to set up and implement the $HSQC_0$ method on their Bruker Avance 600 MHz instrument using the following compounds;

- Vitamin E (alpha-tocopherol)

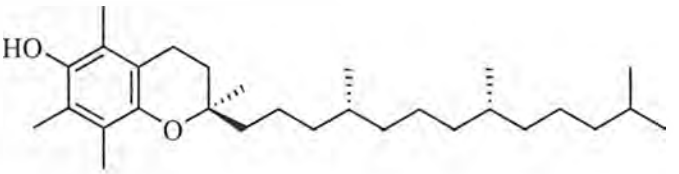

(17)

- Cholesterol

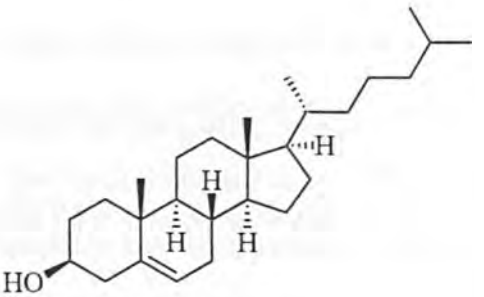

(18)

- Caffeine

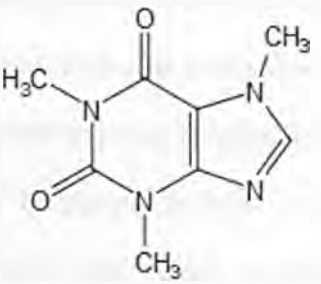

(19)

- Methamphetamine

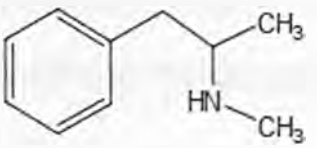

(20)

The aim was to implement the $HSQC_0$ method on their instrument; successful set up of the $HSQC_0$ method was achieved and ran perfectly with the above compounds using maleic acid, durquinone and dimalonic acid as internal standards. Sample preparation protocols were also assessed in an attempt to standardise sample preparation steps as this is the greatest source of error during qNMR. Each NMI has different sample preparation protocols and having witnessed NIST's protocol was an indispensable benefit to the project. From sample preparation (sample size used, weighing methods, balance practises), handling of reagents/lab tools to data acquisition (pulse programs used, relaxation delays and number of repeat experiments) were marginally different to LGC's practices nevertheless key strengths were seen at NIST which could easily be incorporated to practises at LGC.

Although the sample diversity gave an interesting outlook on biases arising from sample related effects the secondment was only for one month, therefore there was limited scope for validating the method further using a common compound of interest between NIST and LGC. Future work is intended where a sample of common interest would be supplied to both institutes for analysis by $HSQC_0$ and potentially coordinate PT schemes or round robin tests with more institutes involved.

3.9 Optimising experiment time

One of the largest drawbacks to 2D qNMR is the impractically long experiment times encountered for each experiment (from 2 hours to 5 hours) due to the multiple FID required for adequate resolution. Reducing the number of scans or data points acquired can potentially infringe in the resolution and quality of spectra.

3.9.1 Increment experiment

The impractical experiment times caused when running three increments for the $HSQC_0$ experiments meant that there was insufficient time to run multiple replicate analyses therefore the necessity of running all three increments was explored. Ideally, if the same result could be obtained by running only two increments the run time would be reduced from 4 hours to 3 hours

per experiment (which could be reduced further by optimising the number of scans and data points acquired). It was found that even samples with limited availability due to high production costs or expensive to obtain, two increment $HSQC_0$ experiments were sufficient for sufficient sensitivity with higher number of scans. Sensitivity of the third increment for these types of samples was very poor due to low concentration of sample and added no value to the dataset unless long scans and high data point acquisition was run to be able to extract data with decent sensitivity. Where sample size was not limited the concentration of solution was increased to a minimum of 30 mg/mL in order to achieve decent sensitivity with a short number of scans and this made running the third increment with a short number of scans possible. The value of the third increment to the result was investigated and found to have an insignificant impact therefore for most experiments only two increment $HSQC_0$ experiments were run.

3.9.2 Processing methods

A new development in the processing of spectra has emerged and is used to cut down experiment time significantly. Non uniform sampling (NUS) methods are widely available on major NMR processing platforms and reduce experiment time by not collecting all the data points from the experiment then predicting the uncollected data points from the data collected. Sparse sampling allows the user to define the amount of data points to collect and the amount the software will need to reconstruct. Sensitivity is increased by collecting more data points (% sampling) where the signal has the highest amplitude [84]. The impact of NUS on the accuracy of measurement and its uncertainty was assessed. It is assumed that the closer to full sampling schemes would generate lower uncertainties therefore the point at which NUS data is no longer deemed suitable was explored.

Multi-dimensional decomposition NMR (MddNMR) is the program used, which allows the missing data points to be reconstructed, which then enables a Fourier transformation of the entire dataset including the missing data points to give a complete spectrum. The two modes under this program used for processing is multi-dimensional decomposition (MDD) and

compressed sensing (CS) modes. After conferring with the Bruker applications team it was advised to use the CS mode for processing as this copes better with sparse datasets and a higher fraction of the original data is recovered [85].

The compounds below were analysed to assess the applicability of NUS to quantitative measurements.

- Glucose (Sigma Aldrich)
- Aldosterone (Sigma Aldrich)
- Celiprolol (British Pharmacopeia at LGC)

Data was collected using the sampling schemes of 25, 50, 75, and 100 % where 100 % is just the standard HSQC with no NUS application. To increase sensitivity further experiments were run using the NUS mode but changing the size of the FID (TD) in the F1 dimension, collecting FIDs of 256 (default), 512 and 1K. For the 1K dataset further reduced sampling schemes of 10 and 15 % were also investigated. Sampling schemes of below 25 % have reported to produce poor spectra due to T_1 noise, which could be overcome with using Poisson-gap sampling where sampling is controlled to minimise gaps between points used [86]. However, for the lower sampling schemes used here standard NUS processing was applied. Low sampling schemes (<25%) is also reported to compromise the accuracy of the peak position, which could be problematic for repeatability and precision studies. From the spectra processed two peaks were chosen to highlight the trends observed from each compound. Figures 30-31 show the absolute signal intensity across the sampling range at different FID data collection points (TD). The replicate experiments were run over three different days.

For glucose, AMP was used as the internal standard and there was an obvious trend in increasing signal area with increasing % sampling amount with good repeatability shown across the three replicates. The 1K TD datasets showed a large deviation at the lower end of the sampling % range for the 8ppm peak (Figure 3.30), and may need reprocessing with baseline correction and manual phasing to further optimise the values. In general, a 15 % sampling

amount gave similar values to the 25 % sampling amount, no major or consistent trends were observed and the uncertainty (% RSD in this case) seemed similar for the different sampling schemes. However, sampling schemes below 15 % are not recommended due to the high % RSD observed between replicate analyses attributable to the high background noise in the spectra. Although using NUS saved valuable experimental time it was found that transforming the 50 % and 75 % sampling amount FIDs took between 5-10 minutes to Fourier transform due to more data points needing to be predicted/reconstructed.

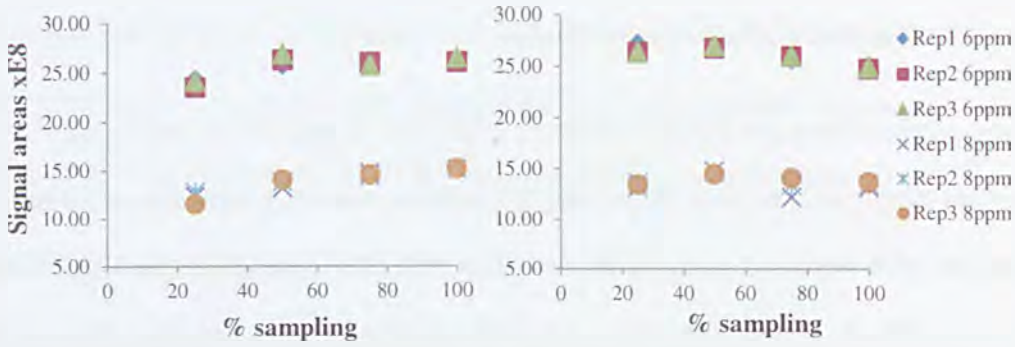

Figure 3.29 – Data comparing signal intensity to the % Sampling levels for Glucose (6ppm) AMP (8ppm) peaks

Left: NS 8, TD of 512 (3 replicates)

Right: NS 8, TD of 256 (3 replicates)

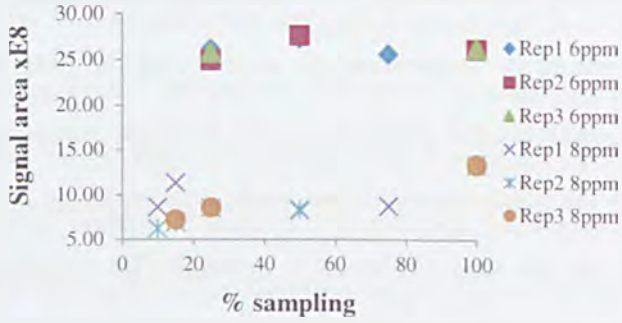

Figure 3.30 – Data comparing signal intensity to the % Sampling levels for Glucose (6ppm) AMP (8ppm) peaks; NS 8, TD of 1K (3 replicates)

Aldosterone (**21**) and Celiprolol (**22**) were chosen for their complexity and the feasibility of NUS sampling on compounds where multiple peaks were assessed. They both showed similar trends as to Glucose therefore the use of NUS for quantitative analysis was deemed acceptable to use across a range of molecules, with a range of sampling schemes all with the benefit of

significantly reducing experiment time. Both aldosterone and Celiprolol were assayed against DMT (Sigma Aldrich) as the internal standard. As the results showed similar trends only the results for Aldosterone are shown below for the TD of 1K dataset, displaying trends of one aldosterone peak and the DMT peak. For aldosterone and celiprolol the % RSD on three replicates of each experiment was generally less than 1 %, which showed that the NUS method worked really well for even moderately complex samples. The glucose % RSD varied from 0.5-3.0 % showing greater error in potentially integration of the data or error in the predicting mechanism of the software.

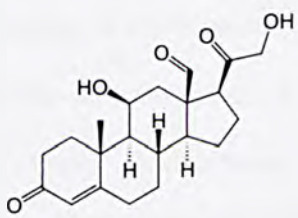

(21)

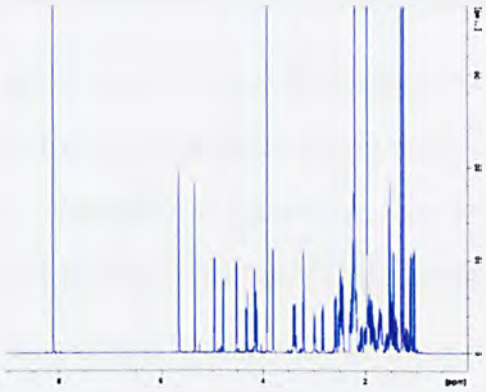

Figure 3.31 – ^{1}H spectrum of aldosterone spiked with DMT in CD_3CN acquired on a 600 MHz Bruker instrument

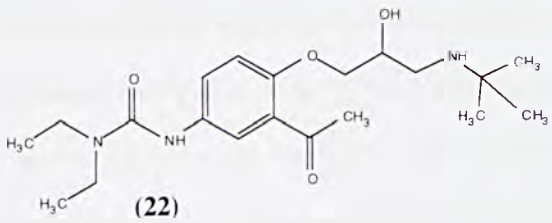

(22)

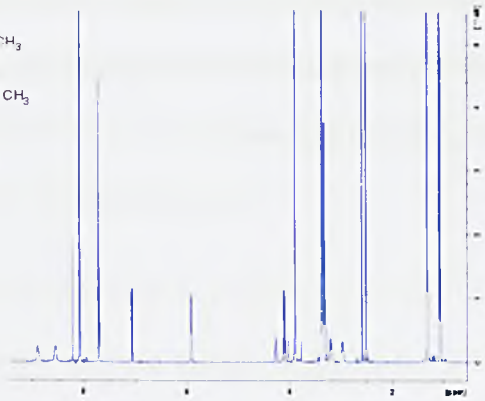

Figure 3.32 – ^{1}H spectrum of Celiprolol spiked with DMT in DMSO-d_6 acquired on a 600 MHz Bruker instrument

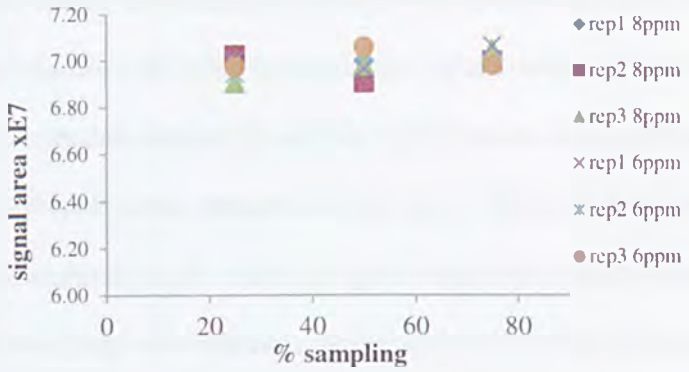

Figure 3.33 – Data comparing signal intensity to the % Sampling levels for Aldosterone (5.6 ppm) DMT (8 ppm). NS 8, TD 1K

3.10 Analyst contribution to uncertainty

Other than the experimental bias there are two principle sources of uncertainty in quantitative experiments; errors from processing spectra and analyst to analyst contribution. To determine the impact of user contribution to uncertainty a set of NUS acquired NMR spectra were processed and analysed by two individual analysts, and the deviation compared. Analyst 1 and Analyst 2 processed the same batch of data containing three replicate analyses of one sample set and the % RSD was reported. Although the mean signal area obtained was similar for both analysts using the same software, the maximum % RSD from a set of three replicate analyses was 1.5 % and 7.7 % for Analyst 1 and Analyst 2 respectively. This indicated significant analyst/user contribution to uncertainty and ultimately the overall result predominantly due to issues in the phasing and baseline correcting of cross peaks. Figures 3.34 and 3.35 show the data plotted for the two analysts.

Figure 3.34 – NUS Results for Analyst 1: Glucose (5.1 ppm) AMP (5.9 ppm); NS 8, TD 512

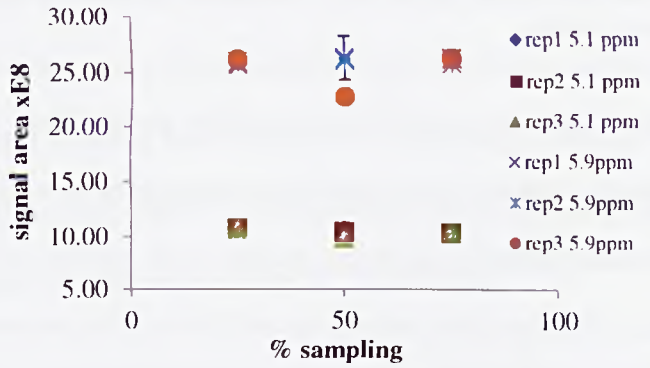

Figure 3.35 – NUS Results for Analyst 2: Glucose (5.1ppm) AMP (5.9ppm); NS 8, TD 512

3.11 Conclusion

HSQC zero is clearly going to be preferable when we have no pure standard to compare against as we cannot calibrate for any nonlinear response, this will be the case in the peptide and more complex samples. Looking at complex mixtures such as amino acids in food supplements where there are readily available pure standards an internal calibration type experiment such as standard addition can be carried out to account for any attenuation of signal. If there are no internal standards available then biases need to be predetermined.

In order for this to work there needs to be consistency between different solutions i.e. a constant bias between measurands. The major concern was the sample dependence on biases seen. Trends were not consistent between samples; therefore if calibration approaches are not used biases need to be fully investigated for that sample to minimise errors.

It has been found that in most cases two increments are sufficient to acquire accurate data for $HSQC_0$ experiments with the option to optimise further to achieve shorter experiment times. The $HSQC_0$ experiment works well for simple molecules however, requires optimisation of J C-H prior to use for complex samples such as peptides. The applicability of NUS to further reduce experimental time proved useful at sampling schemes greater than 15 %, however, this needs to be confirmed for constant time HSQC experiments as it was only run on standard Bruker HSQC experiments, but in principal should have the same effects. This would save time for simple 2D quantitative measurements.

Linearity and reproducibility proved to be successful giving values of >0.995 % and <1.5% respectively on the compounds investigated for concentrations between 0.25-50 mg/mL. This is in line with traditional validated approaches such as HPLC and GC, where a requirement of the above criteria is used to deem data suitable or not. For complex molecules such as peptides the $HSQC_0$ method will need optimisation prior to running the experiments. Parameters such as the coupling constants and relaxation delay will need to be corrected for. For small molecules and peptides in the molecular weight range of 1000 g/mol HSQC experiments with a D1 of 3 seconds and coupling constant value of 145 is deemed sufficient for accurate results.

The greatest sources of error were found to be from the acquiring of data using insufficient resolution in the ^{13}C dimension, insufficient S/N of data, inadequate T_1 and badly matched coupling constant values. The analyst to analyst variation was also seen to be significant for processing of data. In order to minimise these uncertainties appropriate optimisation of parameters is needed as required for 1D qNMR but more critical in 2D cases due to the complexity of the data and spectra. Better guidelines are also needed to reduce analyst induced processing bases.

Chapter 4 Applications

4.1 Background

qNMR has a widespread role in industry and research institutes, providing state of the art measurement science for users worldwide. As little as six years ago, reported use of NMR as a quantitative tool was scarce outside of a few niche areas with little confidence in the results, however over the years the mind-set of measurement scientists has changed, with more papers published showing how to achieve smaller errors with qNMR measurements. Applications and the role of qNMR in industry will be discussed in this chapter with the focus on metrological applications and forensic applications.

It is imperative that worldwide harmonisation of measurement is achieved, as legislation and important decisions in trade, commerce and society depend on these measurements. For most chemical analysis this can be achieved by ensuring that measurement results are traceable to a known reference such as the base units of the Système International d'Unités (SI). By maintaining such a link, results can be compared over time and space enabling informed decisions to be made and minimising the social and economic consequences. However, whilst the required metrological tools such as reference measurement procedures and certified reference materials are established for small molecules, difficulties still remain in the provision of such standards in the area of larger molecules such as peptides/proteins, macrolides and large complex organic molecules.

The provision of Primary Calibration Reference Services has been identified as a core technical competency for National measurement institutes (NMIs) to allow them to disseminate SI traceability into their respective countries [87]. NMIs providing measurement services in organic molecules and peptide/protein analyses are expected to

have ISO 17025 calibration accreditation for the experimental techniques they use and Guide 34 accreditation for the production of reference materials. In addition to this, they need to participate in a limited number of comparison studies that are intended to test and demonstrate their capabilities in the relevant areas. These international inter-laboratory studies take place amongst the major National Measurement Institutes signed up to the metre convention including those from the USA, Germany, Japan and China and are classified as Consultative Committee on the Quality of Material (CCQM) studies which are usually co-ordinated by the Bureau International des Poids et Mesures (BIPM) in Paris. Primary Calibration Reference Services refers to a technical capability for composition assignment, usually as the mass fraction content of an organic molecule in the form of high purity solids or standard solutions thereof.

Over the course of this PhD I have participated in numerous CCQM studies representing the UK's designated institute within the LGC facility at Teddington which have further helped validate the quantitative aspect of my work. The samples ranged from simple molecules to peptides and each study was designed with the aim to produce a qNMR best practice guide for NMI's and reference material producers all over the world to use as reference for good NMR practice.

4.2 CCQM studies

The ability to undertake suitable purity assessment on materials that are to be provided as pure substances or calibration solution reference materials or are used as the internal primary calibrators of measurement services is considered essential for the provision of SI-traceable measurement services in organic analysis. CCQM comparison studies allow NMIs and DIs to provide objective evidence that the procedures they use for purity assessment, and the property value with its associated uncertainty that is assigned, as a result of the application of their procedure, are suitable for their intended purpose.

Comparison is intended to demonstrate a laboratory's performance in determining the mass fraction of the main component in a high purity organic material. The measurement results should be indicative of the performance of a laboratory's measurement capability for the purity assignment of organic compounds and the outcome is usually in the form of reports addressing key measurement problems, which can later be disseminated to smaller local labs.

For the CCQM studies reported in this chapter a range of samples were analysed over 5 years, varying in molecular size and complexity. The common NMI's who take part in CCQM studies and to whom results are compared to are given below;

- LGC (UK)
- Bureau International des Poids et Mesures (BIPM) (France)
- National Institute of Standards and Technology (NIST) (USA)
- National Metrology Institute of Turkey (UME) (Turkey)
- Instituto Nacional de Metrologia, Qualidade e Tecnologia (INMETRO) (Brazil)
- National measurement institute of South Africa (NMISA)
- National measurement institute of Australia (NMIA)
- Centro Nacional de Metrologia (CENAM) (Mexico)
- National Research Council Canada (NRC)
- D.I. Mendeleyev Scientific and Research Institute for Metrology (VNIIM) (Russia)
- Institute for Reference Materials and Measurement , IRMM (Belgium)
- Bundesanstalt für Materialforschung BAM (Germany)
- Korea Research Institute of Standards and Science KRISS (South Korea)
- National Metrology Institute of Japan (NMIJ)
- Health Sciences Authority HAS (Singapore)
- Government Laboratory of Hong Kong SAR (GLHK)
- National Institute of Metrology (NIM) (China)

- Laboratoire National de Métrologie et d'Essais (LNE) (France)
- National Institute of Metrology (NIMT) (Thailand)
- National Metrology Laboratory (SIRIM) (Malaysia)
- Instituto Nacional de Tecnologia Industrial (INTI) (Argentina)
- Hellenic metrology institute (EXHM-EIM) (Greece)

Historically the purity related CCQM studies for mass fraction of a sample has been carried out using traditional analytical techniques such as High performance liquid chromatography (HPLC) or gas chromatography (GC) to look at chemically related impurities in combination with additional analyses for water, solvents, inorganic constituents *etc* and known as the mass balance approach (100-imps technique). qNMR was rarely applied and many NMIs didn't even have access to an NMR spectrometer. However, a handful of institutions (commonly around five) did submit complimentary results along with the mass balance results to confirm their value using an orthogonal method, with the result even then being overlooked.

It wasn't until the results CCQM (k55.b) on Aldrin **(23)** were reported that the power of NMR was finally demonstrated to the international NMI community with participants starting to consider qNMR as a viable technique for high quality purity certification and perhaps even more robust than the traditional techniques. Figure 4.1 shows the results from Aldrin across the NMIs and clearly shows a discrepancy between the mass balance approach and the NMR results. The mass balance approach (Figure 4.2) included combined results from HPLC, GC and DSC analysis. During the initial stage of reporting results the majority of the NMIs disregarded the NMR results whilst the results were being investigated. NMIJ was the only NMI which detected the presence of a significant non-volatile organic impurity, which was not reported by any other laboratory. The final investigation showed that there was a polymer in the sample which wasn't accounted for in the mass balance approach but was accounted for in the NMR approach.

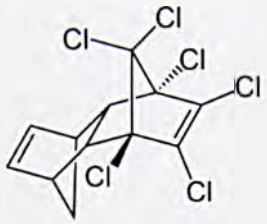

(23)

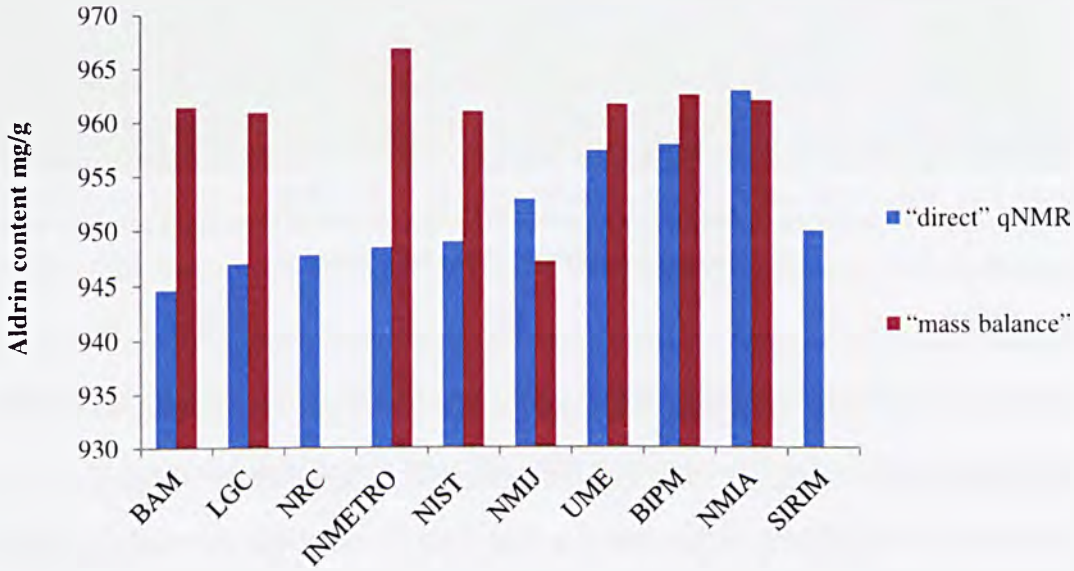

Figure 4.1 – qNMR *vs* mass balance results for Aldrin for each NMI

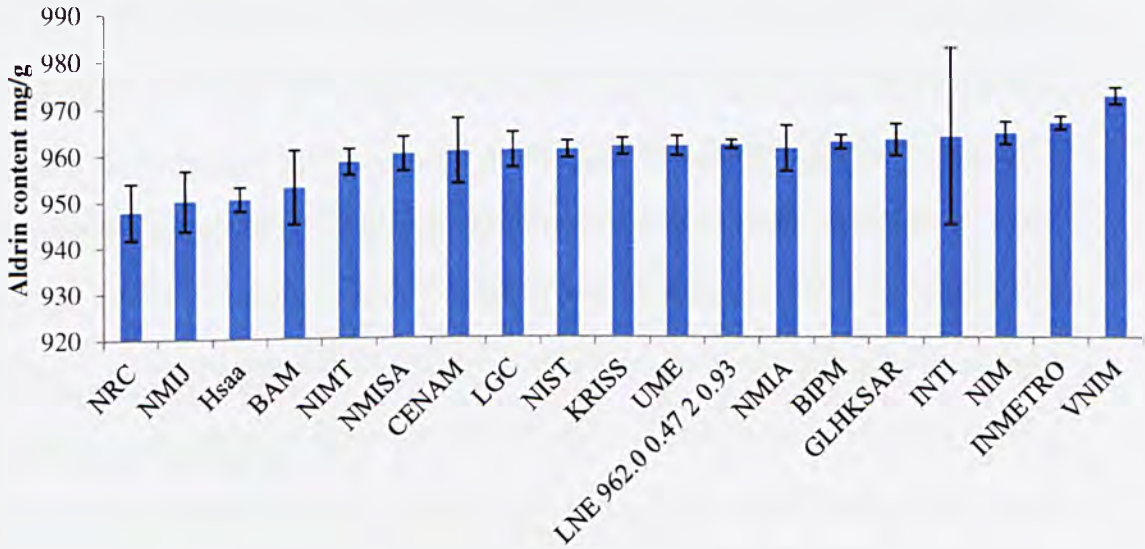

Figure 4.2 – Complete set of mass balance results from NMIs

The Aldrin CCQM was performed by myself before the start of this thesis however, subsequent CCQMs reported are within the scope of this thesis.

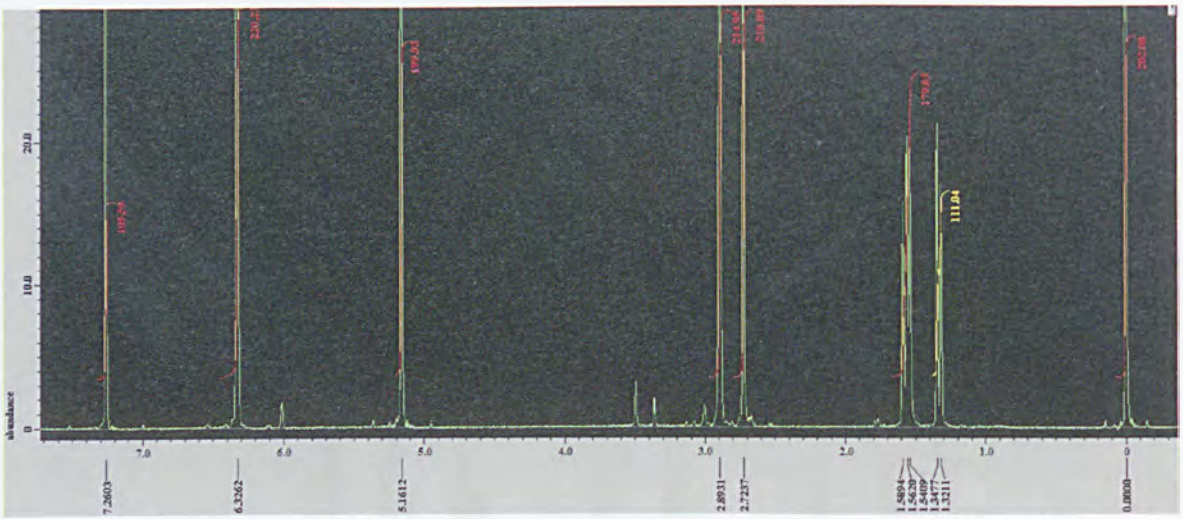

Figure 4.3 – ^{1}H spectrum of Aldrin run on a 400 MHz instrument at Kingston University using the processing software Delta for processing

4.2.1 Valine

L-Valine was selected as the measurand for the first CCQM comparison study performed during this thesis and was the first time that LGC participated in an international comparison using qNMR, in this case as a pilot study in addition to the traditional direct method with both approaches being performed by the author. This study was chosen not only as a part of LGC's requirement to demonstrate competence in the low molecular weight, high polarity quadrant of the BIPM chemical space as outlined in the OAWG (Organic analysis Working Group) strategy document but important as an amino acid in LGCs move into peptide and protein analysis.

The SI traceable quantitation of amino acids is a key first step in the traceability chain and purity assignment of larger peptides and proteins. The availability of properly characterized high purity amino acid standards will play a critical role in underpinning the traceability of peptide and protein quantifications that rely on MS related quantitation of peptides and amino acids derived from selective and total digestion from the proteins and thus the need for certified standards of these materials.

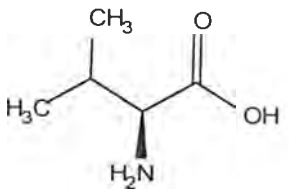

(24)

An analytical grade of L-valine **(24)** was purchased from an unknown commercial supplier by BIPM who co-ordinated the study. The certificate of analysis provided with the material describes its purity as ≥ 99.5%. The mass fraction of the main component and impurity profile of the batch was determined at the BIPM, including assessment of the homogeneity and stability of the various components. The mass fraction content of valine was determined to be in excess of 990 mg/g and the homogeneity and stability of the valine and the associated impurity components were determined as being suitable for the purposes of the comparison.

Eighteen NMIs and DIs, participated in the comparison for valine, submitting results for valine based on qNMR data compared to using a mass balance approach. Assessment of the enantiomeric purity of the material was not required. When using the mass balance approach the following sub-classes of impurities were reported for valine:

i. total related structure organic substances

ii. water

iii. residual organic solvent

iv. total non-volatiles/inorganics

qNMR analysis was a key focus for the study and was used:

1. as a stand-alone, "direct" method to assign the valine mass fraction content

2. to provide an independent estimate of valine content that was combined with other assignment methods (e.g. mass balance)

3. to obtain supporting data for a mass balance assignment.

4.2.1.1 Experimental method

The mass balance approach was developed within LGC by myself using HPLC, KF, TGA and HSGCMS. The direct approach using qNMR used internally standardised assays to determine the % content of Valine and structurally related impurities using protocols from Chapter 2. The amino acid impurity standards for known impurities in Valine were purchased in from Sigma Aldrich and spiked in to evaluate their content. All solutions were prepared gravimetrically using a minimum of 10 mg for each preparation. For the qNMR D_2O was used as the solvent and a minimum of 10 mg of benzoic acid (**25**) as the internal standard. The experimental parameters used were NS:16, D1: 30s and a SW of 20.5 ppm.

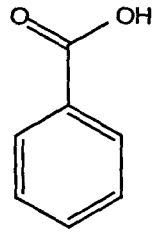

(25)

4.2.1.2 Results

For the direct assignment of valine content by qNMR the signal due to either beta CH was used for quantification which gave a T_1 of 0.8 seconds when using an internal standard of Benzoic acid, Benzoic acid itself had a T_1 of 2.0 seconds.

The main issues with quantification were that there was related impurities under all the other signals impeding on using them for quantification. To assess and identify these impurities standards were brought in to show this. As the beta CH was the only peak free of imps

This was selected for quantification. The mass balance approach involved using GC-FID techniques and derivitising Valine prior to analysis. The mass balance results and the

qNMR results for valine reported by each participant are shown in Figure 4.4. The reference 'true' value was established as 992 +/- 0.3 mg/g by BIPM which is shown by the red dashed lines.

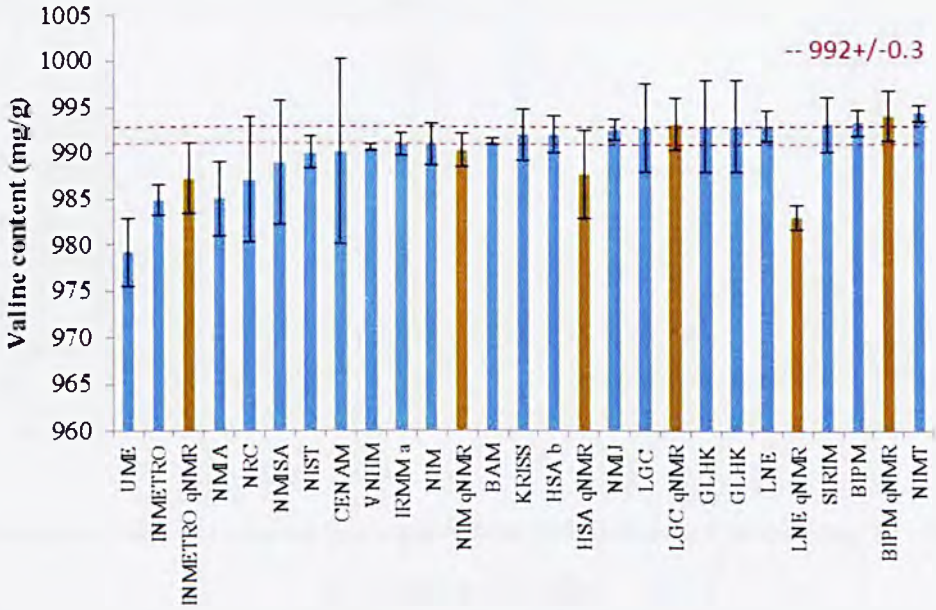

Figure 4.4 – qNMR and mass balance results for Valine. Red dashed lines indicate the reference 'true'value. NMI's results within the red lines all reported the correct value

Five impurities were quantified as being in the valine sample; L-alanine, L-leucine, L-isoleucine, aminobutyric acid and L-methionine. The impurities were quantified using the appropriate methods by each NMI and reported, in our case standard addition using the impurity standards which were bought.

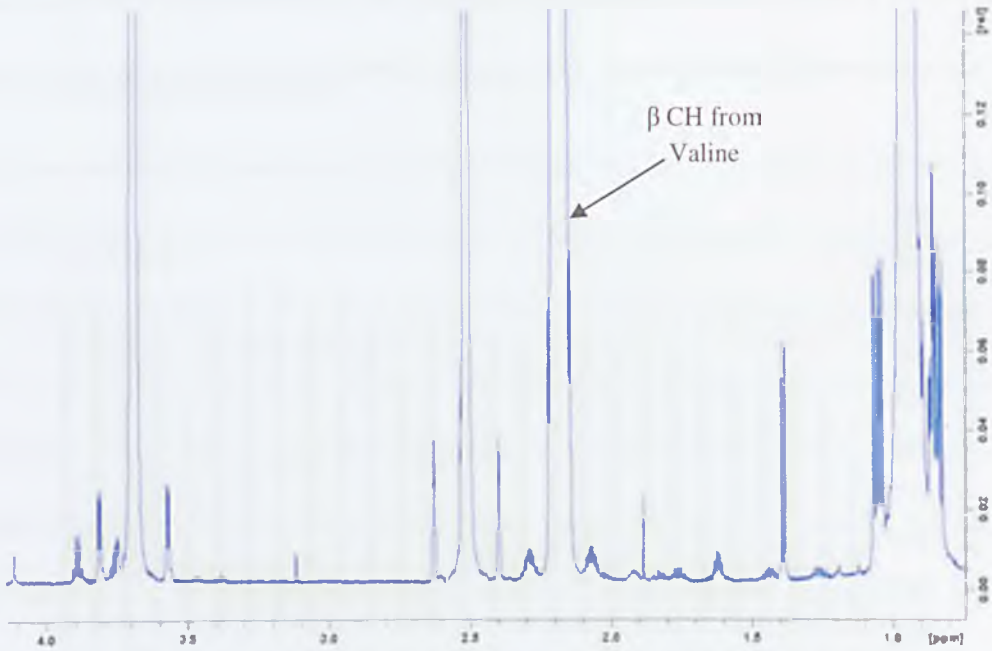

Figure 4.5 – ^{1}H spectrum of Valine in DMSO-d_6 showing signal used for integration acquired on a 600 MHz Bruker instrument

From the study, there was a clear spread of results across the different NMIs in both the mass balance approach and the qNMR approach indicating that even for a simple molecule like valine greater efforts was required to standardise measurement across the NMIs. The values reported ranged from 979.2 – 994.3 mg/g (shown clearly in Figure 4.4).

4.2.2 Dimethyl Sulfone

The spread in results from the Valine study prompted a qNMR pilot CCQM study to assess the source of the variability from qNMR across the NMIs, this was a feasibility study and not a requirement for NMIs to participate in. The study was coordinated by the national measurement institute of Japan (NMIJ) with the reference 'true' value generated by both NMIJ and LGC (UK) through traditional indirect assay. Strict guidelines on how to prepare, run and process the data for NMR was provided by NMIJ and all raw spectra were then sent to NMIJ who later processed the spectra independently and reported the findings. The internal standard used was 3,5-bis(triflouromethyl)benzoic acid (3,5-BTFMBA) **(26)**

supplied by NMIJ. Figure 4.6 shows the structure for the $DMSO_2$ **(27)**, the internal standard used **(26)** and a representative spectrum. The individual NMI spectrometer used and manufacturer of spectrometer was also documented, with the majority of NMIs using a Bruker instrument with a few Varian all ranging from 400-800 MHz.

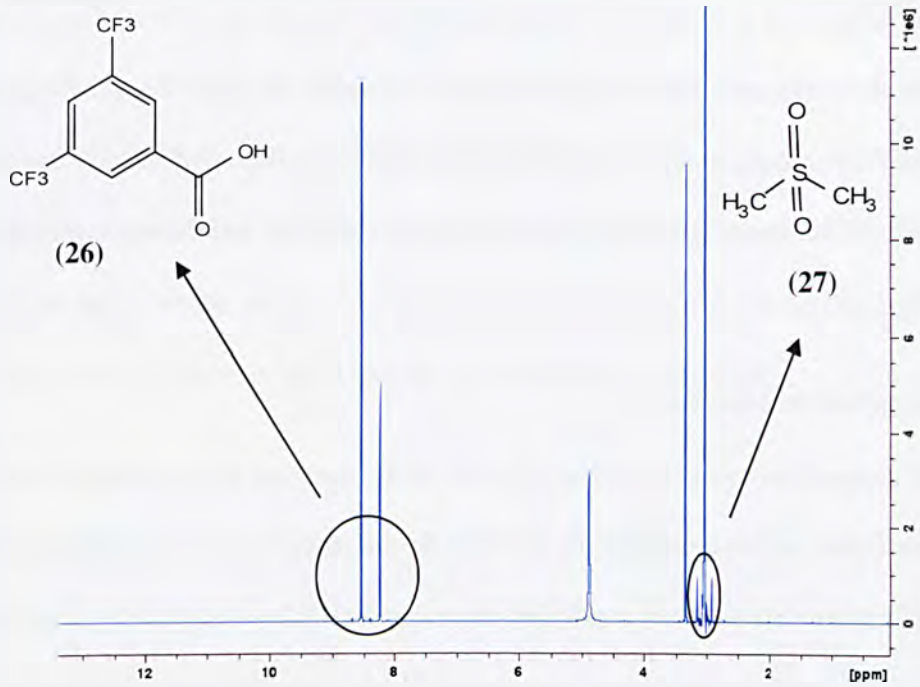

Figure 4.6 – ^{1}H spectrum of $DMSO_2$ (27) and 3,5-BTFMBA (26) in methanol-d_4 acquired on a 600 MHz Bruker instrument

For the sample preparation a minimum sample size of 5 mg was recommended weighing on a four figure balance or higher. A ^{1}H qNMR experiment was to be run with no ^{13}C decoupling, however all other instrumental paramters such as relaxation delays were left for each NMI to independantly optimise and determine.

The reference value was determined by LGC and NMIJ *via* a mass balance approach using gas chormatography. The reference impurity content was determined by Karl Fisher titration, thermal gravimetric analyser and head space GCMS techniques using Equation 4.1.

$$P_{ref} = 1 - (C_{Org} + C_{VOC} + C_{water} + C_{redidue})$$

P_{ref} : Purity of $DMSO_2$
C_{Org} : Components of non-volatile organic compounds
C_{VOC} : Components of volatile organic compounds
C_{water} : Component of water
$C_{redidue}$: Component of residue

Equation 4.1

The provisional reference value was determined by NMIJ as 999.73 ± 0.18 mg/g which equates to 99.97 % m/m, and by myself at LGC as 999.55 ± 0.56 mg/g which transcribes to 99.96 % m/m, combined the reference value used for the study was determined to be 999.64 ±0.84 mg/g.

4.2.2.1 Experimental method

The NMR parameters were disclosed by each NMI, showing the breadth of variation in acquisition. Table 4.1 captures this information, as the study has not been published yet the other NMI information has been concealed other than LGCs.

Paticipant	spectral width (ppm)	Acquisition points	Acquisition time (s)	Transmitter offset (ppm)	Pulse angle	Relaxation delay (s)	Number of scans
A	15	128K	7.3	5.5	90	73	16
B	12	288K	20	5	90	40	8
C	12	128K	9	5.5	90	35	128
D	10	66K	8	6	30	30	80
E	16	33K	3.4	6	90	40	32
F	15	33K	2.2	5.5	90	44	64
G	15	66K	2.7	6	90	60	16
H	20		4.1	6.175	90	30	32
I	100	238K	4	5	90	60	32
J	12	85K	10		90	55	8
LGC	20	128K	5.3	6.2	90	60	16
K	7.3	128K	11.2	6	90	30	16
L	20	132K	5.5	6.175	90	60	64
M	30	128K	4.45	6	90	52	32
N	14	128K	7.7	6	90	30	32
O	9.5	34K	3.4	5.8	90	28	32
P	20	64K	3.28	6	30	20	16
R	12		6.8	6	90	30	16

Table 4.1 – Experimental acquisition parameters as reported by each laboratory

Data processing was done to each NMI's individual methodology. Integration of peaks is known to be a contributing factor to the end result, as this varies from institute to institute

and even between users within the same laboratory [88]. Many NMI's did automatic phasing whilst others chose to do manual phasing. The baseline corrected ranged from using a polynomial, Whittaker smoothing quadratic algorithms as well as automated correction.

The integration of peaks ranged from including the ^{13}C satellites to integrating within them, but all NMI's managed to integrate over a range of 160 or more Hz of the peak at half height, with UME and FTMC using only 120 and 80 Hz respectively. These sources or biases and uncertainties were all assessed during the early stages of this PhD study and selective parts of the work were presented at a workshop within the CCQM Organic analysis sub-committee in 2014 to help the evaluation of the results.

4.2.2.2 Results

The ^{1}H qNMR results obtained by the NMIs who participated in this study are shown anonymised in Figure 4.7. The red dotted lines indicate the uncertainty tolerances deviating from the reference value and only six results were within the red dotted lines (shown in Figure 6). Again this study showed that there was a significant distribution of results across the different NMIs with a maximum deviation of 9 % away from the reference value.

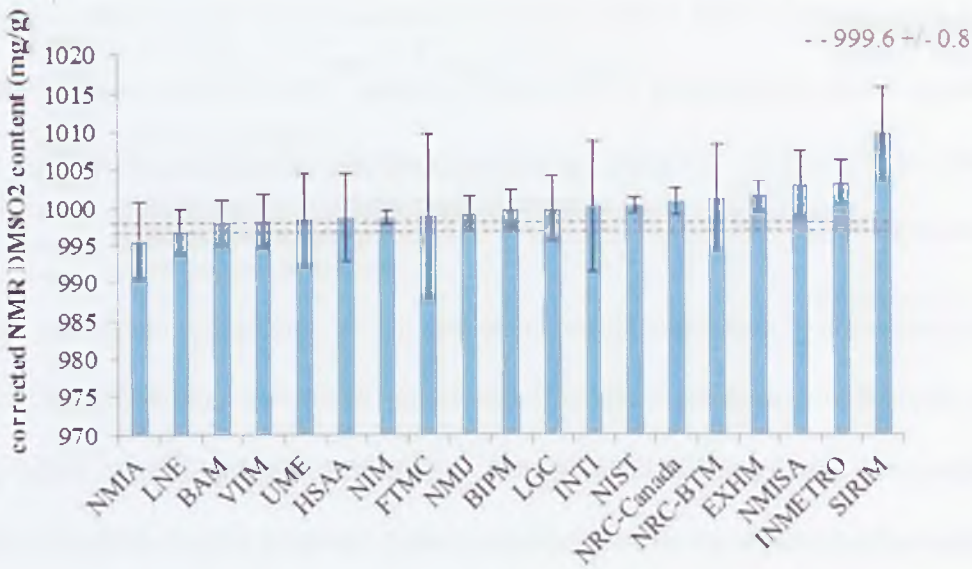

Figure 4.7 – qNMR results for the content of $DMSO_2$ corrected for the purity of the internal standard

From analysing the data and information submitted on how the samples were prepared, the greatest source of error seemed to come from the resolution of the balance used and sample preparation. In the reporting of the results, this lead to recommendations from a well-known paper being cited and ultimately given as guidance for sample preparation to all the NMI's (Figure 4.8) [89].

NMI's using a four figure balance or less had the greatest deviation from the reference value with large errors as expected.

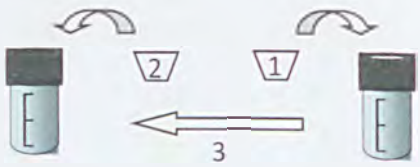

Figure 4.8 - Sample preparation recommendation; 1: prepare a stock solution of solvent and internal standard. 2: Weigh sample into vial. 3: Add stock solution to vial with sample in

The first qNMR pilot CCQM study was successful and informative about the sources of major errors in measurement. A qNMR best practice guide is being drafted by NMIs

including LGC through data and conclusions generated during this PhD. This will include work from many CCQM studies and is aimed to act as a document detailing recommendations on measurement practises and parameters for NMIs, reference material producers and accreditation bodies worldwide ensuring harmonisation of qNMR measurements across time and space.

4.2.3 C-peptide (hCP)

Human C-peptide (hCP) **(28)**, a short (1 kDa to 5 kDa), non-cross-linked synthetic peptide was proposed as the measurand for a Key comparison study K115 and pilot study P55, to look at peptide purity. Human C-peptide is defined as human proinsulin with an amino acid sequence of EAEDLQVGQVELGGGPGAGSLQPLALEGSLQ and molecular weight of 3020 g/mol.

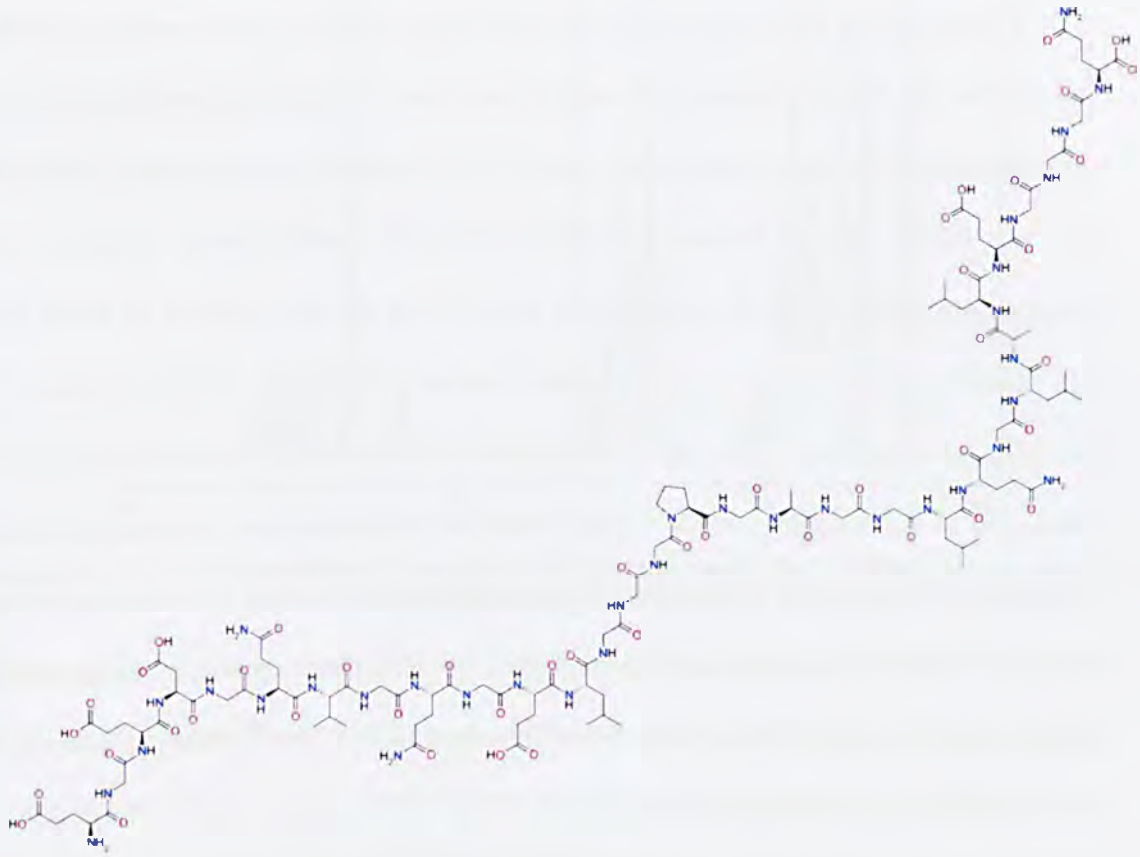

(28)

Currently quantification of peptides and proteins is routinely done by amino acid analysis (AAA) or peptide impurity corrected amino acid analysis (PICAA), a technique which can take up to a week to perform and requires quantification of constituent amino acids following hydrolysis of the material and correction for amino acids originating from impurities. It requires identification and quantification of peptide impurities for the most accurate results. Traceability of the amino acid analysis is achieved by using pure amino acid certified reference material (CRM) standards. Few pure amino acid CRMs are commercially available and they are extremely expensive, with the little quantities available, adding to the complication for the provision of traceable peptide/protein measurements.

4.2.3.1 Experimental method

LGC participated in this study by PICAA for the key study by others and by qNMR by myself. For the PICAA, amino acid analysis was used to digest the peptide followed by quantification using mass spectrometry and HPLC (methods were developed individually by each NMI). Due to limited quantities of the test material being available to the coordinators at BIPM and the subsequently small 50 mg samples supplied by BIPM it was not feasible to perform the traditional water content experiments by MS. In lieu of this analysis, the samples were allowed to equilibrate in the laboratory prior to analysis and a correction to the weighings made applied based on the temperature and relative humidity recorded in the laboratory at that time. For the qNMR quantification, LGC used an in-house reference standard of phenyl glycine (originally measured against certified standard Benzoic acid from NIST). The sample was dissolved in D_2O and 2mmol phosphate buffer and the following ^1H NMR parameters used;

- Number of scans 1600
- Water Suppression NOESY presat pulse program (Bruker)
- Receiver delay 10 seconds

- Data points 32K
- Spectral width 20.5 ppm

Peak purity was ascertained through analysis of NMR and spiking of impurity standards. The methylene peak of hCP was chosen for quantification as it was found to be the only clean peak not overlapped by any other impurities.

A typical NMR spectrum of hCP (unspiked with phenyl glycine as the internal standard) is shown below. The aromatic peaks for the phenyl glycine was used along with the downfield doublet of methylene peak from the aspartic acid of Cpeptide.

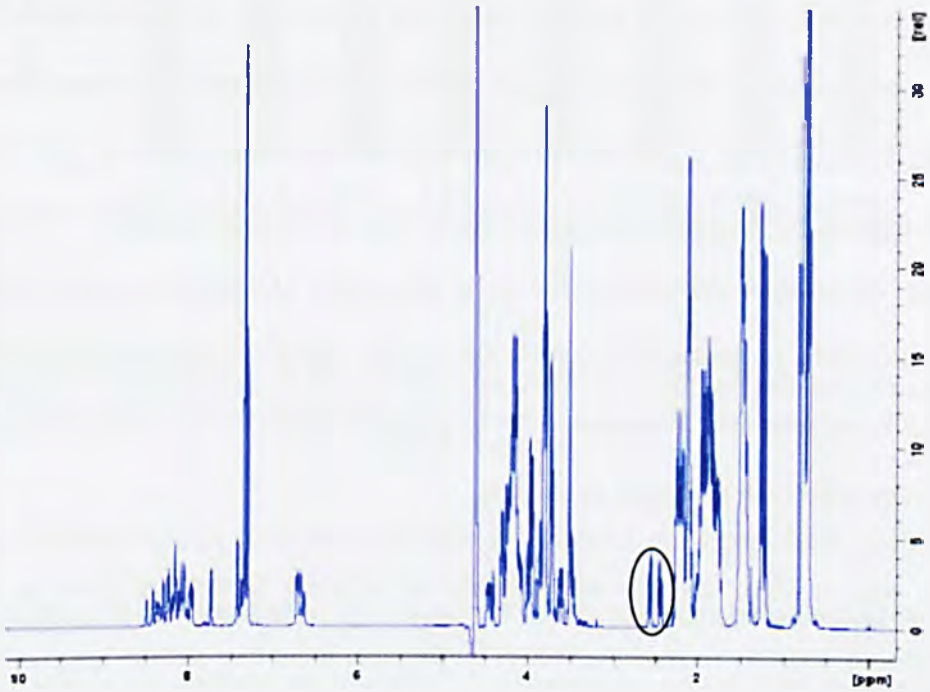

Figure 4.9 – A ^{1}H NMR spectrum of C-peptide in D_2O showing peaks used for integration acquired on a 600 MHz Bruker instrument

This peptide is at the limit of structural complexity of what is normally accepted as suitable for quantitative NMR. The chance of overlap of NMR signals from related impurities including truncated peptides, a repeated amino acid *etc* is very high and thus qNMR cannot be used as a standalone approach in this case. No knowledge of likely impurities was known in the literature and no reference materials of them available to allow calibration of any analysis. The major impurities were tentatively identified by LCMS and 3 of them custom

synthesised by Thermo Fischer to allow confirmation of identity and allow determination of response factors. Two of the three synthesised impurities;

- LQVGQVELGGGPGAGSLQPLALEGSLQ
- EAEDLQVGQVELGGGPGAGSLQPLALEGSLQ

were found to co-elute and give similar MS spectra to signals seen in the sample The cost of custom synthesis of these impurities prevented further impurities being synthesised, particularly due to the tentative nature of a lot of the peptide assignment and thus high risk of the purchasing of incorrect potential impurities.

These impurities were used to generate calibration solutions for the LC-MS and LC-UV which were quantified using qNMR. As a large number of minor impurities were discovered in this sample by LC-MS, it was decided to quantify the major impurities by HPLC due to the expectation of more similar response factors than the MS data. Further refinement of the impurity quantitation was made by the use of preparative LC, performed on an analytical scale column. Resulting solutions of C-peptide and isolated impurity where then analysed by both LC and NMR and tentative UV response factors generated based on the relative integrations of the two peaks under both analytical techniques.

These were used to confirm the UV relative response factors and used to validate the assumptions made on the response factors for the other impurities without impurity standards.

The linearity of the UV response was demonstrated for the C-peptide peak from using varying concentrations of the impurity peaks giving an R^2 of 1, which was acceptable.

4.2.3.2 Results

The Peptide was prepared by two co-ordinating NMI's (who cannot be named as the report has not officially been finalised), by characterization of a commercially sourced sample of synthetic human C-peptide. NMI's were evaluated on their capability to assign mass fraction values using peptide impurity corrected amino acid analysis (PICAA) and qNMR

with complementary HPLC data. In addition, peptide hydrolysis capabilities for the mass concentration assignment of peptide solutions were evaluated as this is a critical step in the PICAA process. The values reported for the hCP mass fraction are shown in Figure 4.10 with their expanded uncertainties shown as error bars. The reference value as reported by the two co-ordinating NMIs, are shown with the red dashed lines.

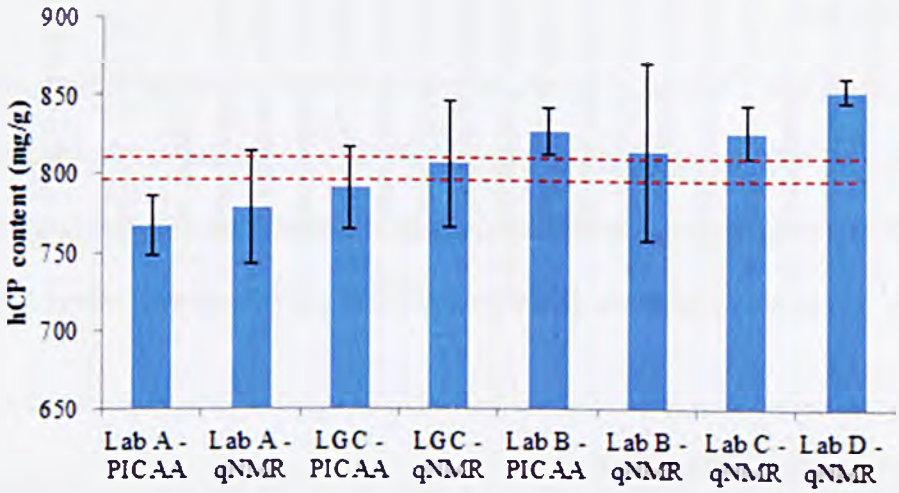

Figure 4.10 – Reported PICAA and qNMR values for hCP, NMIs unidentified as results not officially reported

The values reported by the two co-ordinating NMI's did not agree with each other. Following a one year investigation it was decided that the reference value would be 801.8 +/- 6.2 mg/g, which still made the co-ordinating NMI's results outside of the range however their uncertainty values overlapped with the reference tolerance values. LGC however were within the range for qNMR and peptide impurity corrected amino acid content (PICAA). In many cases, only a very small number of impurities were identified/quantified resulting in an under estimation of the peptide related impurity mass fractions and consequently in an overestimation of the mass fraction value for hCP and *vice versa*. It has been discussed that an overestimation of the peptide related impurity mass fraction values could be caused by in source fragmentation due to poor chromatographic separation. It has been pointed out that

the use of synthesised impurity standards has a positive impact on the quantification of the peptide related impurity mass fraction. From LGC's perspective it has clearly shown that the careful application of LC and qNMR has been able to generate purity assessment of equal quality and uncertainty to the traditional PICAA approach, but with considerably less resource.

4.2.4 Folic acid

Folic acid (**29**) was selected as the measurand for the fourth round of the comparison because it provides a significant analytical challenge, representative of a laboratory's capability for the purity assignment of compounds of moderate complexity and high polarity. It is also a well-known vitamin supplement with a common interest for many NMIs.

4.2.4.1 Experimental method

For the mass balance approach HPLC was used and impurities such as water and residual solvent characterised by Karl Fischer, thermal gravimetric analyser and head space GCMS techniques.

^{1}H qNMR analysis was performed using the following experimental parameters:

- Number of scans: 16
- Relaxation delay: 60 seconds
- Spectral width: 20.6 ppm
- Temperature: 298.0 K

The internal standard used was maleic acid (Sigma Aldrich) dissolved in D_2O/Sodium carbonate buffer.

4.2.4.2 Results

Seventeen NMIs or DIs as well as the BIPM registered to participate in the CCQM-K55.d comparison, and all submitted results giving eighteen in total. Figure 4.11 shows the results

from the provisional mass balance approach (no reference values were assigned to this at the time of writing). NMIs identities have been concealed as the report for this study has not been published at the time of writing.

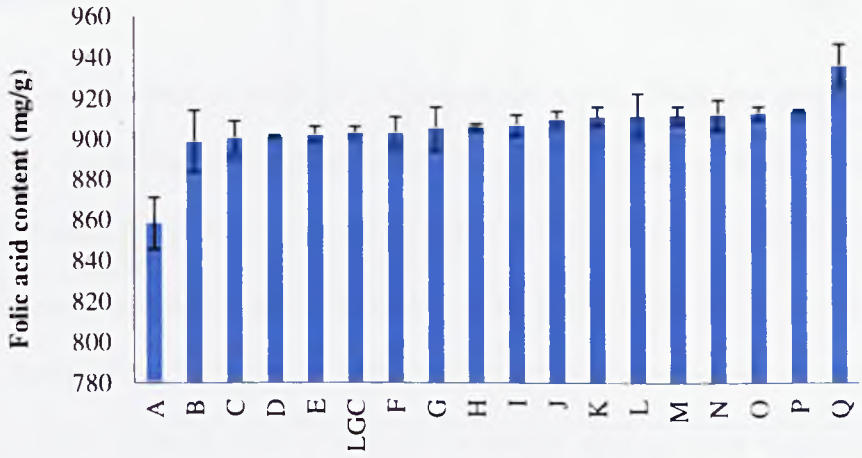

Figure 4.11 – Provisional mass balance results for Folic acid (mg/g) using traditional techniques

Many NMIs which reported folic acid content by mass balance methods for CCQM-K55.d obtained independent estimates by qNMR which they submitted within the parallel CCQM-P117.d study. The signal for the hydrogen at position 7 of the pterin ring was the basis for quantification by all participants. The low solubility of folic acid presented challenges for analyte dissolution and sample preparation for qNMR. Half the participants reporting qNMR results used the higher solubility of folic acid in basified aqueous solution whilst the other half prepared sample solutions in deuterated DMSO, generally with the addition of a drop of D_2O. Figure 4.13 shows the qNMR results. A slight bimodal distribution is seen with marginally lower purity level being determined by qNMR over that seen by the mass balance approach (although a much smaller disparity seen between the two approaches than that seen in the previous aldrin study).

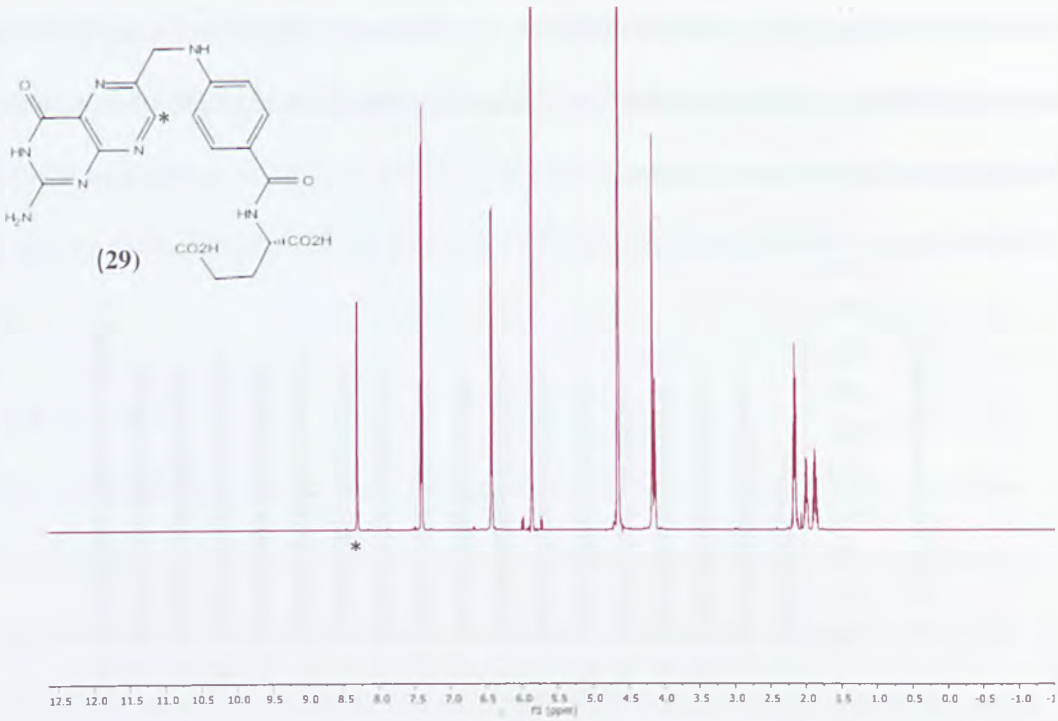

Figure 4.12 – Spectrum of folic acid * shows the proton used for integration and its assignment on the spectrum

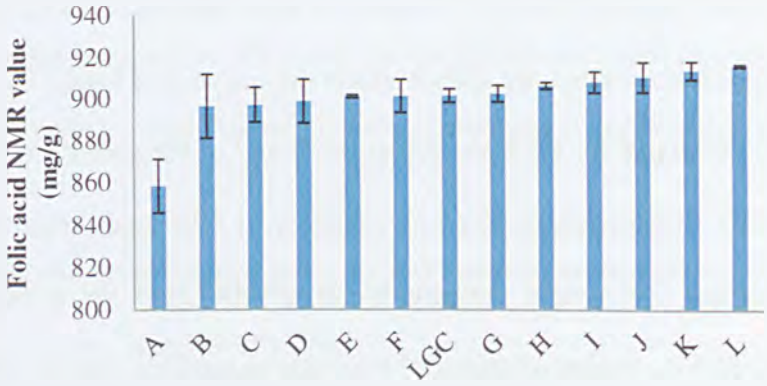

Figure 4.13 – qNMR results for folic acid

4.3 Forensics of drugs of abuse - applications in qNMR

Traditionally the analysis of forensics of drugs of abuse is done by validated mass spectrometry based methods providing high throughput assays with additional ID analysis. However, these analyses are only applicable to chemical substances from databases which have been previously characterised and assayed. The drugs sector has a major issue with the

rise of new analogues of existing psychoactive drugs which are not covered by the existing screening methods. Drugs authorities have had to seek alternative screening methods and this is where NMR has been significantly advantageous in filling the gaps in existing methodologies.

For this reason, forensics of drugs of abuse applications in qNMR has grown considerable over the last decade but also due to simpler sample preparation, NMR providing a non-invasive technique and easy structural elucidation on offer. In general NMR applications for forensic analysis of drugs of abuse provide a wide range of versatility in the information collected. Samples can be analysed without the addition of deuterated solvents [90]. Using NMR can also determine the origin of the drugs giving better information on the distribution of drugs, as ratios of minor components from a drug are associated to its geographical origin [91].

For forensic applications one of the main aims is to identify if any illegal substance is present in a seized sample and if so in what quantity. For quantitative analysis it has been highlighted that sampling procedures play an important role in the outcome of results; it is important to make sure the sample is homogenised and a minimum of 1g is used where possible [92].

As part of the validating ^{1}H qNMR methods on complex molecules a range of forensic compounds (in different matrixes) were analysed by qNMR to assess the technique.

As part of the validating ^{1}H qNMR methods on complex molecules a range of forensic compounds (in different matrixes) were analysed by qNMR to assess the technique.

4.3.1 Quantification of para methoxy-N-methylamphetamine

Para methoxy-N-methyl amphetamine (PMMA) **(30)** is a Class A psychedelic drug and causes serious side effects or death if taken in excess. Structurally it is not too complex however is

commonly distributed in tablet form. The tablet matrix may contain small amounts of the active PMMA and other organic components such as sugars making analytical quantification somewhat challenging.

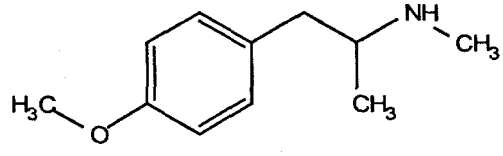

(30)

4.3.1.1 Experimental method

Four bags of pink powdered crushed tablets of PMMA (sourced from LGC), were used to determine the quantity of active component by qNMR. Approximately 12 mg of crushed tablet and 6 mg of the internal standard, Benzoic acid (NIST) were accurately weighed dissolved in DMSO-d_6. For qNMR analysis a D1 of 30 seconds was used and other parameters remained at the default settings.

4.3.1.2 Results

The aromatic signals at 7.51 ppm and 7.63 ppm from the benzoic acid reference standard and the aromatic signal at 6.90 ppm from the PMMA were used for the assay calculations. The results are summarised in Table 4.2 and an example ^{1}H NMR spectrum is shown in Figure 4.14.

The analysis assumed that all of the PMMA in the tablets was solubilised, and the results were therefore representative of a minimum level of PMMA present.

Sample	PMMA %	Mean PMMA %
Bag 1_rep1	41.49	41.68
Bag 1 _rep2	41.87	
Bag 2_rep1	41.97	41.93
Bag 2_rep2	41.88	
Bag 3_rep1	41.8	41.91
Bag 3_rep2	42.02	
Bag 4_rep1	42.21	42.2
Bag 4_rep2	42.18	

Table 4.2 – Results from the different replicates of PMMA content

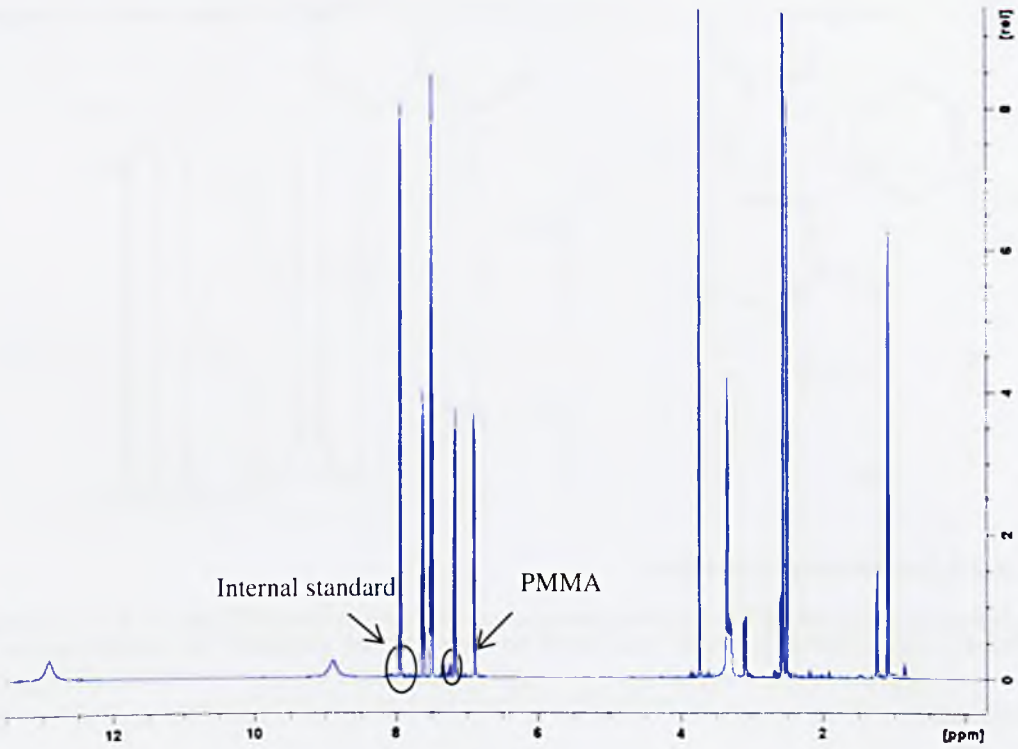

Figure 4.14 – A PMMA ^{1}H spectrum spiked with benzoic acid as internal standard

There was a good agreement between the four bags and the two replicates of each bag with a 0.5 % RSD across the 8 replicates.

4.3.2 Quantification of diclazepam & nitracaine

The feasibility of 2D $HSQC_0$ was explored using a sample of Diclazepam and nitracaine (sourced from LGC). Both ^1H qNMR and 2D $HSQC_0$ were run on the sample to compare the values obtained. Diclazepam **(31)** is an analogue of the anti-depressant Diazepam and possess potency 10x that of Diazepam. Nitracaine **(32)** is a stimulant which has similar characteristics to cocaine.

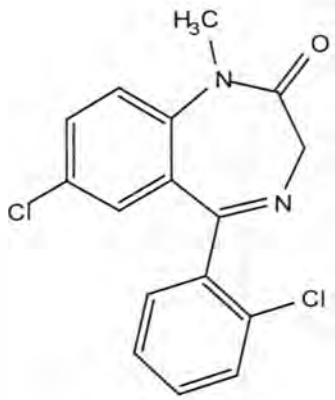

(31)

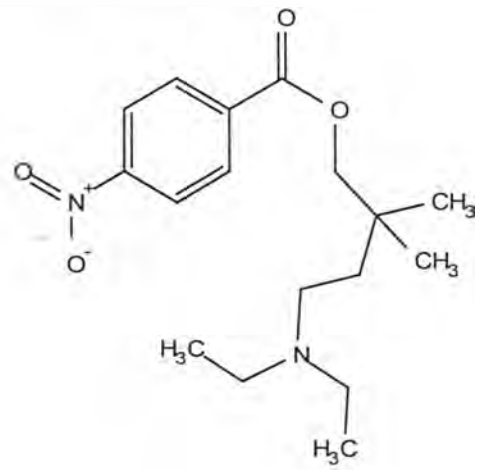

(32)

4.3.2.1 Experimental method

Maleic acid (Sigma Aldrich) was used as the internal standard for quantification of both diclazepam and nitracaine by 1D and 2D qNMR and dissolved in DMSO-d_6. For the 1D assay a D1 of 60 seconds was used and for the 2D HSQC experiments a D1 of 5 seconds was used. A Hetjres experiment was run to determine to optimal coupling constant and a T_1 experiment to determine the optimal relaxation delay. Maleic acid had a T_1 of 2 seconds whilst the peaks used for quantification from the diclazepam and nitracaine had a T_1 of <0.5 seconds.

4.3.2.2 Results

The ^1H qNMR result gave a Diclazepam content of 95.98 % with a % RSD of 0.6 % on three replicates, whereas the $HSQC_0$ results gave a Diclazepam content of 84.38 % with an % RSD of 1.3 % also on three replicates. The low $HSQC_0$ value is most likely due to the short D1 used (5

seconds) during the experiment, whereas the T_1 for the maleic acid is 2 seconds. $HSQC_0$ experiments do not account for T_1 loss only for the delays seen during the pulse program before the acquisition of data. The standard Bruker HSQC without any calibration gave a result of 86.9 % and after theoretical calculations of T_1 and coupling constant bias was corrected to give a value of 85.45 %. However this experiment needs refining for the 2D experiments due to the multiplicity of the peak. The peak used is a non-equivalent methylene peak and therefore the coupling it has is to its other methylene proton. Protons coupled to themselves evolve differently during the pulse program and therefore is not an ideal representative model. The nitracaine is a better suited model as no multiplicity factors need to be considered.

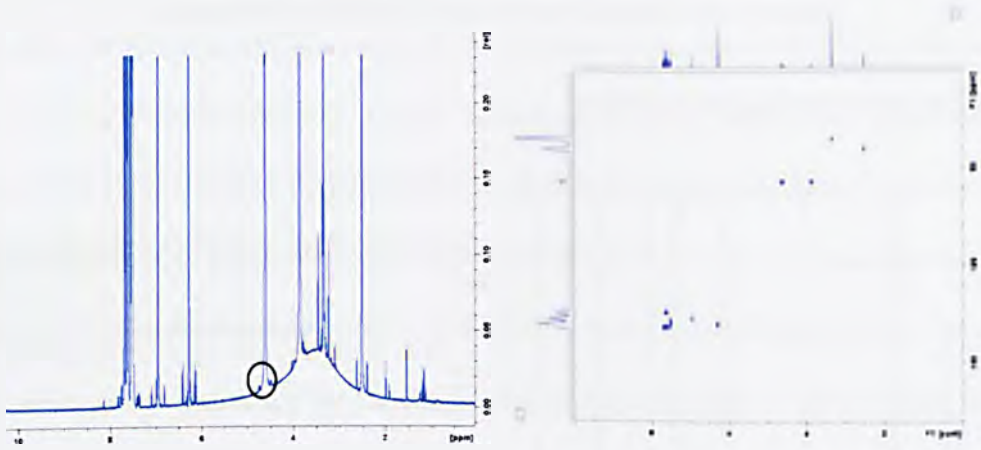

Figure 4.15 – A ^{1}H and 2D spectrum of diclazepam (peak used for integration circled) spiked with MA

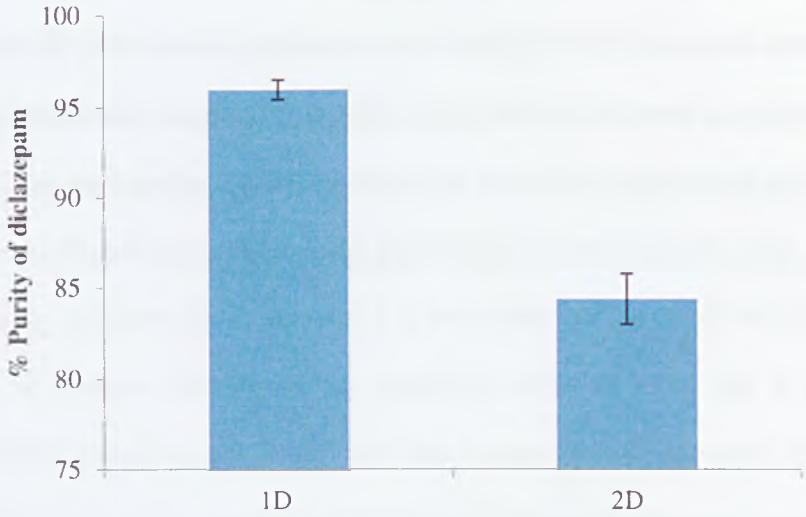

Figure 4.16 – Results from 1D and 2D qNMR of diclazepam

The nitracaine results are shown below.

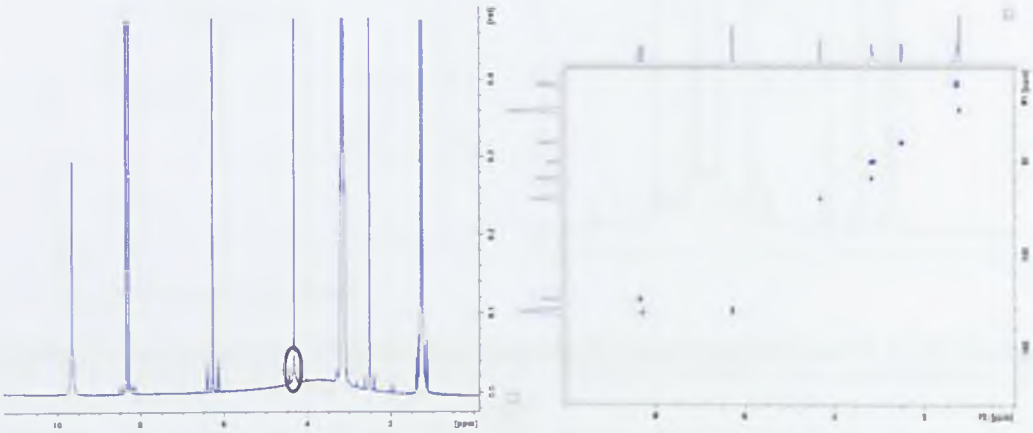

Figure 4.17 – A ^{1}H and 2D spectrum of nitracaine (peak used for integration circled) spiked with MA

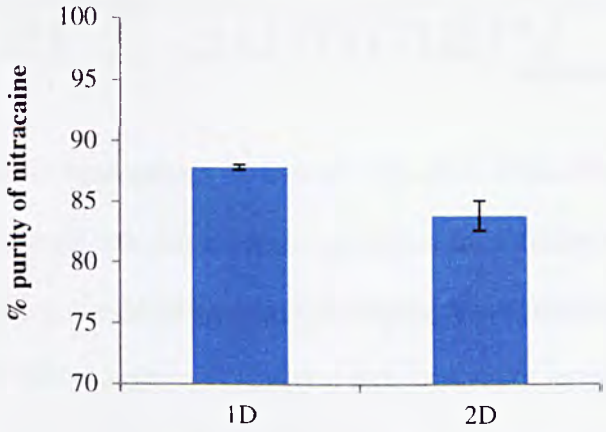

Figure 4.18 – Results from 1D and 2D qNMR for nitracaine

The ^{1}H qNMR result gave a nitracaine content of 87.89 % with a % RSD of 0.2 % on three replicates, whereas the $HSQC_0$ results gave a nitracaine content of 83.79 % with a % RSD of 1.1 % also on three replicates. The standard Bruker HSQC without any calibration gave a value of 93.43 % but after compensating for theoretical homo and hetero nuclear coupling constant bias and T_1 bias gave a corrected value of 88.91 % which is consistent with the 1D value. Again the discrepancy between the $HSQC_0$ value is most likely due to the short D1 used which is not accounted for in $HSQC_0$, the T_1 for nitracaine is <0.5 s whilst the MA is still 2 seconds.

4.4 Conclusions

In this chapter a great deal of industrial applications for qNMR has been represented. Several compounds ranging in simplicity and complexity have been analysed by both 1D qNMR and 2D qNMR.

The CCQM studies showed great success in the qNMR work reported. LGC/Kingston university's results in all cases showed great assurance in the values reported as there was little discrepancy between the reference values and reported values.

The forensics quantification work also showed promising applications and although the 2D qNMR results gave results with larger uncertainties this can further be optimised to get the

% RSD down to below 3% (for samples in complex matrices) through careful optimisation of instrumental parameters.

The forensics quantification work also showed promising applications and although the 2D qNMR results gave results with larger uncertainties this can further be optimised to get the % RSD down to below 3% (for samples in complex matrices) through careful optimisation of instrumental parameters as evidenced in my earlier chapter.

Chapter 5 Summary

5.1 Conclusions

To provide comparability of any measurement through time and space standardisation of results is essential. Standardisation ensures that quality and traceability is maintained throughout the measurement system. This is primarily achieved by ensuring measurements are traceable back to a known reference such as the base units of the Système International d'Unités (SI). This can be done by using reference methods and reference materials to ensure comparability of data is achieved. Inter-laboratory comparison studies are also a major facilitator of standardisation of measurements, where the capability of a lab is assessed for an analytical technique and ultimately for well documented guidelines and reports which are drafted to disseminate into local labs.

NMR is theoretically a perfect technique for quantification of measurements, the problem at the moment is that NMR is inconsistently applied to quantitative analysis, which doesn't always yield the unbiased results that it is assumed to. Because the NMR community within the NMI institutes operate at the highest level of measurement science, it is important to understand and quantify these minor biases.

The first step to standardising NMR measurements for quantitative work would be to have validated reference methods. 1D and 2D qNMR measurements can be validated for simple molecules with key biases derived and accounted for. However, the relatively low resolving power of 1D NMR limits its applications when analysing complex molecules or mixtures. 2D NMR can offer improved resolution through spectral editing and dispersion of signals into additional dimensions overcoming the low resolving power as seen in 1D analysis, however, additional biases have to be determined, understood and accounted for. Validating

2D HSQC can be achieved on simple model systems and then applied to more complex mixtures with minimum method development or biases can be corrected for by application of calibration methods.

Recently many papers have been published emphasising the importance of validated qNMR measurements and recent PANIC conferences and Bruker Users' meetings have had a strong emphasis on validation of NMR methods. Labs around the world have different protocols and interpretation of measurements and results in a significant spread of reporting data from the same measurement analysis. If this was applied to analysis underpinning legislative decisions, the impact can be substantial both socially and economically. Reference standards are used routinely in labs worldwide sold from common suppliers therefore utilisation in a common manner is also essential for correct applications and commutability. Commutability is defined as '*the ability of a material to yield the same numerical relationships between results of measurements by a given set of measurement procedures, purporting to measure the same quantity, as those between the expectations of the relationships obtained when the same procedures are applied to other relevant types of material*' by ISO 17511:2003 [93]. In simplistic terms and how commutability was determined within this thesis, commutability assesses whether different techniques yield the same measurement results, i.e. HPLC compared to qNMR.

Figure 5.1 shows a process flow diagram used to determine the path of qNMR analysis in this thesis;

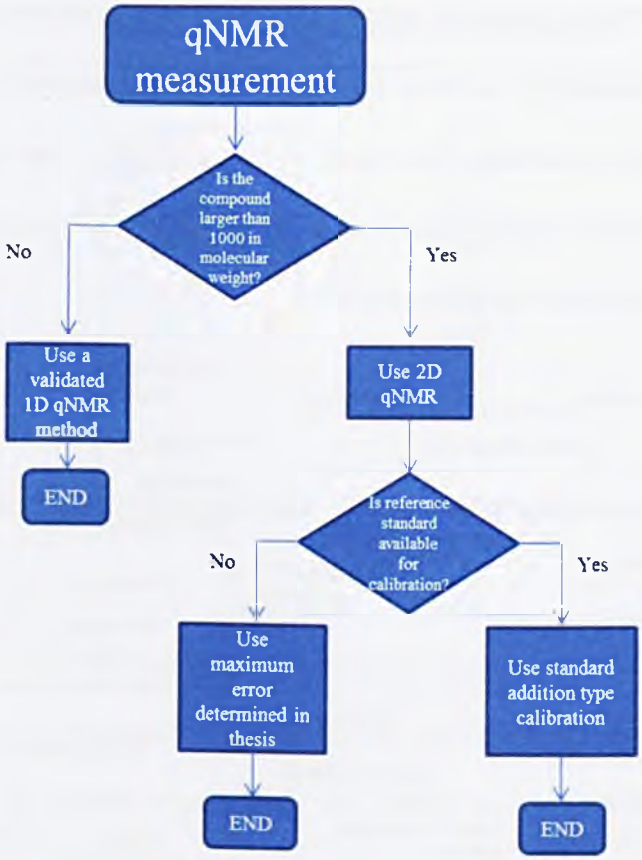

Figure 5.1 – Simple flow diagram to show path of analysis for 1D or 2D measurements. It may be the case that molecules smaller than 1000 g/mol still require to go down the 2D path however a simple 1D acquisition would determine this. The standard addition type calibration is described in Chapter 3

The outcome of this PhD is to report what influences NMR measurements and how to correct for them so that SI traceability is adhered to and a close to perfection, unbiased, 'standardised' NMR method is delivered.

In this thesis a collection of compounds, have been subjected to analysis by 1D and 2D qNMR with the aim of determining major sources of uncertainty and validation of the methods using simple model systems with the use of reference standards to achieve SI traceable measurements. For SI traceable results reference standards are required which have either been assigned a reference value in-house using the NIST Benzoic Acid or bought in from other NMIs.

As a first step towards standardisation of 1D qNMR measurements, the standard ^{1}H qNMR method was exhaustively validated for both internal and external standards using various traceable reference standards. The biases were investigated and documented; Figure 5.2 shows the biases investigated with the uncertainties reported which can be applied to any ^{1}H qNMR measurement for simple molecules.

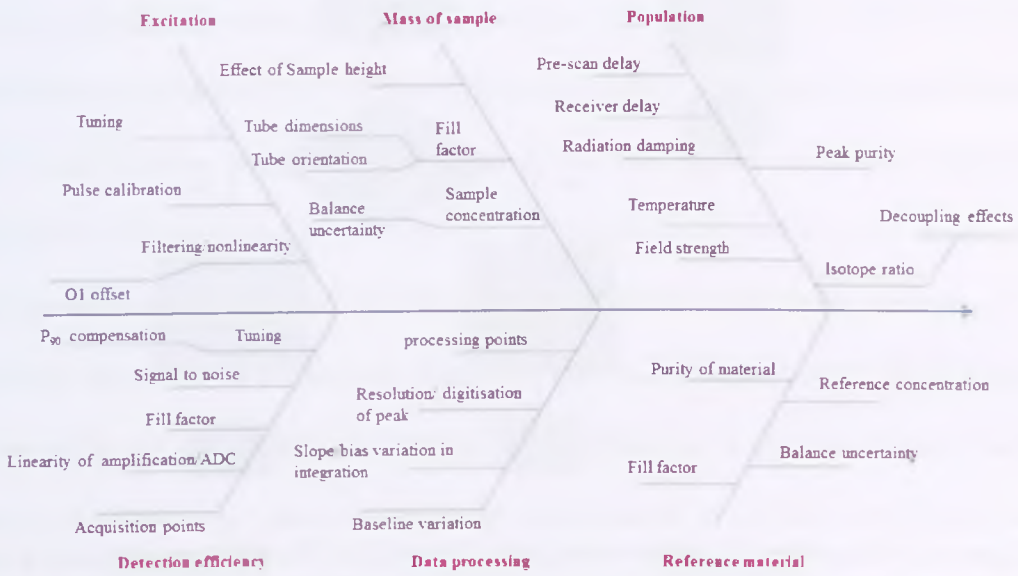

Figure 5.2 – Biases established for 1D qNMR analysis

It is desired that the uncertainty of measurement be kept low to give more confidence in the reporting values, for this reason where possible the biases are corrected or calibrated for. The work in Chapter 2 focused on minimising and correcting for where possible the biases seen in ^{1}H qNMR, with the aim of reducing measurement uncertainty to <1% for all analytes with a target of 0.1% for simple cases. By optimising the instrument appropriately the uncertainties in Table 5.1 can be eliminated, however, if the biases aren't or cannot be eliminated Table 5.1 presents typical uncertainty contributions associated to each parameter as determined in Chapter 2. T_1 uncertainty is not listed in Table 5.1 as T_1 optimisation is a pre-requisite for any qNMR measurement and optimisation of that parameter is essential prior to analysis.

Parameter	Uncertainty contribution (%)*
O1P variation	0.70
Use of different RG	0.15
Incorrect P1	0.70
Insufficient S/N	0.14
Incorrect fill volume	0.08
Repeatability	0.03
Resolution (TD)	0.05
Operator bias	0.50

*From RSD and STD Dev data

Table 5.1 – Typical uncertainty contribution from each parameter if not optimised prior to runs for 1D qNMR analysis

In Chapter 3 Initial 1D qNMR measurements on small peptides showed limited applications due to the complexity of the spectrum, therefore the need for a 2D qNMR method became critical. However, 2D qNMR experiments are limited by the availability of reference standards which are used to calibrate the additional errors seen and signal attenuation becomes an issue.

The $HSQC_0$ and standard addition calibration methods show great potential in reducing the additional biases and also require initial determination of T_1. Chapter 3 reports for the first time validation of $HSQC_0$ and calibration methods whilst maintaining SI traceability. The results shown in Chapter 3 give agree with gravimetric and ^1H qNMR methods (validated in Chapter 2) showing the methods to have great potential. The additional biases seen in 2D approaches are scrutinized to ultimately give uncertainty values to compensate for them if a calibration type method cannot eliminate them. $HSQC_0$ results of the GFFYTPKA peptide gave excellent agreement to the amino acid results, whereas the ^1H qNMR approach gave a 10 % discrepancy. The standard addition calibration approach using HSQC and ^1H NMR methods also gave excellent results for the date nectar commercial sample, quantifying the % glucose found in the original date nectar bought from a supermarket.

Chapter 4 reports the various CCQM studies reported in this thesis, showing the importance and need for standardising qNMR measurements to ensure commutability within the metrological community. Methods optimised and validated in Chapter 2 and 3 are utilised within international studies and industrial applications proving that NMR is a powerful tool in achieving fast, reliable, SI traceable quantitative measurements. Where other techniques show pitfalls qNMR has led the way in providing state of the art measurement.

The work carried out in this thesis has shown great impact as seen in Chapter 4, however two of the greatest outcomes from this thesis is the inclusion of its validation data to obtain UKAS calibration status accreditation to a recently installed Bruker 600 MHz instrument at LGC. The work in this thesis has also had an impact and been acknowledged for recommendations being compiled in IUPAC guidance documents in project IUPAC Project 2013-025; SI Value Assignment of Organic Purity for outlining a 'Best practise Guide for qNMR'. The potential to use the techniques described in this thesis in routine labs can significantly change the way analytical measurements for quantitative analysis is carried out as shown by the results obtained for the date nectar, highlighting that current measurement methods in the food industry is not effective in providing accurate values for consumer needs especially in the daily consumption recommendations listed on the packaging of products. NMR has gone from strength to strength over the last decade and if the advancements in its applications carry on, showing its benefits over other conventional techniques then NMR will soon become a principal technique used as a default as part of a suit of experiments for analysing compounds.

Lastly, to show how effective qNMR can be compared to other techniques, the example of Brain natriuretic-32 peptide (BNP) can be used. The reason why this project was initiated at LGC was to help a sub division within the Organic Analysis team. The protein analysis team use amino acid analysis (AAA) for the basis of all their quantitative work. However, this can take up to a month to do one analysis of a compound. BNP was required to be

quantified by both qNMR and AAA. qNMR took two days to prepare the samples, run the experiment, process the data and report the purity value. By AAA however, the result took two weeks to obtain with steps such as hydrolyzation, freeze drying and Isotope Dilution Mass Spectrometry analysis being involved. The efficiency of qNMR was clear and both yielded values +/- 0.5 % of each other. Figure 5.3 shows a spectrum of BNP, BNP offered a histidine singlet at 8 ppm free of overlap therefore worked perfectly in the 1D state. The method was robust and ideally quantitative measurements should all be applicable to qNMR. For peptides such as the BNP 1D qNMR was viable due to the fortuitous histidine signal however, this is not always the case and the work done in this thesis shows alternative methods yielding results as good as the 1D approach.

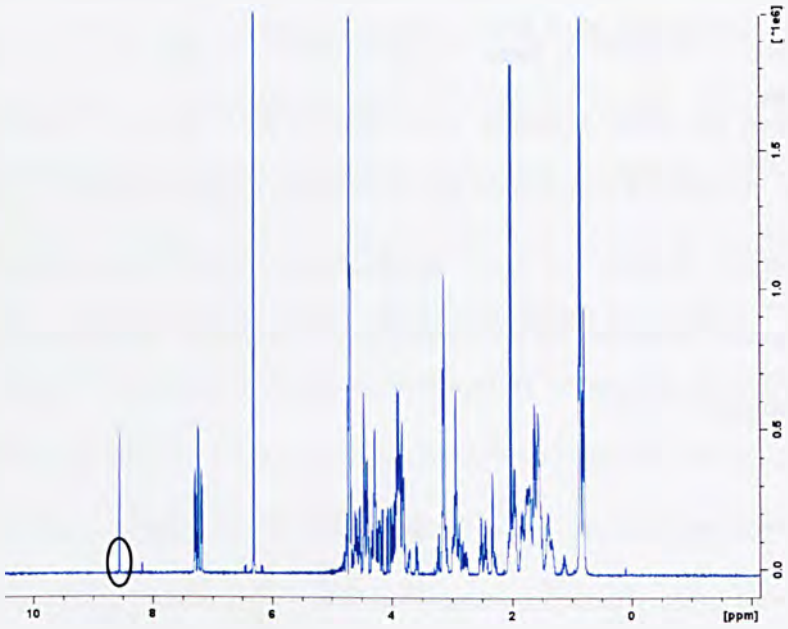

Figure 5.3 – ^{1}H Spectrum of BNP (histidine peak circled) spiked with MA in D_2O acquired on a 600 MHz Bruker instrument

5.2 Future work

The fundamental drawback in employing 2D qNMR is the experiment time required. Standard experiments with sufficient D1 and number of scans take up to 6 hours per experiment which is not viable, ideally each 2D experiment should be less than 50 minutes

without compromising resolution and T_1. There are methods which are aimed at minimising experimental time; therefore the next obvious step would be to look into ways to reduce the duration of experiments whilst also accounting for biases.

The use of non-uniform sampling has already been investigated within the scope of this thesis and seems promising in reducing experimental time, (36 minutes compared to 2 hours and 24 minutes). The repeatability for these experiments were acceptable and gave good precision (<2%).

Another method would be to use paramagnetic relaxing agents to reduce the T_1 effects, however the implications to uncertainty by doing this will need to be investigated. If relaxation delays are reduced using relaxing agents, the error coming from D1 in the pulse program is reduced however, there is additional loss of signal through relaxation during the delays within the pulse sequence itself (Figure 5.4). Therefore although it may seem favourable, the reduced experimental time comes at a cost. Obviously these effects need to be investigated, because for many applications the error may be within the required precision needed. However for the metrological community the compensated precision may not be acceptable.

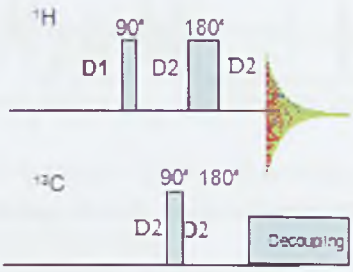

Figure 5.4 – A pulse sequence showing how if T_1 is reduced the other delays within the excitation pathway such as 'D2' could be compromised as they aren't relaxed to equilibrium due to the short experiment time

The two methods described above require numerous scans to achieve spectra with reasonable sensitivity. In 2003 a single scan 2D approach was developed by Frydman and his group which uses gradient pulses to spatially encode spin interactions and in the last decade the application to this method to quantitative analysis has been investigated [94]. It would be beneficial to investigate the uncertainties for single scan HSQC experiments and investigate how $HSQC_0$ and standard addition type experiments could be used with this. However, the negatives which come with the single scan method could outweigh the positives of reduced experiment time. Issues such as phasing, baseline, noise and non-linearity need to be investigated.

Ultimately it would be ideal if all experiments could all be run under 1D proton NMR conditions rather than 2D experiments. Less biases need to be considered under proton 1D experiments and there is no significant issue of experiment time. Therefore, a method within 1D experiments to increase resolution of complex molecules would be perfect. A method reported by R. R Ernst and co-workers is the Pure Shift NMR experiment, which is a 1D experiment where the conventional 1D proton NMR pulse sequence is altered to generate a proton decoupled proton spectrum, therefore increasing resolution of complex peaks [95]. However, this is a multiple pulse experiment and the impact on the ratio of signals needs to be assessed as well as additional biases arising from the complex pulse sequence. It would be interesting to evaluate some compounds using this technique and begin to ascertain the sources of uncertainty and how they may be overcome.

In conclusion, although 1D qNMR is preferred to 2D qNMR, it is not always viable. There is still inconsistency of how qNMR is applied, particularly in the under reporting of measurement uncertainty and for complex mixtures, and therefore undermines the potential of qNMR over alternative analytical techniques. If used correctly and consistently qNMR both in the 1D and 2D approaches have tremendous advantages and this has shown to improve the knowledge on the biases associated with both techniques and helping to

standardise protocols whilst maintaining SI traceability. There are many PT schemes out there where the 'true' measurement value is selective to that study and cannot be transferred to other measurements. The work carried out in this thesis shows transferrable expertise to analysis over a wide range of chemical organic molecules and has given an in-depth analysis to report new capabilities. A National Measurement Institute will always attempt to measure purity by more than one independent method to ensure no method specific bias, but the robustness of these methodologies are showing stand-alone capability in all but the most stringent of applications.

6 References

[1] F. Bloch, W. W. Hansen, M. Packard, *Phys. Rev.* 1946, **69**, 127

[2] R. R. Ernst, W. A. Anderson, *Rev. Sci. Instrum.* 1966, **37,** 93

[3] U. Holzgrabe, R. Deubner, C. Schollmayer, B. Waibel, *J. Pharm. Biomed. Anal.* 2005, **38,** 806-812

[4] F. Malz, H. Janke, *J. Pharm. Biomed. Anal.* 2005, **38,** 813-823

[5] S. Liu, C. Hi, *Analytica Chimica Acta*, 2007, **602,** 114-121

[6] N. J. Rankin, D. Preiss, P. Welsh, K. E. V. Burgess, M. S. Nelson, A. D. Lawlor, N. Sattar, *Atherosclerosis* 2014, **237**, 287-300

[7] U. Holzgrabe, W. K. B. Diehl, I. J. Waiver, *J. Pharm. Biomed. Anal.* 1998, **17,** 557-616

[8] U. Holzgrabe, M. Malet-Martino, *J. Pharm. Biomed. Anal.* 2011, **55,** 679-687

[9] N. G. Goger, H. K. Parlatan, H. Basan, A. Berkkan, T.Ozden, *J. Pharm. Biomed. Anal.* 1999, **21,** 685-689

[10] U. Holzgrabe, *Prog. Nucl. Magn. Res. Spec.* 2010, **57**, 229–240

[11] M. Ritota, L. Casciani, B. Han, S. Cozzolino, L. Leita, P. Sequi, M. Valentini, *Food Chemistry* 2012, **135,** 684-693

[12] P. N.; Vidal, J. M. Manzanos, E. Goicoechea, D. M. Guillen, *Food Chemistry*, 2012, **135,** 1583-1591

[13] N. A. Portela, E. C. S. Oliveira, C. A. Neto, R. T. Rodrigues, S. R. C. Silvam, V.R.E Castro, P. R. Filgueiras, *Fuel*, 2016, **166**, 12-18

[14] Cunha, A. D.; Montes, R. L.; Castro, V. R. E.; Barbosa, L. L. *Fuel*, 2016, 166, 79-85

[15] M. Malet-Martino, U. Holzgrabe, *J. Pharm. Biomed. Anal.* 2011, **55,** 1-15

[16] S. P. Mielke, *Prog. Nucl. Magn. Reson. Spec.* 2009, **54,** 141-165

[17] M. P. L. Galvao-Botton, A. M. Katsuyama, C. R. Guzzo, F. C. L. Almeida,S. C. Farah, P. A. Valente, *FEBS Letters*, 2003, **552,** 207-213

[18] V. Katta, B. T. Chait, *Rapid Commun. Mass. Spectrom.* 1991, **5,** 214-217

[19] G. Wider, L. Dreier, *J. Am. Chem. Soc.* 2006, **128**, 2571-2576

[20] International vocabulary of Metrology – Basic and General Concepts and Associated Terms, JCGM 200:2012, VIM3.

[21] http://www.bipm.org/en/worldwide-metrology/metre-convention/ (last accessed 25/02/2016)

[22] http://www.bipm.org/en/publications/guides/gum.html (last accessed 10/05/2016)

[23] http://jcgm.bipm.org/vim/en/2.26.html (last accessed 10/05/2016)

[24] R. Zeleny, H. Schimmel, *Trends in Analytical Chemistry*, 2012, **33**,107-116

[25] E. Prichard, V. Barwick, *Quality Assurance in Analytical Chemistry*, Wiley, 2007.

[26] T. Shoenberger, *Anal. Bioanal. Chem.* 2012, **403,** 247-254

[27] S. K. Bharti, R. Roy, *Trends Anal. Chem.* 2012, **35**, 5-26

[28] F. Malz, H. Jancke, *J. Pharm. Biomed. Anal.* 2005, *38* **(5),** 813–823.

[29] R. J. Wells, J. Cheung, J. M. Hook, *Accred. Qual. Assur.* 2004, **9,** 450-456

[30] T. Saito, T. Ihara, M. Koike, S. Kinugasa, Y. Fujimine, K. Nose, T. Hirai, *Accred. Qual. Assur.* 2009, **14**, 79-86

[31] T.Rundlof, M. Mathiasson, S. Bekiroglu, B. Hakkarainen, T. Bowden, T. Arvidsson, *J. Pharm. Biomed. Anal.* 2010, **52,** 645-651

[32] T. Rundlof, I. McEwen, M. Johannson, T. Arvidsson, *J. Pharm. Biomed. Anal.* 2014, **93,** 111-117

[33] G. Shao, R. Kautz, S. Peng, G. Cui, R. W. Giese, *J. Chromatogr. A*. 2007, **1138,** 305-308

[34] S. T. Deen,B. D. Hibbert, J. M. Hook, R. Wells, *J. Analytica Chimica Acta*, 2002, **474,** 125-135

[35] R. Watanabe, T. Suzuki, Y. Oshima, *Toxincon,* 2010, **56,** 589-595

[36] I. W. Burton, M. A. Quillam, J. A. Walter, *J. A. Anal. Chem.* 2005, **77,** 3123-3131

[37] Y. Huang, B. Su, Q. Ye, V. A. Palaniswamy, M. S. Bolgar, T. V. Raglione, *J. Pharm. Biomed.* Anal. 2014, **88,** 1-6

[38] G. F. Pauli, S. Chen, C. Simmler, D. C. Lankin,; T. Godecke, B. V, Jaki, B. Friesen, J. McAlpine, J. Napolitano, *J. Med. Chem.* 2014, **57**, 9220-9231

[39] S. Akoka, L. Barantin, M. Trierweiler, *Anal. Chem.* 1999, **71**, 2554-2557

[40] N. Michel, S. Akoka, *J Magn. Reson.* 2004, **168,** 118-123

[41] K. Mehr, B. John, D. Russell, D. Avizonis, *Anal. Chem.* 2008, **80**, 8320-8323

[42] Y. B. Monakhova, M. Kohl-Himmelseher, T. Kuballa, D. W. Lachenmeier, *J. Pharm. Biomed. Anal.* 2014, **100**, 381-386

[43] J. Jeener, B. H. Meier, P. Bachmann, and R. R. Ernst, *J. Chem. Phys.* 1979, **71**, 4546

[44] H. Koskela, I. Kilpelainen, S. Heikkinen, *J. Magn. Reson.* 2010, **202,** 24-33

[45] P. Giraudeau, *Magn. Reson. Chem.* 2014, **52,** 259-272

[46] W. P. Aue, J. Karhan, R. R. Ernst, *J. Chem. Phys.* 1976, **64,** 4226–4227

[47] H. Koskela, I. Kilpelainen, S. Heikkinen, *J. Magn. Reson.* 2005, **174**, 237-244

[48] K. Hu, W. M. Westler, J. L. Markley, *J. Am. Chem. Soc.* 2011, **133,** 1662-1665

[49] K. Hu, J. J. Ellinger, R. A. Chylla, J. L. Markley, *Anal. Chem.* 2011, **83,** 9352-9360

[50] K. Hu, T. P. Wyche, T. S. Bugni, J. L. Markley, *J. Nat. Prod.* 2011, **74,** 2295-2298

[51] N. Michel, S. Akoka, *J. Mag. Reson.* 2004, **168,** 118-123

[52] L. Frydman, T. Scherf, *J. Am. Chem. Soc.* 2003, **125,** 9204-9217

[53] P. Giraudeau, G. S. Remaud, S. Akoka, *Anal. Chem.* 2009, **81**, 479-484

[54] M. Mayzel, J. Rosenlow, L. Isaksson, V. Y. Orekhov, *J. Biomol. NMR.* 2014, **58,** 129-139

[55] J. Wirandi, A. Lauber, *Measurement* 2006, **39**, 612-620

[56] W. Kessel, *Thermochimica Acta,* 2002, **382,** 1-16

[57] T. Saito, T. Ihara, M. Koike, S. Kinugasa,Y. Fujimine, K. Nose, T. Hirai, *Accred. Qual. Assur.* 2009, **14,** 79-86

[58] V. Rizzo, V. Pinciroli, *J. Pharm. Biomed. Anal.* 2005, **38**, 851-857

[59] S. Liu, C. Hu, *Analytica, Chimica, Acta,* 2007, **602**, 114-121

[60] A. Le Gresley, F. Fardus, J. Warren, *J. Crit. Rev. Anal. Chem.* 2015, **45,** 300-310

[61] G. A. Barding, R. Salditos, C. K. Larive, *Anal. Bioanal. Chem.* 2012, **404,** 1165-1179

[62] A. Le Gresley, F. Fardus, J. Warren, *J. Crit. Rev. Anal. Chem.* 2015, **45**, 300-310

[63] R. Evilia, *Anal Letters*, 2001, **34(13),** 2227-2236

[64] F. Fardus-Reid, J. Warren, A. Le Gresley, *Anal Methods*, 2016, **8**, 2013-2019

[65] A. J. Charlton, W. W. H. Farrington, P. Brereton, *J. Agric. Food Chem.* 2002, **50**, 3098-3103

[66] E.Caytan, E. P. Botosoa,. V. Silvestre, R. J. Robins, S. Akoka, G. S. Remaud, *Anal. Chem.* 2007, **79**, 8266-8269

[67] S. Kim, G. D. Cruz, J. G. Fadel, A. Clifford, *J. Food Sci. Biotechnol.* 2012, **21,** 295-298

[68] L.Elflein, K. Raezke, *Apidologie*, 2008, **39**, 574–587

[69] T. M. De Swiet, *J. Magn. Reson.* 2005, **174**, 331–334

[70] D. J. Marion, H. Desvaux, *J. Magn. Reson.* 2008, **193**, 153–157

[71] H. Mo, D. Raftery, J. Harwood, J. *Magn. Reson. Chem.* 2010, **48**, 235–238

[72] P. Giraudeau, *Magn. Reson. Chem.* 2014, **52**, 259–272

[73] S. K. Bharti, R. Roy, *Trends Anal. Chem.* 2012, **35**, 5-26

[74] P. Giraudeau, G. S. Remaud, S. Akoka, *Anal. Chem.* 2009, **81**, 479-484

[75] S. Heikkinen, M. M. Toikka, P. T. Karhunen, I. A. Kilpelainen, *J. Am. Chem. Soc.* 2003, **125,** 4362-4367

[76] R. K. Rai, P. Tripathi, N. Sinha. *Anal. Chem.* 2009, **81**, 10232–10238

[77] W. Gronwald, S. M. Klein, H. Kaspar, R. S. Fagerer, N. Nurnberger, K. Dettmer, *Anal. Chem.* 2008, **80**, 9288–9297

[78] K. Hu, J. J. Ellinger, R. A Chylla, J. L. Markley, *Anal. Chem.* 2011, **83(24)**, 9352–9360

[79] S. H. Ahn, J. W. Kang, J. H. Moon, K. P. Kim, S. H. Leea and M. S. Kimm, *J. Mass Spectrom.* 2015, **50**, 596–602

[80] K. J. Bronsema, R. Bischoff and N. C. van de Merbel, *Anal. Chem.* 2013, **85**, 9528–9535

[81] C. Pritchard, F. A. Torma, C. Hopley, M. Quaglia and C. O'Conner, *Anal. Biochem.* 2011, **412,** 40–46

[82] R. W. Walker and M. I. Goran, *Nutrients* 2015, **7,** 5850-5867

[83] https://www.nist.gov/news-events/news/2008/11/nist-releases-final-wtc-7-investigation-report - last assessed on the 5th September 2016

[84] M. Mayzel, *J. Biomol. NMR.* 2014, **58**, 129-139

[85] E. C. Lin and S. J. Opella, *J. Magn. Reson.* 2013, **237**, 40–48

[86] P.J Sidebottom, *Magn. Resn. Chem.* 2016, **54**, 689-694

[87] M. G. Cox and P. M. Harris, *Meas. Sci. Technol.* 2006, **17**, 533–540

[88] S. K. Bharti, R. Roy, *Trends in Anal. Chem.* 2012, **35**, 5-26

[89] T. Yamazaki, T. Ohtsuki, T. Miura, T. Suematsu, T. Horinouchi, M. Murakami, T.Saito, T. Ihara, A. Tada, M. Tahara, Y. Goda, H. Akiyama, S. Nakao, Y. Yamada, R.Koike, N. Sugimoto, *Bunseki Kagaku.* 2014, **63,** 323–329

[90] L. A. Gama, B. B. Merlo, V. Lacerda Jr., W. Romão, A. C. Neto, *Microchemical Journal.* 2015, **118**, 12–18

[91] B. Pagano, I. Lauri, S. De Tito, G. Persico, M. G. Chini, A. Malmendal, E. Novellino, A. Randazzo, *Forensic Science International.* 2013, **23**, 1120–124

[92] L. Dujourdy, T. Csesztregi, M. Bovens, A. Franc, J. Nagy, *Forensic Science International.* 2013, **231**, 249–256

[93] ISO 17511:2003. Metrological traceability of values assigned to calibrators and control materials. Geneva, Switzerland: *http://www.iso.org/iso/iso_catalogue/catalogue_tc/catalogue_detail.htm?csnumber=30716* - (last accessed 06/12/16)

[94] Frydman, L.; Scherf, T. *J. Am. Chem. Soc.* 2003, **125**, 9204-9217

[95] W.P. Aue, J. Karhan, R.R. Ernst, *J. Chem. Phys.* 1976, **64,** 4226–4227

Appendix A - Day to Day variation of tubes

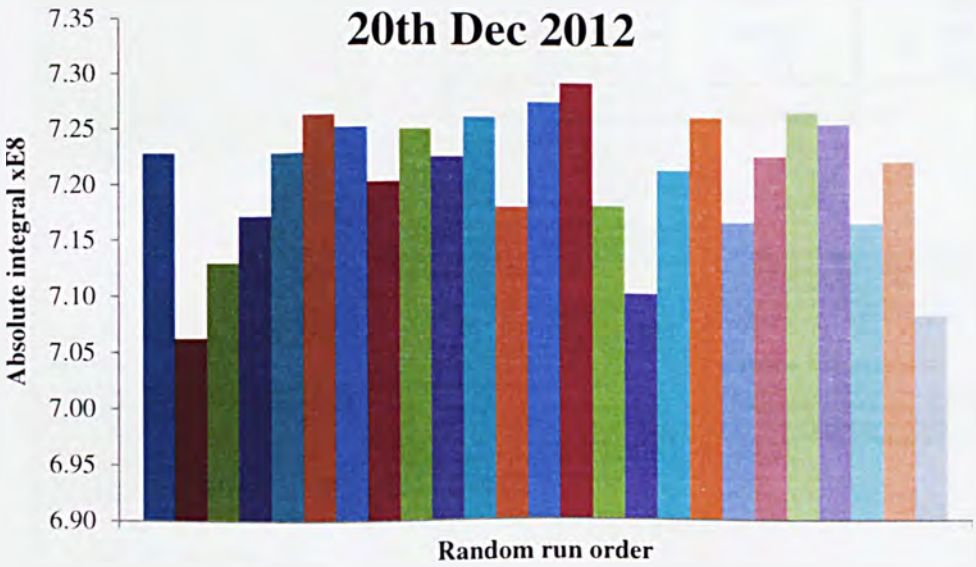

Five NMR tubes run randomly over two different days to show there are no significant trends. Axis different due to different RG used on the different days. NS: 16, D1:60s, all acquired on a 600 MHz Bruker instrument in deuterated Toluene.

Run order of tubes labelled 1 to 5 for the 20th:

1,2,3,4,5,5,3,2,1,4,3,4,1,5,2,2,1,4,3,5,5,4,1,2,3

Run order of tubes labelled 1 to 5 on the 12th :

1,2,3,4,5,2,1,4,5,3,5,4,2,1,3,4,5,1,3,2,1,2,3,5,4

Appendix B – Table showing % RSD of average integrals using different Pulse widths

Table supporting Figure: 2.15

Pulse width (μs)	Std dev of absolute integrals	% RSD
6.50	8579.2	0.15
6.80	18652.1	0.32
6.90	11983.6	0.21
6.95	6710.1	0.12
7.00	8278.0	0.14
7.05	7679.9	0.13
7.10	9298.7	0.16
7.20	16384.5	0.28
7.50	13121.3	0.23
	Average RSD	0.19

Appendix D - Poster presented at PANIC showing data from Chapter 3

Calibration and measurement uncertainty in quantitative HSQC experiments

Fahmina Fardus[1,2], Michael Nelson[3], Adam Le Gresley[2], John Warren[1]
[1]LGC Ltd., UK, [2]Kingston University, UK, [3]NIST, USA

Introduction

The aim of this project was to assess the potential of HSQC-based quantitative NMR (qNMR) to support SI traceable reference material characterisation and determine its suitability for analysis of structurally complex species and chemical mixtures. Such applications include assays of peptide and oligonucleotide solutions with a target expanded uncertainty of <2%.

Universal linearity of signal intensity with respect to proton content is lost during HSQC experiments and calibration of each unique heteronuclear signal is required to obtain comparable quantitative information for each chemical moiety.

The relative merits and realistic uncertainties associated with external calibration, internal standard and HSQCzero ($HSQC_0$) based approaches were assessed using solutions of adenosine and guanosine 5 monophosphates as a model system.

Figure 1 HSQC spectrum of the 2 nucleotides used

Repeatability

A single solution was analysed 6 times over 3 days by a conventional HSQC experiment, a constant time HSQC (CT-HSQC, shown in Figure 2) experiment and a CT-HSQC with a dummy repeat pulse sequence to generate 2-point HSQC calibrations. From these 18 experiments repeatability was assessed for the absolute intensity of three unique peaks (Figure 3).

Figure 2 CT HSQC pulse sequence

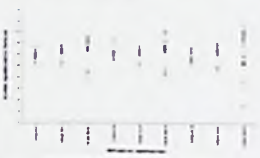

Figure 3 Repeatability of HSQC-based experiments

These experiments were performed with a default 145Hz 1JCH and relaxation delay of 1.5s. It is important to acquire data using the optimal J value so bias can be kept minimal. Attempts to modify the experiments to cycle through a range of J values proved unsuccessful due to issues of badly phased spectra within realistic experiment times.

Intermediate Precision

The between sample variation was examined by comparing 6 independent solutions. The standard deviations of the replicate analyses are shown below.

	SD of Absolute intensity		SD of Relative intensity	
	Repeat of same solution	Between solution	Repeat of same solution	Between solution
HSQC	3.0%	9.8%	1.0%	2.8%
HSQC CT	3.0%	12.5%	0.8%	3.0%
HSQC CT-2	4.4%	17.3%	0.9%	3.8%

Table 1 Repeated measurement and between sample precision

For external calibration, the intermediate precision of the absolute intensity is key to its viability as a suitable analytical method. The high value of the standard deviation of the absolute signal intensity of the guanosine 5MP C1 methine between sample preparations was clearly unacceptable for our purposes.

The normal proviso of using 5-7x T1s is not required in both external calibration and the use of internal standards but the use of such a short relaxation delay does make the method susceptible to variation in T1 due to concentration and matrix effects.

Analysis of T1s across sample preparations showed the T1s to vary between 1.5 and 2.0s due to concentration effects which generated the standard uncertainties in the table below.

	Range of T1s	T1 based standard uncertainty in			
		External calibration		Internal standard	
		1.5s D1	5s D1	1.5s D1	5s D1
Guanosine 5MP	1.7 to 2.0 s	9.30%	2.20%	1.40%	0.70%
Adenosine 5MP	1.5 to 2.0 s	5.80%	1.10%		

Table 2 Standard uncertainties from a D1 of 1.5-5s

Additional replicate HSQC experiments utilising a range of different relaxation delays confirmed that a recycle delay (D1) of >5s was required for highly repeatable integration evaluation. A minimum D1 of 3s was required to allow acceptable precision of 2% with an internal standard.

Figure 4 D1 effects

Linearity

The linearity of C1 methine signal intensity with respect to concentration was assessed using D1 values of 1.5s and 5s (Figure 5). Neither sets of data showed acceptable linearity for an external calibration approach within the target range of measurement uncertainty.

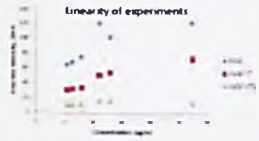

Figure 5 Linearity

Comparison of approaches

Adenosine was assayed against guanosine as an internal standard on 5 solutions (A-E) by 4 approaches: 1H qNMR, HSQC, CT HSQC and $HSQC_0$ (Figure 6). Figure 6A shows the assay using well matched peaks (C1s of both nucleotides); whilst Figure 6B shows the assay using random peaks (C1 vs an aromatic methine).

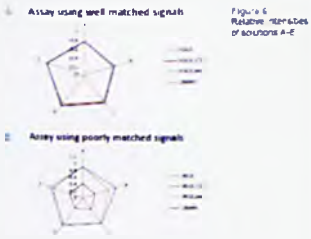

Figure 6 Relative intensities of solutions A-E

The data showed the assay for the HSQC-CT experiment using a well-matched standard to be within the criteria of +/- 2% of the qNMR result, however the mis-matched assay requires a standard addition approach to calibrate for the bias.

Application in a peptide assay

A small peptide (GFFYTPKA) was assayed against an internal standard of phenyl glycine. The results yielded a relative expanded uncertainty of less than 2 % (at the 95% CI K=2) in agreement with the 1H qNMR value.

Figure 7 HSQC spectrum of GFFYTPKA

Summary

Crucial to achieving acceptably narrow uncertainty intervals to characterise chemical reference materials (RM) the $HSQC_0$ demonstrated the best overall experimental repeatability. This approach demonstrates significant potential for allowing comparison of poorly matched signals, though the advantage of its implementation is limited for well-matched signal systems. This limitation is largely due to poor precision unless impractically long experiment times are used.

Phenyl glycine was found to be a useful standard for quantifying α-methines of the amino acids, with the dual advantage of possessing comparable coupling constants and cross peaks with similar but distinct chemical shifts. A modified RM with comparable relaxation properties to peptides is being investigated.

NIST National Institute of Standards and Technology U.S. Department of Commerce

Kingston University London